University of Groningen

Master Thesis

Revenue maximization of distributed Ocean Battery systems through Model Predictive Control

Author:
Kirsten Niekolaas - S2763605

Supervisors:
prof. dr. ir. B.Jayawardhana
prof. dr. A.Vakis

March 5, 2020

Abstract

With the world moving towards the adoption of renewable energy sources in the electricity grid, the inclusion of storage becomes unavoidable to ensure energy availability on demand. From this perspective, off-shore wind farms can be expanded by Ocean Batteries. Ocean Batteries are on-site lossless storage units of the hydropower type of system. To maximize their potential in a wind farm, multiple Ocean Batteries should be in operation. How these Ocean Batteries communicate with one another to behave optimally in the system has been investigated in this research.

A control model is developed that has a supervisory control that determines the optimal system control actions before sending the control variables to the distributed control units. After a comparison is made between a Rule-Based Control strategy and a Model Predictive Control strategy from a simplified representation of the system, a case study is performed to provide insight into the behavior of the individual Ocean Batteries and wind turbines in the real system. The focus of the control model is to obtain higher revenues from a wind farm with connected Ocean Batteries compared to a wind farm without.

From the analysis it is concluded that the design of the Model Predictive Control strategy is a suitable choice that increases revenues significantly compared to a wind farm without storage. Sensitivity analyses have been executed on the level of the turbine capacity and the depth of the Ocean Batteries, but could not result in better system performance with the current Ocean Battery design. In addition, the control model has been extended with the possibility to buy energy from the market, which significantly increases the performance of the Ocean Batteries in terms of revenues. The developed control model serves as a basis for other extensions, such as reduction of cable capacity to shore, and increased potential is therefore expected.

Contents

List of Abbreviations iv

List of Figures v

List of Tables vii

1 Introduction 1
- 1.1 Towards a sustainable future . . . 1
- 1.2 The Ocean Battery: a product with potential . . . 2
- 1.3 Problem analysis . . . 4
- 1.4 System description . . . 6
- 1.5 Stakeholder analysis . . . 7
- 1.6 Research goal . . . 8
- 1.7 Research design . . . 12
  - 1.7.1 Research questions . . . 13
  - 1.7.2 Operationalization . . . 14

2 The system of connected Ocean Batteries 16
- 2.1 Ocean Battery: the concept . . . 16
- 2.2 Design of the system . . . 16
- 2.3 Wind energy . . . 18
- 2.4 Electricity markets . . . 27

3 Dynamical model of the Ocean Batteries 31
- 3.1 Factors affecting the efficiency of the Battery . . . 31
- 3.2 Equations describing the Ocean Battery dynamics . . . 33
- 3.3 Simulations . . . 36
- 3.4 Validation of the dynamical model . . . 37
- 3.5 Dynamical model for the distributed system . . . 39

4 The control systems model 41
- 4.1 The distributed control system . . . 41
- 4.2 Control strategies . . . 41
- 4.3 Design of the control model . . . 45
- 4.4 The optimization algorithm . . . 46

5 Validation of the distributed storage control system 51
- 5.1 Validation of the MPC 1S1G model . . . 51
- 5.2 Validation of the RBC 1S1G model . . . 52
- 5.3 Validation of the MSMG model . . . 55

6 Results 58
- 6.1 Simulation set-up . . . 58
- 6.2 Reference model: without storage . . . 59
- 6.3 Results of the simulations: One-Storage-One-Generator . . . 60
- 6.4 Results of the simulations: Multiple-Storage-Multiple-Generator . . . 69

6.5 Sensitivity analyses 76
6.6 Model extension: possibility to buy from the market 78

7 Discussion **82**
7.1 Summary of the research 82
7.2 Limitations 83
7.3 Further research 84

8 Conclusion **86**

References **88**

Appendices **94**

A Generation of wind data set **94**

B Calculation of the volume of the Ocean Grazer storage **97**

C Dynamical model of the Ocean Grazer storage **98**

D Validation of the dynamical model **100**

E Basic settings for the validation simulations **101**

F One-Storage-One-Generator RBC simulation model **103**

G One-Storage-One-Generator MPC simulation model **105**

H Multiple-Storage-Multiple-Generator MPC simulation model **109**

I Reference model: without storage **115**

J Simulation results **117**

K Optimization problem in Chapter 6.6 **124**

List of Abbreviations

1S1G One-Storage-One-Generator.

aFRR automatic Frequency Restoration Reserves.

BRP Balance Responsible Party.

BSP Balancing Service Provider.

CTO Chief Technology Officer.

DCS Distributed Control System.

EU European Union.

MPC Model Predictive Control.

MSMG Multiple-Storage-Multiple-Generator.

OG Ocean Grazer.

PaT Pump as Turbine.

PHES Pumped Hydro Energy Storage.

RBC Rule Based Control.

RTM Real-Time electricity Markets.

SLSQP Sequential Least SQuares Programming.

List of Figures

1 The share of renewable energy in 2017 (REN21, 2019). 1
2 Artist's impression of the Ocean Grazer 3.0 (Origins, 2019). 3
3 Higher-level system: stages of renewable energy utilization. 6
4 Optimize electricity output from wind energy from a revenue perspective. . . 7
5 Optimize electricity output from wind energy from a revenue perspective (decomposition). 7
6 The conceptual model. 11
7 The engineering cyle by Wieringa (Wieringa, 2014). The implementation phase is not incorporated for this research. 13
8 Depiction of the possible energy flows in the system. 17
9 Annual European onshore and offshore mean wind speeds at an 80 meter height (Rodrigues et al., 2015). 19
10 Configuration of the Hons Rev wind farm, which is located near Denmark (Rudion et al., 2008) 20
11 A power curve for a 2 MW wind turbine as a function of the wind speed (Moskalenko et al., 2010). 22
12 Normalized power output as a function of turbine row for a wind direction with minimal deviation (Porté-Agel et al., 2013). 23
13 Normalized power output as a function of turbine row for two wind directions with minimal deviations (Wu and Porté-Agel, 2015). 23
14 A depiction of the configuration of the OG-WindFarm with different wind direction and how they affect the rows in the farm in (a) and (b). 24
15 Converting eight wind directions (a) to four wind directions (b) in order to generate a wind power data set. 25
16 The power curve for the MHI Vestas Offshore V164-8.0 MW turbine. 26
17 An overview of the different electricity markets and their relation to the actual point of delivery (KULEnergyInstitute, 2015). 28
18 Example of the Ocean Grazer storage system design. 32
19 Results change in energy level from filling and draining the bladder once. . . 37
20 Illustration of the working principle of Model Predictive Control(1) 43
21 Illustration of the working principle of Model Predictive Control(2) 44
22 The behavior of the simulation model when simulated for a day in terms of storage level (a) and price (b). 52
23 The effect of efficiency on the storage levels with the day-ahead market (2019). The efficiencies are (a) $\eta_P = 0.75, \eta_T = 0.8$; (b) $\eta_P = 0.8, \eta_T = 0.85$; (c) $\eta_P = 0.85, \eta_T = 0.9$; (d) $\eta_P = 0.9, \eta_T = 0.95$; (e) $\eta_P = 1, \eta_T = 1$. 53
24 The behavior of the simulation model when simulated for a day in terms of storage levels (a) and price (b). 55
25 The behavior of the simulation model when simulated for a day in terms of storage levels (a) and price (b). 56
26 The calculated revenues from the day-ahead market (a) and aFRR market (b). 60
27 The set-up of the system for the 1S1G case study. 60
28 The calculated revenues from a variable number of storage systems in a cluster for the 1S1G MPC model. 62

29 The calculated revenues from different prediction horizons for the 1S1G MPC model. 63
30 The computation times for different prediction horizons for the 1S1G MPC model. 64
31 The resulting revenues from varying efficiencies for the pump and turbine mode of the PaT for the 1S1G MPC model. 65
32 The resulting revenues from varying efficiencies for the pump and turbine mode of the PaT. 67
33 Yearly revenues from the reference case and the RBC and MPC strategies for the day-ahead market. 68
34 Yearly revenues from the reference case and the RBC and MPC strategies for the aFRR market. 69
35 Set-up of the system for the MSMG case study. 70
36 Revenues of the MSMG simulations for the years 2017-2019 of the day-ahead market. 71
37 Revenues of the MSMG simulations for the years 2017-2019 of the aFRR market. 73
38 Revenues of the MSMG simulations for the years 2017-2019 with varying prediction horizons. 75
39 Revenues of the sensitivity of the turbine capacity with the MSMG simulations. 77
40 Revenues of the possibility to buy energy from the market from the MSMG simulations. 80
41 Distribution of the wind directions in the data set (left) and average wind speed per wind direction (right). 94
42 Configuration and allocation of turbines in the grid. 95
43 Power output per wind turbine produced with the wind data set. 95
44 Top-view of the Ocean Grazer. 97

List of Tables

1 Efficiencies of the rows of turbines when the wind is blowing straight. 24
2 Efficiencies of the rows of turbines when the wind is blowing slantwise. 24
3 Combined efficiencies for the turbine rows. 25
4 Model parameters for generation of a wind turbine power production data set. 26
5 The percentages that the prices of the aFRR-up market and aFRR-down market are equal. 29
6 The highest, lowest and mean prices of the retrieved data sets. All prices are in €/MWh. 30
7 Model parameters. 36
8 Efficiencies of the Ocean Battery. 36
9 Relation between the sampling time and the total simulation time when filling and draining the storage once. 38
10 Comparison between the simulation model and analytical calculations. 38
11 Effects of changing the efficiency parameters on the amount of energy sent to the storage and sold from the storage. 54
12 The amount of times the mean of the data set is exceeded for various price data sets, by the Excel model. 54
13 The amount of times the mean of the data set is exceeded for various price data sets, by the Python model. 54
14 Effects of changing the efficiency parameters on the amount of energy stored from the wind turbine and the revenues generated by the system. 57
15 Parameters used for the 1S1G simulations. 59
16 Parameters used for the MSMG simulations. 59
17 Computation times for a yearly simulation with MPC 1S1G code in $hh : mm : ss$. 61
18 Yearly revenues for the 1S1G MPC strategy. 64
19 Yearly revenues for the RBC strategy. 67
20 The computation times for a yearly simulation of the MSMG MPC model for the different price markets in *hh:mm:ss*. 70
21 The computation times for a monthly simulation of the MSMG MPC model for a varying prediction horizon in *hh:mm:ss*. 71
22 Maximum storage levels (day-ahead market) for the MSMG simulations with the MPC strategy. 72
23 Total energy sent to storage (day-ahead market) for the MSMG simulations with the MPC strategy. 72
24 The proportion of energy sent to storage for both models over the years 2017-2019. 73
25 Maximum storage levels (aFRR market) for the MSMG simulations with the MPC strategy. 74
26 Total energy sent to storage (aFRR market) for the MSMG simulations with the MPC strategy. 74
27 The proportion of energy sent to storage for both models over the years 2017-2019. 75
28 The proportion of energy sent to storage for both prediction horizons over the years 2017-2019. 76

29 Total amount of energy stored as a result of increasing the turbine capacity with the MSMG simulations. 77
30 Yearly revenues from the sensitivity analysis to the depth of the Ocean Batteries. 78
31 Total amount of energy stored as a result of increasing the depth of the Ocean Batteries with the MSMG simulations. 78
32 The percentage of time that the wind production is lower than 2 MW. 79
33 The percentage of time that prices are negative. 79
34 The amount of energy stored from the wind turbine and bought from the market for 2017-2019. 80
35 Parameters for the calculation of the volume of the Ocean Grazer. 97
36 Volume of the Ocean Grazer storage. 97
37 Basic settings for the validation of the MPC 1S1G model by prediction validation and parameter variability. 101
38 Basic settings for the validation of the MPC 1S1G model by prediction validation and parameter variability. 101
39 Basic settings for the validation of the MPC MSMG model by prediction validation and parameter variability. 102
40 Test whether one iteration for the optimizer is sufficient with 1S1G MPC model. 117
41 Test the effects of sampling time on the yearly revenues with 1S1G MPC model. 117
42 Test the relation between the number of Ocean Batteries in a cluster and the yearly revenue with 1S1G MPC model. 117
43 Test the effects of prediction horizon on the yearly revenues with computation times of the simulation in *hh:mm:ss* with 1S1G MPC model. 118
44 Test the effects of the efficiency of the PaT on the yearly revenue with 1S1G MPC model. 118
45 Yearly revenues for the 1S1G MPC strategy. 118
46 Test the effects of the efficiency of the PaT on the yearly revenues of the RBC model. 118
47 Yearly revenues for the RBC strategy. 119
48 Yearly revenues (day-ahead market) for the MSMG simulations with the MPC strategy. 119
49 Maximum storage levels (day-ahead market) for the MSMG simulations with the MPC strategy. 119
50 Total energy sent to individual storage units (day-ahead market) for the MSMG simulations with the MPC strategy. 119
51 Total energy sent to storage units (day-ahead market) for the MSMG simulations with the MPC strategy. 120
52 Yearly revenues (aFRR market) for the MSMG simulations with the MPC strategy. 120
53 Maximum storage levels (aFRR market) for the MSMG simulations with the MPC strategy. 120
54 Total energy sent to individual storage units (aFRR market) for the MSMG simulations with the MPC strategy. 121
55 Total energy sent to storage units (day-ahead market) for the MSMG simulations with the MPC strategy. 121
56 Yearly revenues from the turbine capacity sensitivity with MSMG MPC strategy. 121
57 Yearly revenues from the depth sensitivity with MSMG MPC strategy. 121

58 Maximum storage levels from the depth sensitivity with MSMG MPC strategy. 122
59 Yearly revenues (aFRR market) for the MSMG simulations with the MPC strategy + buy from market. 122
60 Maximum storage levels (aFRR market) for the MSMG simulations with the MPC strategy + buy from market. 122
61 Total energy sent to individual storage units (aFRR market) for the MSMG simulations with the MPC strategy + buy from market. 122
62 Total energy sent to storage units (day-ahead market) for the MSMG simulations with the MPC strategy + buy from market. 123

1 Introduction

This first chapter is dedicated to understanding the context of the problem and defining the system that is subject to this research. First, the need for innovative solutions to expand renewable energy systems by storage in order to deliver a constant energy output is explored. Thereafter, the recent developments of the Ocean Battery systems proposed at the University of Groningen are discussed and the relevant stakeholders are analyzed. Furthermore, the problem the research deals with is analyzed and relevant research questions are presented that serve as the main focus of this thesis. Finally, the research design leading up to answering the research questions is presented.

1.1 Towards a sustainable future

Sustainability, or the lack thereof, is one of the most discussed and researched topics nowadays, driven by climate change and the rising CO_2 level (Drew et al., 2009). It is widely acknowledged that a change in energy generation and consumption is inevitable to keep the world as livable as it is today. The energy generation is mainly concerned with limiting the CO_2 emissions, whereas energy efficiency and responsible utilization of energy are most important for energy consumption. The focus of this research is on the side of energy generation. Nearly all governments have reached consensus that more renewable energies have to be deployed in the future to overcome environmental pollution and climate change, and to ensure energy security(Alagappan et al., 2011; Dincer, 2000). Over the past years, renewable energy has become widely accepted and has reached a mainstream position in society (Smith, 2017). Target goals on the global renewable energy share have been defined as a result of this development, focusing on a share of at least 30% in 2030, both nationally and globally (Rijksoverheid, 2016; IRENA, 2014). However, it can be observed that the world is not on track to meet these goals. Figure 1 depicts the share of renewable energy in 2017. It can be observed that only 18.1% of all energy is renewable, of which 10.6% consists of modern renewables (REN21, 2019). From the target goals set by the government it can be derived that a large increase in the utilization of modern renewables is expected in the upcoming years.

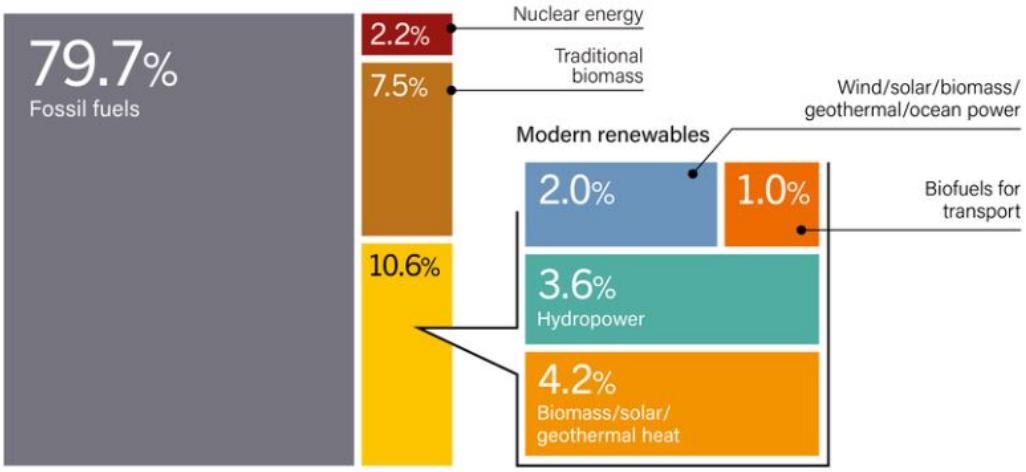

Figure 1: The share of renewable energy in 2017 (REN21, 2019).

Although it is necessary to expand the amount of renewable energy sources deployed, it is difficult to extend the amount of renewable energy sites on-land. One of the major reasons is that local acceptance of various types of renewable energies, such as wind power, has been proven difficult and is definitely a factor to consider when designing renewable energy policies. Negative public perception towards renewable energy development driven by for example landscape pollution have led to the delay or even cancellation of renewable energy projects (Guo et al., 2015). An option to overcome part of the negative public perception is to shift the focus of on-land renewable energies towards off-shore (Ladenburg, 2008). An example of a widely used type of off-shore renewable energy source is wind energy. Advantages include abundance, stronger power extraction and consistency in terms of the availability compared to on-land wind energy (Perveen et al., 2014).

Currently, off-shore wind farms cover a large surface area, of which the area between neighboring wind turbines can only be used for a limited amount of operations such as limited shipping purposes (Rijksoverheid, 2015). To utilize this area in a more efficient way, one may look into using this area to capture solar energy or wave energy. Nowadays there are many initiatives to develop technologies that may harvest wave energy, but they are relatively underdeveloped compared to other renewable energy technologies (Drew et al., 2009). An example of a novel wave energy converter system which is currently in development is the Ocean Grazer WEC (van Rooij et al., 2015). A large amount research is executed at the moment on the optimization and feasibility of this WEC and it may be considered a promising application for the future.

One of the challenges regarding renewable energy sources is its intermittent character (Gowrisankaran et al., 2016). Storage systems may be incorporated to balance the electricity output from renewable energy sources (Suberu et al., 2014; Garcia-Rosa et al., 2013). Another argument in favour of incorporating storage systems is that a shift can be observed towards a decentralized renewable energy generation (Karger and Hennings, 2009). This requires the adoption of energy storage systems and its demand is therefore increasing for a wide range of applications. Large renewable power generators, such as the wind farm, are said to be amongst them (Rehman et al., 2015). The aforementioned Ocean Grazer also has its own incorporated lossless storage system, the 'Ocean Battery' (Dijkstra et al., 2016), which is currently the main focus of Ocean Grazer BV in its road towards launching a product to the market. This research is focused on the Ocean Battery.

1.2 The Ocean Battery: a product with potential

The Ocean Battery is a bottom-fixed device that receives its take-off power from renewable energy sources, such as wind energy or wave energy. The Ocean Battery is an on-site hydropower type of storage system, which offers energy buffering capabilities that enable satisfied energy market demand and maximized system revenue. The storage system consists of a concrete structure that is gravity-based and enables the system to store potential energy (Wei et al., 2019). Its working principle is as follows: an internal fluid is pumped from a reservoir with atmospheric pressure to a flexible bladder in a closed system. The bladder has the same hydrostatic pressure as the ocean water surrounding the Ocean Battery, thereby creating a pressure difference between the bladder and the concrete reservoir. A turbine subsequently converts the potential energy into electricity by means of the pressure difference

Figure 2: Artist's impression of the Ocean Grazer 3.0 (Origins, 2019).

when the electricity is demanded by the market. The greater the depth at which the Ocean Battery is situated, the greater the pressure difference, and the higher the capacity of the Ocean Battery in MWh. It is therefore desirable to incorporate the Ocean Battery at a high depth, possibly connected to wind turbines that are already existent.

The version of the Ocean Battery described above is an improvement to the latest Ocean Grazer concept that has been visualized, the Ocean Grazer 3.0. The Ocean Grazer 3.0 is depicted in Figure 2. Changes with respect to this design include the shape of the storage bladder: the new storage system has a square shape instead of a round shape such that the rubber bladder behaves in a beneficial manner. Furthermore, wave energy is disregarded for this project, as the Ocean Battery may also receive electricity from other renewable energy sources such as wind turbines or solar panels. Finally, the Ocean Batteries can be placed next to wind turbines instead of only beneath them, which opens up the possibility of incorporating Ocean Batteries in existing wind farms. These arguments have led to the development of a new Ocean Battery concept for Ocean Grazer BV.

One of the newest ideas concerning the project is to use the Ocean Batteries as an anchor for floating wind turbines. Fixed tower type wind turbines are placed on near shore locations due to the necessity to place the turbines on the seabed. Floating wind turbines, however, are not bound by this requirement and can therefore be placed in deeper waters, opening up the possibility to harvest energy from stronger and steadier wind fields (Koo et al., 2014). With the advantage of placing the Ocean Batteries at greater depth, the idea of using the Ocean Batteries as an anchor for floating wind turbines was generated. It must be noted that the Ocean Batteries are still in the development phase and it has to be investigated whether the storage system may result in economic benefits compared to having no storage system at all: it must be considered that the choice to implement ready-to-sell electricity as the power take-off

for the Ocean Battery instead of harvesting wave energy has the following consequence. The electricity from another power source can also directly be sold to the market, which means that the benefits of storing the electricity must be large enough to overcome the negative effect of the Ocean Battery's efficiency. These benefits include for example sufficient fluctuations in electricity price, reduced cable costs and stable supply. Multiple Ocean Batteries may be adopted in one wind farm, that consists of a number of wind turbines, to store a large amount of energy. The number of Ocean Batteries connected to one wind turbine is also a variable to study. The topic of this thesis is to transform the aforementioned system of Ocean Batteries into a revenue maximization study. To achieve this, a control model has to be developed that decides on the individual Ocean Battery's actions.

1.3 Problem analysis

In this section the problem is analyzed from its background and a problem statement is defined. From the problem statement, the project is scoped in order to define the boundaries of the research.

Problem background

Ocean Grazer BV is interested in launching a product. As mentioned above, their main focus at the moment is the Ocean Battery, or the storage system. If Ocean Grazer BV succeeds to launch this product to the market and to fully integrate this product, it can be considered a novel technology that efficiently reuses the area between neighboring wind turbines and that can be a valuable addition to wind farms. Moreover, the Ocean Battery is a lossless storage system, which means that no energy is dissipated from keeping the energy in the storage for a large amount of time. This leads to advantages compared to other storage systems when for example seasonal fluctuations with respect to the electricity production are significant. It can be concluded that the new design may contribute to the needs of the market significantly, especially since the Ocean Batteries are powered by renewable energy sources.

To efficiently manage the aforementioned system consisting of a number of Ocean Batteries and wind turbines, an appropriate distributed control system is necessary. This control should be able to process information about the price market and the electricity production, and to deliver electricity from the individual storage systems to the electricity grid when it is demanded. Currently, such a control does not exist, which means the product cannot be launched to the market as long as this control has not been developed. For this research, a distributed control system has been developed that attempts to maximize the revenues obtained by the system of connected Ocean Batteries as opposed to for example securing a stable energy supply, as this approach suits the business aspect of the master Industrial Engineering and Management better. Costs are not included in this research, which means that the focus of the revenue maximization study is on the fluctuations in electricity price rather than on a restricted cable capacity.

Problem statement

From the problem background the problem statement is defined as follows

The problem is that a control for multiple connected Ocean Batteries does not exist yet, whereby insight in the individual Ocean Battery's behavior in a distributed system is lacking.

When there is no control over the Ocean Batteries, there is nothing that decides on the actions of the individual storage systems. There may be three states of the Ocean Battery: it may be storing energy, generating electricity or not doing anything at all. Having a control gives insight in the desired behavior of individual Ocean Batteries at each time step and can therefore be considered a valuable tool. There may also be other reasons why Ocean Grazer BV is not able to launch the Ocean Batteries to the market yet, such as a knowledge gap on its economic feasibility or design choices that are still open to discussion. The distributed control model developed in this research should therefore be adaptable to different designs of the system and different designs of the Ocean Batteries. In this way, the control model may also be able to provide some insights in the optimal design choices. Ultimately, the revenue is calculated by the model and maximized by a selected control strategy.

Scope of research

The scope of the research is limited to the following. The control model developed in this research requires several inputs. These inputs can be categorized as follows.

- **System design**: the design of the system is concerned with the amount of wind turbines in the considered wind farm, the amount of Ocean Batteries connected to a single wind turbine and the location of the system.
- **Ocean Battery design**: the design of the Ocean Batteries are concerned with the dimensions and efficiency of the system, the capacity of the pump and turbine, and the water depth at which the Ocean Batteries are situated, which determines the storage capacity.
- **Information on power production**: information on the power production is necessary for the control to determine the storage possibilities. For this research only power production from wind turbines is considered. The model simulations are run with historical data sets. Data sets with the individual wind turbine's power production in a wind farm are not publicly available, so the generation of wind power data set is included in the scope of the research.
- **Market prices**: to eventually maximize revenues generated by the system it is necessary to have knowledge on the prices for which the electricity can be sold. A historic data set from a local price market may be retrieved as an input for the control model to run simulations with.

The scope of the research is limited to developing the distributed control model and retrieving the aforementioned inputs. Costs are not considered in this research. This means that the actual costs of the Ocean Batteries, the wind turbines and the cable infrastructure are considered out of the scope of this research.

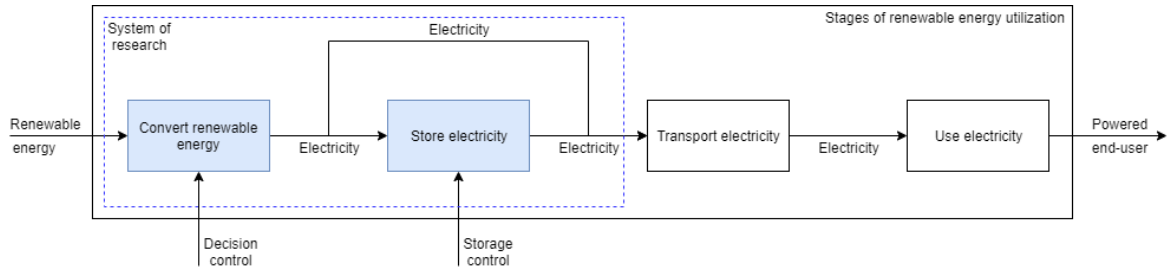

Figure 3: Higher-level system: stages of renewable energy utilization.

1.4 System description

From the aforementioned research boundaries the system boundaries have been defined. In this section the system that is subject to this research is explained and graphically presented. A distinction is made between the higher-level system that the system of this research fits into and the actual representation of the system that is studied in this research.

Higher-level system

The higher-level system is concerned with all the stages of renewable energy utilization: from converting renewable energy to transporting and to using renewable energy. The higher-level system is a physical system, of which all elements may be optimized in terms of for example its efficiency or costs. A graphical representation of the higher-level system is depicted in Figure 3. Control actions are applied at the point where it is decided whether the electricity should be stored or should directly be transported to the end-user, and at the point at which it is decided at which time step the storage is drained. The input of the system is the renewable energy and the output is the end-user that is powered by the electricity.

The focus of this research has been indicated by the dashed lines in Figure 3. The research is focused on the renewable energy type 'wind' as much potential is expected in this area, such as the aforementioned distribution of Ocean Batteries applied as anchors for floating wind turbines. The focus has been chosen such that both the generation of wind data and the storage are included. The distributed control model that is developed eventually controls the decisions on the storage of the electricity.

Focus of research

The focus of the research is depicted in Figure 4. Within the system the conversion of wind energy to electricity takes place. In the end, the focus is on the control that ensures the electricity output from wind energy is optimized in terms of the revenues that can be generated by the system. In the represented system there may be a number of Ocean Batteries connected to one wind turbine and there are also several wind turbines present in the studied system.

The focus of research can be further decomposed. The decomposition is depicted in Figure 5. In this figure, all consecutive operations from the generation of electricity to the optional storage of electricity to draining the storage again are included. The upper blocks represent the decomposition of the 'convert wind energy' block from Figure 4 and the lower blocks

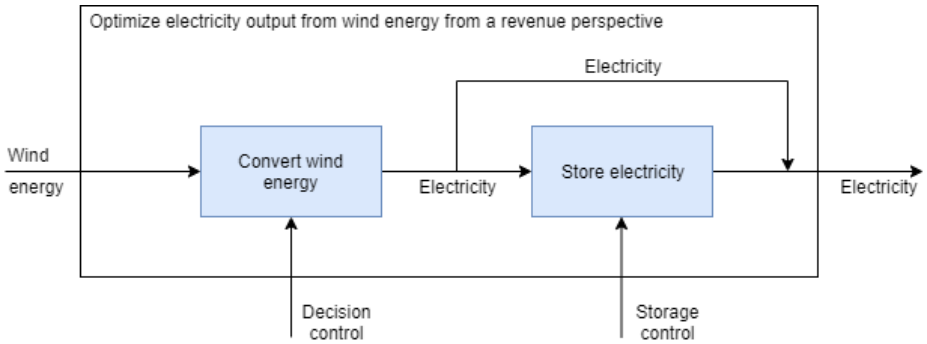

Figure 4: Optimize electricity output from wind energy from a revenue perspective.

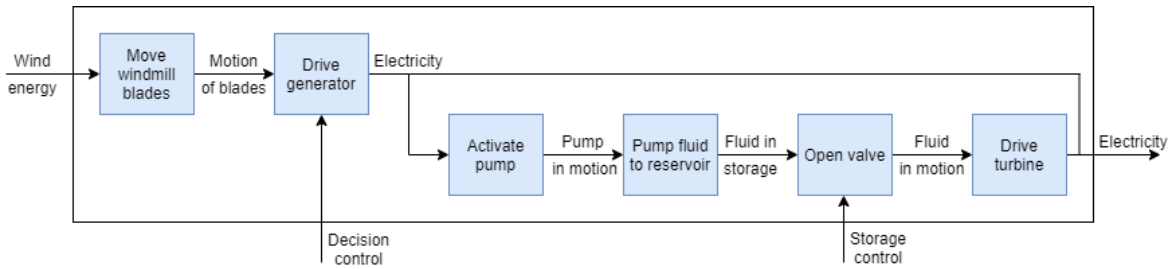

Figure 5: Optimize electricity output from wind energy from a revenue perspective (decomposition).

represent the decomposition of the 'store electricity' block from Figure 4. The system gives more insight in the operations to study during the project.

1.5 Stakeholder analysis

From the problem analysis and system description there may be several parties identified that have a stake in the project. There are several types of stakeholders that can be identified for this research. The most important stakeholder is the problem owner, who is the initiator of the project and usually has an idea about a possible solution. He is also the one most interested in the solution to the problem. Then there are stakeholders who have an interest in the research or are in another way affected by the research. Different stakeholders may have different requirements of the research and an analysis of the stakeholders is therefore relevant to ensure all requirements are incorporated (Wieringa, 2014). All of the aforementioned types of stakeholders are taken into account for this research and the relevant stakeholders are mentioned in this section.

Problem owner

The problem owner is the CTO of Ocean Grazer BV: Marijn van Rooij. Along with the company itself, Marijn will benefit from a distributed control model that is able to optimize revenue of the system. He will therefore not only have an interest in the outcome of the research, but also a high influence in the development of the model. Once this model is developed, Marijn may have more knowlegde on the best design of the Ocean Grazer and he

may be one step closer to launching the Ocean Grazer to the market. It may also be considered valuable information once it appears the revenues may not be sufficient to outperform a system without storage.

Other stakeholders

The other stakeholders are divided into stakeholders that have an influence or interest in the research and stakeholders that are affected by the research.

Stakeholders that have an influence or interest in the research

The Ocean Grazer research group, with in particular the supervisors of this research, prof. dr. ir. B.Jayawardhana and prof. dr. A.Vakis, have an influence in this project. Their influence mainly focuses on ensuring the research has sufficient academic level and makes a contribution to science, rather than only developing the model for one or a few specific situations. The research group also has an interest in the outcome of the research as the outcome contributes to the knowledge base of the Ocean Grazer project and may lead to insights about the direction to choose for the project.

The government becomes a stakeholder once the product is launched as regulations concerning the placement and operation of the Ocean Batteries will then play a role. However, since the project is still in the early stage of innovation, the government does not have an influence for this research and is therefore not taken into account.

Stakeholders that are influenced by the research

The company behind the Ocean Batteries, Ocean Grazer BV, is influenced by the outcome of the research, as the tool that is developed may provide insights in the optimal design for the Ocean Battery and the tool itself may be used for the distributed system of Ocean Batteries in the future.

Wind farm owners may also be influenced by the research as they are a possible target customer of Ocean Grazer BV. This influence will exist once the Ocean Battery is further developed. When this happens, other project partners should be attracted and become a stakeholder as a result. However, for this research this is not the case, which means that wind farm owners and other project partners are not incorporated in this research.

1.6 Research goal

In this section the goal of this research is derived from the problem analysis. It is also explained how the research contributes to both the business aspects and the technological aspects of an IEM master thesis. Thereafter, the proposed distributed control model is introduced and a conceptual model representing all variables to be taken into account for this research has been derived.

Goal statement

The problem that my research is concerned with is that there is no control model yet to be implemented for a distributed system of Ocean Batteries. The distributed Ocean Batteries can only be in operation after an appropriate control model has been developed and adopted. For the purpose of this research, the control model should outperform the situation in which there is no storage at all in terms of revenues. The goal statement is therefore as follows:

The goal is to develop a control model that ensures higher revenues of the distributed system of Ocean Batteries compared to a system without storage.

By feeding the required inputs to the model, the revenue can be calculated. The control model is the final deliverable of this research project as it can be considered a useful tool to calculate the revenue of the system when different inputs are fed to the model. The control model has been developed within the time-span of the IEM research project, which is five months. A suitable control strategy is selected and adopted to optimally control the system of Ocean Batteries.

Business aspect & technological aspects

The business aspect that this research is concerned with is to develop a control model that may be adopted to launch a particular product to the market, namely the Ocean Battery. The aim is, however, to make this model adaptable to different designs of a system, different designs of the storage, different power take-off sources and different locations of the wind farm. The final control model may therefore become an interesting tool in the business of launching deep-sea storage systems. The technological aspects are mainly concerned with the description of the physics of the Ocean Batteries and how formulas can be derived to make the required calculations to maximize the revenue of the system. The control model, that is be developed in Python code, is the tool to realize this and makes a contribution to science by providing insight in the behavior of individual storage units in a distributed control system.

The control model

In this section the initial scoping of the control model to be developed is described. There exists a requirement for the model to be adaptable to the aforementioned inputs. In order to achieve this, first the Ocean Batteries are modelled in Python to describe their dynamics. Thereafter, the cost function for the optimization is determined and the optimization algorithm is developed. As there are many parameters to be determined or even varied during this research, the largest requirement for the control model is that is should be adaptable to various inputs and parameters.

As all Ocean Batteries within the distributed system are equal with respect to the dimensions and location variables. It should therefore be reasoned why the system cannot simply be approached as a lumped model. A lumped model in this case means that all storage and turbine capacities of the Ocean Batteries in the system are summed. If it would be possible to approach the grid as a lumped system, the control model would be simplified significantly compared to when each of the Ocean Batteries is modelled individually. There are several arguments providing reasoning why a lumped model is not suitable for the comparison to reality:

- The storage level of the various storage units may differ. In the lumped model case, an external stimulus would require the system to deliver a particular amount of energy over a given time period based on the available total electricity and the summed turbine capacities. Problems may arise regarding the fact that one storage unit may empty sooner than another especially in a situation where a storage is filled to its maximum before being drained and vice versa. The system cannot deliver the expected amount of electricity over the given time period anymore, as the turbine capacity of the remaining storage units may not suffice the demanded amount of electricity.
- Some storage systems may have downtime at some point due to maintenance or failure. This storage unit can then be taken out of operation without affecting the other storage units. It is difficult to model the downtime of storage units into a lumped model. For example, if a certain percentage would be selected to represent the average downtime of the whole system, the model cannot work in reality as it is important to know when the individual storage units are out of operation. Maintenance operations and downtime are, however, out of scope for this research.
- The energy input may differ among various places in the wind farm. Storage units are in this case able to store electricity independent of the other storage units and the storage levels will differ as a result. This factor is dependent on the cable infrastructure describing the connections between the storage units and wind turbines in the system.

Summarizing the above arguments it is concluded that it is necessary to develop a control model on the level of individual Ocean Batteries.

Conceptual model

Before a control model can be developed, it is investigated which factors have to be accounted for in the distributed control model. From the analyses above, a conceptual model has been constructed to visualize all these factors. The conceptual model is depicted in Figure 6. In this figure, the boxes that are blue represent the parameters and inputs that have to appear in the distributed control model.

Explanation of variables

All variables mentioned in the conceptual model and its requirements are explained in this section. A distinction is made between variables that are dependent on the location of the grid, variables that are kept constant in this research and variables that should be researched in-depth.

Variables that depend on the location of the grid

- **Predicted wind power production**: the control model is able to read and incorporate power production as an input. For this research, a data set is used of the power generated by a wind farm based on historical wind data. The model is designed such that also other power production information may serve as an input.
- **Forecasted market prices**: the control model is able to read and incorporate forecasted market prices. The market prices differ for each electricity market. For this research, historical data sets with market prices are used.

- **Number of wind turbines in the system**: the control model is able to incorporate different system designs, which means that the model is generic and applicable to multiple locations for the Ocean Batteries.

Variables that are constant in this research

- **Volumetric capacity**: the storage capacity can be varied by changing the depth of the Ocean Batteries or by changing the dimensions of the Ocean Batteries. The dimensions of the Ocean Batteries are considered constant in this research, which means that the volumetric capacity of the Ocean Batteries does not change.

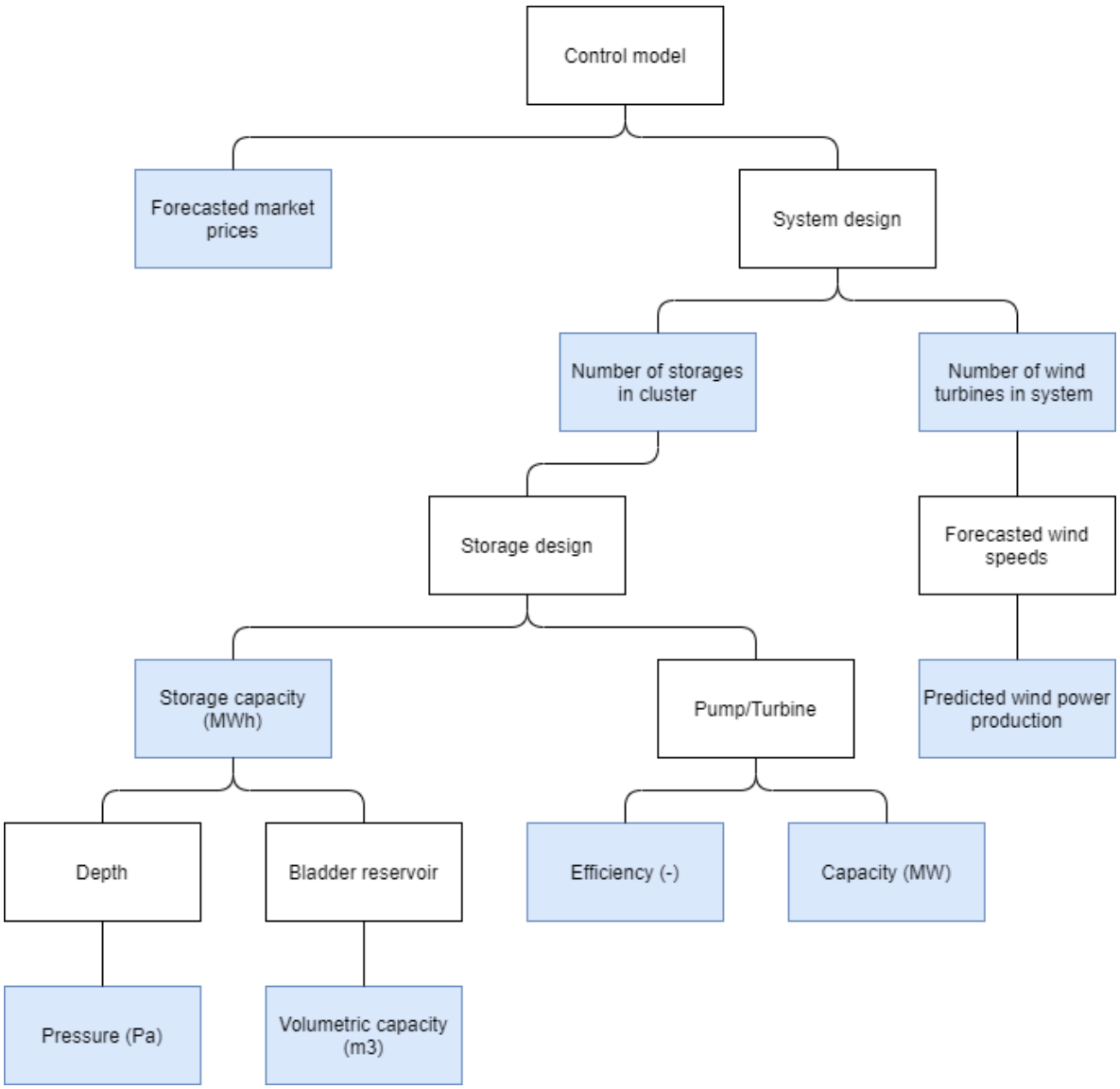

Figure 6: The conceptual model.

Variables that are researched in-depth

- **Pump/Turbine capacity**: for the major part of this research, the turbine capacity is assigned a constant value. To observe the effects of changing the turbine capacity, a sensitivity analysis is executed.
- **Pump/Turbine efficiency**: a literature study is conducted to find realistic values for the pump and turbine efficiencies. The effect of changing the efficiency of the pump and turbine is studied intensively as changing the efficiency may have a major effect on the decision to store energy based on the electricity prices. A pump and turbine have a start-up time, which means that it takes some time to reach its maximum efficiency. However, it is assumed that the effects of the start-up time are minor effects and the start-up time is therefore disregarded for this research.
- **Ocean pressure**: the storage capacity may also be varied by changing the depth of the Ocean Batteries. Similar to the pump and turbine capacity, the storage capacity is assigned a constant value for the major part of this research. The effects of changing the depth of the Ocean Batteries are studied in a sensitivity analysis.
- **Number of storage units in a cluster**: in this research, each Ocean Battery represents a cluster of a number of Ocean Batteries, all kept at the same storage level. This can be seen as a lumped model of N Ocean Batteries with N times the capacity of one Ocean Battery. The number of storage units in a cluster determines the total amount of energy that can be stored. The size of the cluster is researched to determine the suitable number of Ocean Batteries per wind turbine.

1.7 Research design

Now that all considerations with respect to the distributed control model have been explained, the design of the research is thoroughly described. First the research questions are formulated, then the process steps and the resources required to execute these steps are listed. Finally, a risk analysis is executed and the structure of the report from this chapter on is explained.

As the research is mainly concerned with designing a generic control model, the engineering cycle as defined by Wieringa is a useful tool to adopt, since the engineering cycle may be used for situations where a solution is needed for a particular problem and its solution is non-trivial (Wieringa, 2014). The engineering cycle therefore serves as a basis throughout this research. The engineering cycle is depicted in Figure 7. The problem investigation phase is treated in the first chapter of this research. In addition, the requirements for the control model have also been investigated and specified in the first chapter for the treatment design phase. The second stage of the treatment design phase is to propose and develop a control model. For the treatment validation phase it is evaluated whether the developed control model is generating the desired output and the sensitivity of the model is tested. Simulations are performed to validate the control model. The second stage of the treatment design phase and the treatment validation phase are executed in the remaining chapters of this research. The treatment implementation phase is disregarded from the research as it is impossible to implement the distributed control model in a real-life situation.

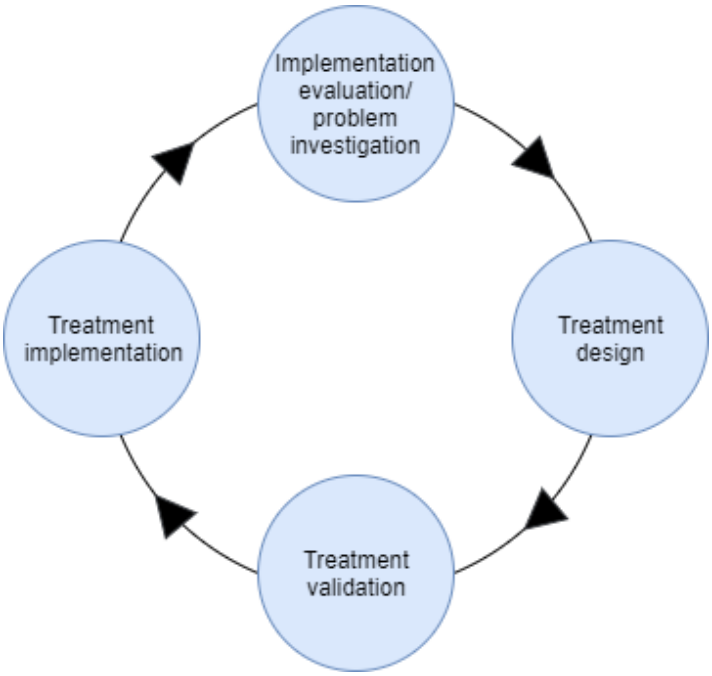

Figure 7: The engineering cyle by Wieringa (Wieringa, 2014). The implementation phase is not incorporated for this research.

1.7.1 Research questions

The main research question that serves as a basis throughout this research to achieve the goal is formulated as follows.

How should the distributed system of Ocean Batteries be controlled?

The research question is answered at the end of the report after the research is executed by answering a number of sub-questions that eventually lead to the answer to the main research question. The sub-questions are formulated as follows:

1. What are the relevant considerations for the design of the distributed system of Ocean Batteries and how may they be incorporated in this research?
2. Which external input is required for the control model?
3. How can the dynamical model of the Ocean Battery be developed?
4. What would be an suitable control strategy and how can this control strategy be applied to the dynamical model?
5. How can the proposed control model be validated?
6. What are the revenues obtained by the control model in comparison with a no storage system for a predefined case study?
7. How are the storage capacity and turbine capacity related to the generated revenue?
8. What are the effects of introducing the possibility to store energy that is bought from the market?

1.7.2 Operationalization

Based on the aforementioned sub-questions, the steps to answer these sub-questions are listed in this section. These steps will ultimately lead to answering the main research question.

1. The first sub-question is answered by studying the system of connected Ocean Batteries in the wind farm on a conceptual level, whereby relevant considerations are identified.

2. The second sub-question is answered by defining the external input required for the model along with a strategy on how to retrieve data to run the simulations with. A logical follow-up action to this sub-question is to retrieve the input data.

3. The third sub-question is answered by describing the dynamics of the Ocean Battery on a conceptual level, followed by the appropriate equations describing the dynamics and a short simulation to validate the dynamical model. In this step, the model is developed in Python

4. The fourth sub-question is answered as follows. First, possible control strategies are investigated and the most suitable option for this research is selected. Second, the selected control strategy is used to formulate an optimization problem and corresponding control algorithm. Third, the control strategy is added to the Python model to construct the final control model.

5. The fifth sub-question is answered by studying validation techniques and applying these techniques on the proposed distributed control model. Once the control model is validated, simulations can be executed with a satisfactory level of confidence.

6. The sixth sub-question is answered by executing simulations and calculating the revenues that can be obtained for different situations. These results are analyzed afterwards.

7. The seventh sub-question is answered by executing sensitivity analyses on the storage capacity, influenced by the depth of the Ocean Batteries, and the pump and turbine capacity. The results of the sensitivity analyses are analyzed to advice Ocean Grazer BV on the optimum design choices for the pump and turbine capacity.

8. The eighth and last sub-question is answered by adding a connection to the electricity market that can be used to buy electricity for storing purposes and studying its effects.

Resources

Several resources are required to be able to answer the sub-questions and ultimately the main research question. These resources include previous work on the Ocean Grazer, available literature and data that should serve as an input for the model. The following data is required to run the model:

- Data about the electricity generation of the single turbines in a particular wind farm. To achieve this, a data set needs to be generated.

- Data about the price market. Important considerations include the location of the wind farm to determine which country the price market should be taken from, and the time slots at which the data was recorded.

It is likely that the data is stored in an Excel file, which means that the control model should be developed in a program that is able to process Excel files. Python is a suitable choice.

Risk analysis

There may be several factors that need to be accounted for in order to analyze the risks that are associated to this research.

- Assumptions have to be made in order to scope the research. For example, the efficiency of the pump and turbine may largely depend on the selected pump or turbine and its capacity. Equivalently, the start-up time may also play a role in the behavior of Ocean Battery. It needs to be noted that this may change the results significantly.
- The data on the performance of individual wind turbines is not readily available. As a data set has to be generated to overcome this issue, the data may deviate from a real-life situation and may not be as reliable as a real data set. The outcomes may change once the data set does not represent reality to a sufficient extent.

Structure of the report

The remainder of this thesis is organized as follows. Chapter 2 gives a description of the distributed system of Ocean Batteries and the application in a wind farm. In addition, the required inputs are studied and the method to retrieve input data is explained, thereby treating sub-questions 1 and 2 in this chapter. Chapter 3 is concerned with the description of the dynamics of the Ocean Battery and the development of the dynamical model in Python, ultimately answering sub-question 3. In Chapter 4, different control strategies are analyzed and the selected control strategy is applied on the dynamical model to develop the final distributed control model, answering sub-question 4. Chapter 5 is dedicated to the validation of the proposed control model, thereby answering sub-question 5. Consequently, sub-questions 6-8 are answered in Chapter 6 that is composed of the simulation set-up, its results, the sensitivity analyses and the extension to the model. Finally, the research is concluded with a discussion and conclusion in Chapters 7 and 8.

2 The system of connected Ocean Batteries

In this section, the system that is studied, including all of its relevant elements, is further explained by a research through literature. This includes the system design considerations, the wind turbines and the wind turbine power production that is required as an input for the model. This chapter is finalized with an explanation on the electricity markets and how the corresponding historical data that serves as an input to the model, may be retrieved.

2.1 Ocean Battery: the concept

Zooming in to the concept of the Ocean Battery, it is observed that its working principle largely resembles the working principle of a Pumped Hydro Energy Storage (PHES). For both concepts, potential energy is stored by elevating water. During the charging process, electricity is converted into mechanical energy to drive the pump that pumps water from a lower reservoir to a higher reservoir, thereby converting the mechanical energy into gravitational potential energy. When discharging, the process is reversed and the potential energy is converted into electricity again by driving a turbine. Globally there are many PHES systems installed (Barbour et al., 2016). Therefore, PHES is nowadays considered a technology that is well-established and commercially acceptable. It is not only a sustainable energy system, but it has also proven a suitable application to improve the grid stability when this grid contains other renewable energy sources such as wind power (Rehman et al., 2015). Like the Ocean Battery, PHES are also lossless storage units, implying that there is no self-discharge over time (Barbour et al., 2016). An interesting development in the area of PHES systems is the introduction of variable speed pump/turbines. The advantage of this technology is that the rotation speed of the pump/turbine can be adjusted, which allows turbines to operate closer to their optimum efficiency (Deane et al., 2010). This may also become an interesting technology for future application in the Ocean Battery.

An important difference between the previous design of the Ocean Battery and the possibilities for the new design is that in previous work about the Ocean Grazer, the pump and the turbine were two separate devices as the pump was driven mechanically by waves (Dijkstra et al., 2016). Now that the pump is driven by the electricity from wind turbines, the possibility arises to implement one device that is both able to pump and operate as a turbine, also known as the Pump as Turbine (PaT), that has proven its applicability already in the aforementioned PHES systems (Rehman et al., 2015). PaT's are able to operate over a large range normally covered by several types of turbines. One of the major advantages of a PaT is the reduction of initial equipment cost, and thereby resulting in a shorter return on investment compared to a separate pump and turbine (Nautiyal et al., 2010). Although the equipment costs of the PaTs are lower, it must also be mentioned that the overall efficiency of PaTs is also lower than the efficiencies of the separate devices (Morabito and Hendrick, 2019). These efficiencies are still in the range of 70-80% and therefore acceptable for this research (Rehman et al., 2015).

2.2 Design of the system

In the previous chapter, the system that is studied in this research is briefly described. It consists of the wind turbines, the Ocean Batteries, the cable infrastructure between them and the control that receives information about the generated power and the price market.

This control should eventually be able to maximize the revenues of the system. In the future, this system may become part of a smart grid, which is an innovation that is said to be the next generation electricity grid. The smart grid has emerged from the accelerated need to modernize the existing distribution network. The modernization of the distribution network should be achieved by the introduction of technologies that assist with demand-side management and revenue protection (Farhangi, 2009). The smart grid is part of the road towards sustainability and the system in this study can therefore contribute to a sustainable future. The research is centered around the energy flows in the system, which is explained in the next section.

Energy flows in the system

Conceptually, it has been studied which energy flows occur within the system. As a result, four different flows or energy are identified:

- From the generator to the storage *(E_{gs})*
- From the generator to the market *(E_{gm})*
- From the storage to the market *(E_{sm})*
- From the market to the storage *(E_{ms})*

The market can be seen as the customer in this system. The energy flow from the market to the storage is initially not included in the control model. Rather it is used as an extension to the model to observe the effect of including this connection. The flows of energy are represented by Figure 8. It should be noted that the studied grid consists of multiple storage systems and wind turbines, but that the market is treated as a single entity.

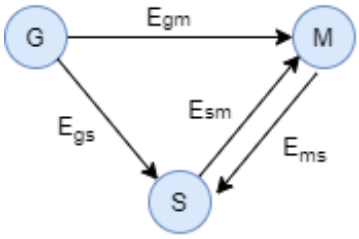

Figure 8: Depiction of the possible energy flows in the system.

The model that is developed focuses on optimizing the energy flows from a revenue perspective. When the energy is stored before it is sold to the customer, the energy is subject to efficiency losses. For the level of detail that this thesis is focused on, it would be desirable to express the efficiency of the Ocean Battery as a single number. The impact of the efficiency losses is investigated in the next chapter.

There are several design considerations associated with the studied system. These design considerations are listed below.

- **Location**: first, the location of the grid is of importance, as it influences the available wind and the electricity prices corresponding to the chosen location.

- **Number of wind turbines**: the number of wind turbines determines the maximum output of the system in terms of power. The more wind turbines in the grid, the higher the system output, but also the more Ocean Batteries may be incorporated.
- **The type of wind turbines**: by this the capacity of the wind turbine would suffice. This factor would make a difference for the amount of Ocean Batteries connected to the wind turbine.
- **Number of storage systems in a cluster**: based on the type of turbine and the desired storage capacity, the number of storage systems in a cluster that is connected to a single wind turbine, can be selected.
- **Definition of interconnections**: it should be defined which storage systems are connected to one another and which storage systems are connected to a wind turbine. The control model is developed such that the adjacency matrix of the system, displaying the interconnections between storage units, wind turbines and the market, serves as an input to the model.
- **The cable capacities**: the cable capacities play an important role in the amount of electricity that can be sold to the electricity grid. For this research, cable capacities have been excluded.

These considerations answer sub-question 2: *What are the relevant considerations for the design of the distributed system of Ocean Batteries and how may they be incorporated in this research?*

2.3 Wind energy

The considered power source in this research is wind energy. The power from wind turbines serves as an input to the model. Wind energy is converted to electricity by a wind turbine of which the rotor is connected to an electric generator (Hansen, 2015). When looking for a suitable location of a wind farm, it appears from Figure 9 that the Northern European seas have great potential for harvesting wind energy. In addition, these seas also have a seabed with relatively low water depths, which makes them suitable for wind turbines. Due to these characteristics, the Northern European countries are the frontrunners of the offshore wind industry nowadays (Rodrigues et al., 2015). A location in the Northern European seas should therefore be selected as the location for this research.

Input wind power production

From the conceptual model in Chapter 1 it was determined that predicted wind power production is an input to the model, and from the resources it was mentioned that a historical data set with power production is not readily available to run the model with and should be generated. In order to generate the wind power data set, calculations should be made using available wind data from the selected location.

Wind turbines convert wind energy into electrical energy as follows: wind energy contains kinetic energy, which is first converted into rotational kinetic energy by the movement of the blades that make up the turbine, and then into electrical energy by the generator. The

amount of energy that can be converted is dependent on the wind speed and the swept area of the turbine. A wind turbine consists of several components that enable the conversion from wind energy into supplied electrical energy to the grid (Sarkar and Behera, 2012).

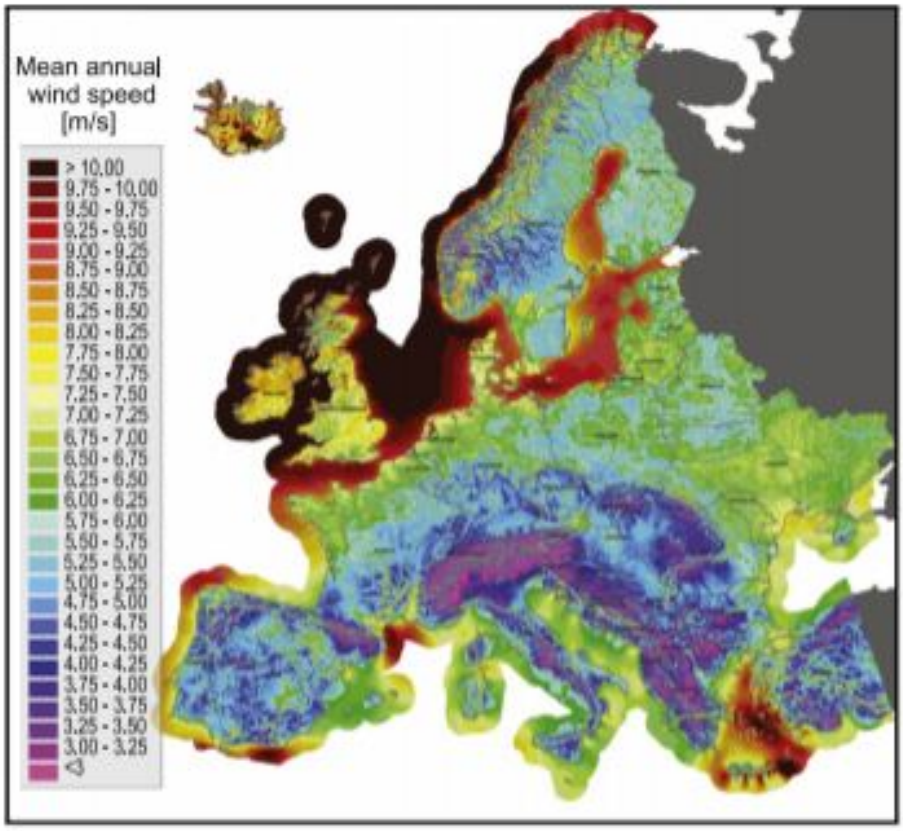

Figure 9: Annual European onshore and offshore mean wind speeds at an 80 meter height (Rodrigues et al., 2015).

On average, a wind turbine situated at a beneficial wind energy site operates at about 35% of its total possible capacity. The amount of electricity that can be produced by a wind turbine is dependent on the following factors (Sarkar and Behera, 2012; Lakshmi and Vasantharathna, 2014; Siahkali and Vakilian, 2010).

1. **Wind speed**: wind speed and the power that may be generated by a wind turbine are related through a power curve that depends on the type of turbine and its location. Wind turbines start producing power at a cut-in speed, which is usually at a wind speed of approximately 4 m/s. In addition, wind turbines stop producing power at the cut-out speed due to safety measures, usually around 25 m/s. The maximum power output is reached from the rated wind speed to the cut-out speed. When the wind speed is between the cut-in speed and the rated speed, there exists a nonlinear relationship between the generated power and the wind speed. The amount of power generated can be described by the wind-power curve, which is a function of the wind speed to the third power. This means that for example if the wind blows twice as hard, the power

will increase with a factor eight. The variability in the available wind energy results in the effect that the turbine operates at power levels that continually change.

2. **Availability wind turbines**: the availability of the wind turbines is dependent on its down-time. When the machine is undergoing maintenance for example, the wind turbine is not available. The availability of wind turbines is disregarded for this research.

3. **Arrangement of wind turbines**: the way the wind turbines are situated in the grid matters for the amount of power produced by a wind farm. When a wind turbine is placed inefficiently, the wind is taken by other wind turbines and its production will be significantly lower. This effect is identified as the wake-effect (Adaramola and Krogstad, 2011) and is elaborated on below.

A wind farm location and configuration should be selected in order to produce a wind data set. An imaginary wind farm, which is based on the Horns Rev wind farm located near Denmark (Rudion et al., 2008), is selected to generate a wind data set. The configuration of the Horns Rev wind farm including its cable infrastructure is depicted in Figure 10. The imaginary wind farm will be referred to as OG-WindFarm from now on.

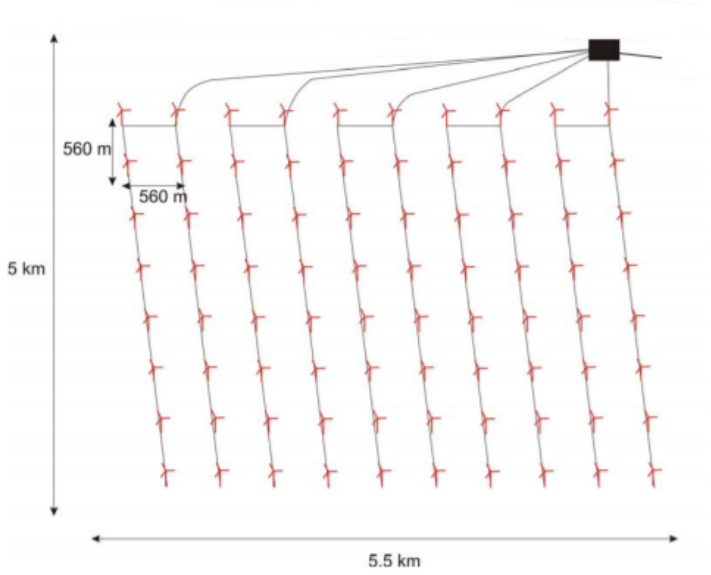

Figure 10: Configuration of the Hons Rev wind farm, which is located near Denmark (Rudion et al., 2008)

The aim of this section is that a wind power production data set can be generated that serves as an input to the control model. Eventually, the power output of the individual wind turbines should be calculated from this study. The formula describing the calculation of the power output of a single wind turbine is given by

$$P = 0.5 \cdot A \cdot \rho \cdot \eta \cdot v^3, \tag{1}$$

where
P is the power output in [W],
A is the swept area in $[m^2]$,
ρ is the density of air in $[kg/m^3]$,
η is the efficiency of the wind turbine [-],
v is the wind speed in $[m/s]$ (Chen, 2008).

The efficiency of the wind turbine is composed of the power coefficient (the rotor efficiency), the gearbox efficiency and the generator efficiency. First, the *power coefficient*, in equations usually denoted by C_p, can achieve values of around 45% nowadays (Hansen, 2015). The maximum theoretically achievable power coefficient is described by the Betz limit, which states that no wind turbine can ever achieve an efficiency of more than 59.26% from an ideal wind stream due to braking of the wind. The achievable values of the power coefficient in practice are lower because of inefficiencies and losses related to configurations, frictions and turbine designs (Ragheb and Ragheb, 2011). Second, the *gearbox efficiency* and the *generator efficiency* have values close to 0.7 and 0.9 (Sarkar and Behera, 2012; Grauers, 1996). The total efficiency of the wind turbine can therefore be calculated as

$$\eta = C_p \cdot \eta_g \cdot \eta_g. \tag{2}$$

A wind turbine is rated at a certain power, implying that the wind turbine cannot produce more than that power even if the power from the wind is high enough to generate more power. The rated power is dependent on the capacity of the turbine. Equation 1 therefore only holds for situations in which the wind speed is lower than the rated wind speed. In fact, a constraint for the power output may be formulated taking into account the aforementioned cut-in and cut-out speed as

$$P(t) = \begin{cases} 0, & v(t) < v_i \text{ or } v(t) > v_o \\ \phi(v(t)), & v_i \leq v(t) < v_r \\ P_max, & v_r \leq v(t) \leq v_o, \end{cases} \tag{3}$$

where
$P(t)$ is the power output at time t in $[W]$,
$v(t)$ is the wind speed at time t in $[m/s]$,
v_i is the cut-in wind speed in $[m/s]$,
v_r is the rated wind speed in $[m/s]$,
v_o is the cut-out wind speed in $[m/s]$.

An example of a power curve for a specific wind turbine is depicted in Figure 11. From this figure, the cut-in speed and the rated speed may be derived. To obtain the total power of the wind farm, all the output powers of the individual wind turbines may be summed as

$$P(t) = \sum_{i=1}^{N} P(i,t), \tag{4}$$

bounded by

$$0 \leq P(i,t) \leq P_r(i), \tag{5}$$

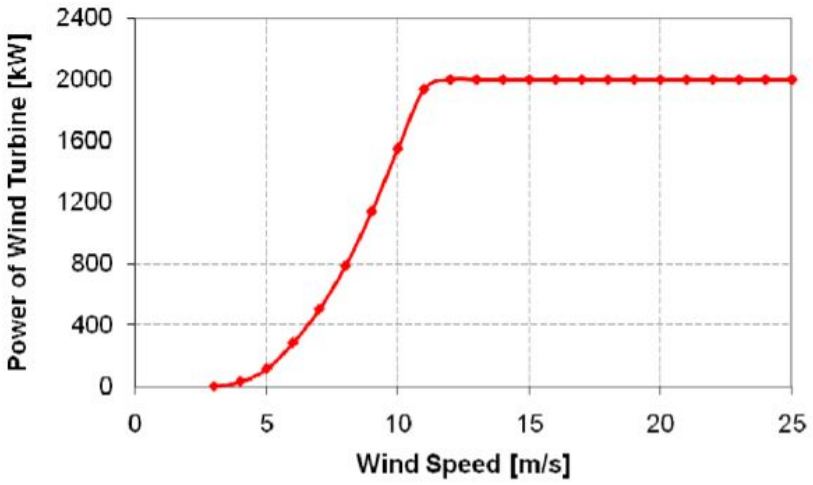

Figure 11: A power curve for a 2 MW wind turbine as a function of the wind speed (Moskalenko et al., 2010).

where
$P(t)$ is the power output of the wind farm at time t in $[MW]$,
$P(i,t)$ is the power output of wind turbine i at time t in $[MW]$,
$P_r(i)$ is the rated power of turbine i in $[MW]$.

As Equation 4 already suggests, the power output of a wind farm with a number of wind turbines with equal rated power is not simply the power output of a single wind turbine multiplied by the number of turbines. The power output of a single turbine is dependent on its location in the grid due to the aforementioned wake-effect.

The wake-effect

The wake-effect entails that the performance of a wind turbine is affected by the wakes of other wind turbines in a wind farm. As a result of this interaction, the total energy output and efficiency of the wind farm are reduced (Gebraad et al., 2017; Castellani et al., 2015). Power losses due to wake effects may be between 20% and 45% compared to a wind farm containing solely unobstructed turbines. The power loss is dependent on the distance between the wind turbines and the operating conditions (Adaramola and Krogstad, 2011). Much research has been executed on how these negative effects can be reduced or mitigated. Possible solutions include placing the wind turbines at a larger distance from each other, placing the wind turbines in a different configuration (Kusiak and Song, 2010), using coordinated control techniques to mitigate the wake effects such that the energy production can be maximized. An example of a coordinated control technique is that upstream wind turbines may reduce power production to minimize the wake effects on downstream turbines (Gebraad et al., 2017). In addition, yaw control may be implemented to change the direction and the velocity of the wake forming that occurs behind a turbine in a wind farm (Gebraad et al., 2016). The wake effect differs with wind direction and the efficiency of the wind farm always differs dependent on the wind velocity and wind direction.

Several papers focused on studying the wake effects on the power output for the aforementioned the Horns Rev wind farm (Moskalenko et al., 2010; Porté-Agel et al., 2013; Rudion et al., 2008; Barthelmie et al., 2010; Wu and Porté-Agel, 2015). For their research, it was attempted to study the wake effects on the various rows or distances of the wind farm and translate this to a normalized power for several wind directions and wind velocities. Resulting normalized power outputs are depicted in Figure 12 and Figure 13. An interesting phenomenon is that power losses due to the wake-effect are significantly higher for the wind turbine in the second row compared to the other rows (Adaramola and Krogstad, 2011).

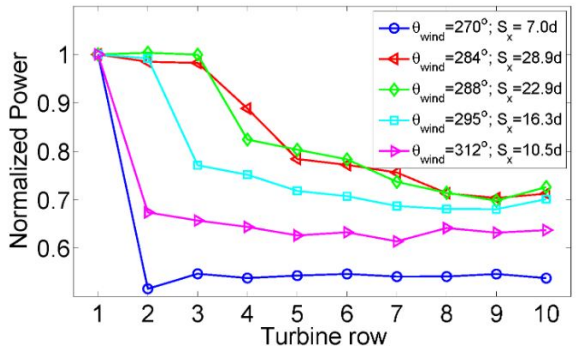

Figure 12: Normalized power output as a function of turbine row for a wind direction with minimal deviation (Porté-Agel et al., 2013).

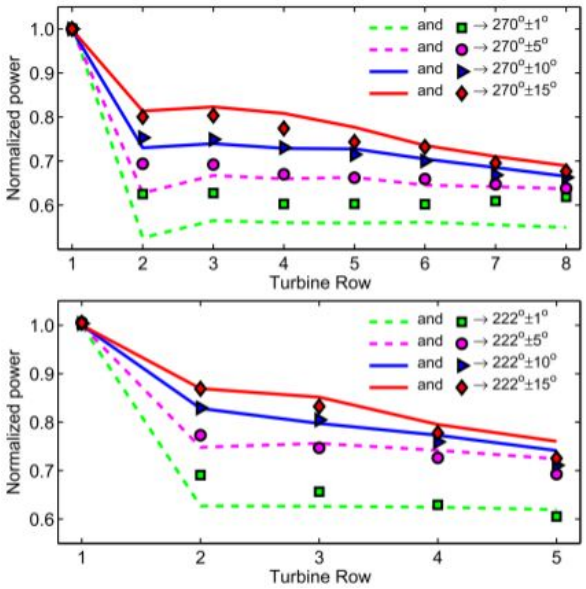

Figure 13: Normalized power output as a function of turbine row for two wind directions with minimal deviations (Wu and Porté-Agel, 2015).

From the results of these papers, the imaginary OG-WindFarm is created with average efficiencies, or wake losses, for the individual wind turbines in the wake farm. The OG-WindFarm consists of 64 wind turbines, in a grid of 8 by 8, with the same configuration angle as the

Horns Rev wind farm (7 °). Figure 14 depicts the configuration of the OG-WindFarm with different wind directions and the effects on the various rows of the wind farm. The left grid (a) in Figure 14 corresponds to the upper normalized power graph in Figure 13 and the right grid (b) in Figure 14 corresponds to the bottom normalized power graph in Figure 14. From the normalized power output in the figures an estimation has been made for the different rows in the OG-WindFarm. The results are listed in Table1 and Table 2. Table 1 represents the case when the wind blows from a straight direction as in Figure 14(a) and Table 2 represents the case then the wind blows from a slantwise direction as in Figure 14(b). The number of turbines in a specific row is also mentioned as this differs for the wind directions.

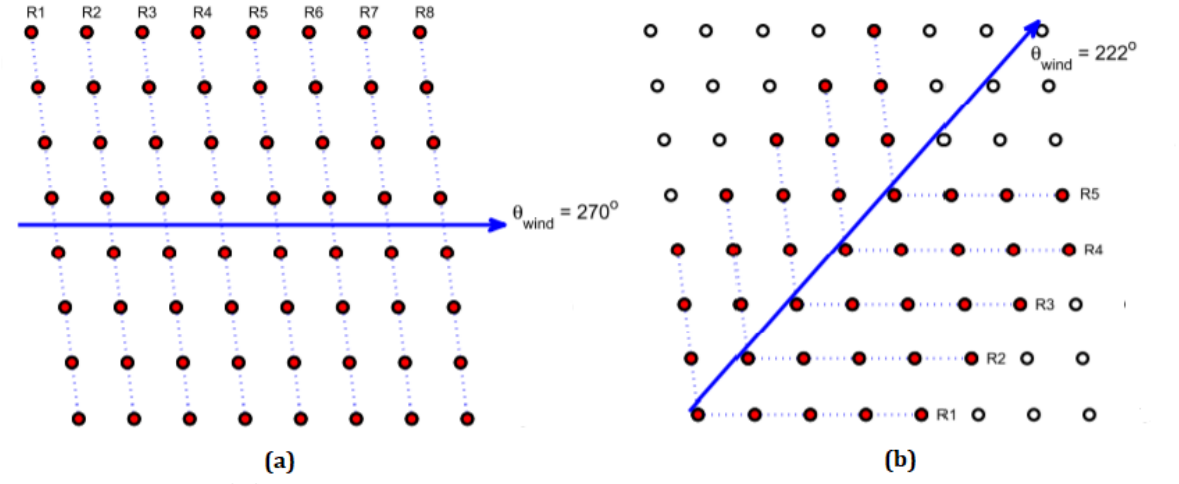

Figure 14: A depiction of the configuration of the OG-WindFarm with different wind direction and how they affect the rows in the farm in (a) and (b).

Turbine row	1	2	3	4	5	6	7	8
# of turbines	8	8	8	8	8	8	8	8
Efficiency	100%	72%	72%	72%	70%	70%	68%	68%

Table 1: Efficiencies of the rows of turbines when the wind is blowing straight.

Turbine row	1	2	3	4	5	6	7	8
# of turbines	15	13	11	9	7	5	3	1
Efficiency	100%	83%	81%	77%	74%	74%	72%	70%

Table 2: Efficiencies of the rows of turbines when the wind is blowing slantwise.

Turbines are denoted by T_N. Each wind turbine, from $T_1 ... T_{64}$ is subject to efficiency losses, dependent on the row that the wind turbine is located in. However, as the wind blows from various directions, the row in which the wind turbine is located differs over time. It is attempted to approach these variations as close as possible, but in an efficient way. When

taking only the straight and slantwise wind directions into account, one is left with eight wind directions that are depicted in Figure 15(a). Taking into account eight different efficiencies corresponding to wind directions for each wind turbine results large computational efforts. It has therefore been decided to only take into account the four main wind directions of which the boundaries correspond to the excluded wind directions, depicted by the dashed lines in Figure 15(b).

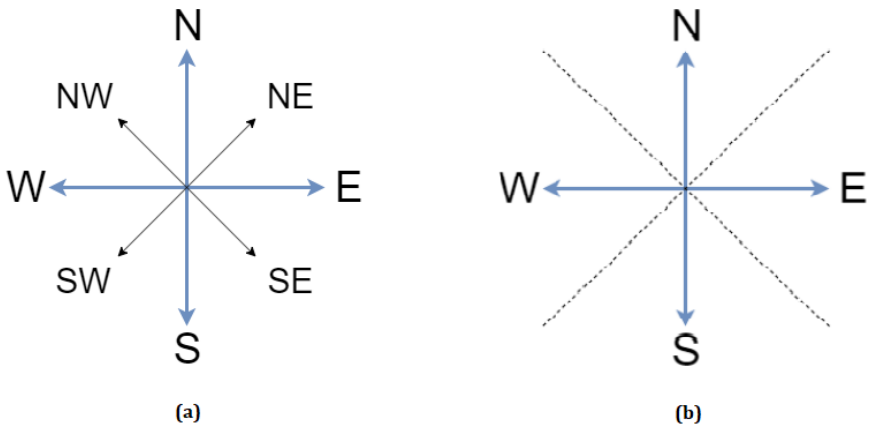

Figure 15: Converting eight wind directions (a) to four wind directions (b) in order to generate a wind power data set.

Taking four different wind directions means that the efficiencies in Table 1 and 2 should be combined. In order to do so, the combined efficiencies corrected for the number of turbines in a row are taken to assign an efficiency per turbine row. The results are given in Table 3.

Turbine row	1	2	3	4	5	6	7	8
Efficiency	100%	79%	77%	75%	72%	72%	69%	68%

Table 3: Combined efficiencies for the turbine rows.

Data set generation

In order to make the calculations, a specific wind turbine should be selected. Data was retrieved for the MHI Vestas Offshore V164-8.0 MW (turbine models.com, 2016). The power curve of the MHI Vestas Offshore V164-8.0 MW is depicted in Figure 16.

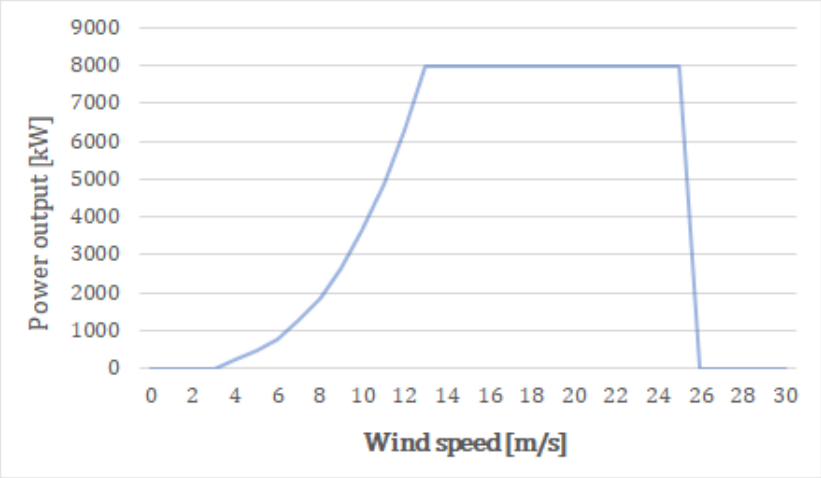

Figure 16: The power curve for the MHI Vestas Offshore V164-8.0 MW turbine.

The relevant parameters of the MWI Vestas Offshore V164-8.0 MW and the other parameters required for calculating the power as in Equation 1 are listed in Table 4. The efficiency of the turbine was calculated from Equation 1 by using the rated power, P_r, at the rated wind speed, v_r.

Parameter	**Value**	**Description [units]**
P_r	8	Rated power of the wind turbine $[MW]$
v_r	4.0	Rated wind speed $[m/s]$
v_o	25.0	Cut-out wind speed $[m/s]$
v_i	13.0	Cut-in wind speed $[m/s]$
A	21164	Swept area $[m^2]$
η	0.2809	Efficiency of the wind turbine [-]
ρ	1.225	Density of air $[kg/m^3]$

Table 4: Model parameters for generation of a wind turbine power production data set.

To calculate the power of a wind turbine in the aforementioned grid, a location should be selected that wind data can be retrieved from. A location in the North Sea is chosen and its data is received from the KNMI (KNMI, 2019). For the calculations, the hourly data of 2017, 2018 and 2019 are used. Whenever the wind data was not available, the data of the days before as used to replace these values. The model that was developed to allocate the power to each wind turbine on a given time step is included in Appendix A. A validation of the data used and generated is also provided in this appendix. The data set generated is used as an input to the control model.

Limitations

There are factors that have an influence on the generation of wind power that have been disregarded in this study. Both factors may have a significant effect on the power production of a wind turbine, but are not included in this research for simplicity reasons. These factors are as follows.

- **Maximum ramp-up/down rate**: A wind turbine has a maximum ramp-up/down rate, which means that its power production can only increase or decrease with a maximum rate per time unit. For example, a wind turbine cannot go from not moving at all to operation at rated wind speed within a second. Usually, a wind turbine can be ramped up with not more than 10% of its rated power per minute (Singh and Singh, 2009).

- **Time it takes to face the wind**: When the wind is changing direction, it takes some time for a wind turbine to face the wind again and harvest the maximum amount of wind energy.

2.4 Electricity markets

The second external input for the model is the price of electricity. In this section, all information required to understand the relevant electricity markets and how to obtain the required historic data is explained. Once a data set containing electricity prices per time step is obtained, the revenues from the model can be calculated.

Since the 90s, many countries have opened their electricity markets to manage the electrical power system as opposed to the old system where electricity was regulated through a state monopoly. The EU has even imposed the open electricity markets on its countries in order to work towards a deregulated electricity market, where production and distribution are separated from transport. The purpose of a deregulated electricity market is twofold (Kiener, 2006):

- To encourage competition between players on the market in order to reduce the costs of electricity. This results in the price of electricity being determined by the supply and demand on the market instead of being determined by a single operator.

- To enable the free circulation of electricity between the countries within the EU to strive for a joint power system which has a common market, as sharing energy resources is one way to stabilize the power system.

A current development in this area is that more and more renewable power sources are adopted in the power systems, while the electricity demand also increases. Both factors influence the power systems' operation and planning significantly. Given this factor in combination with the rapid development of communication technology, the Real-Time electricity Markets (RTM) are implemented. Building an efficient and effective transaction platform in order to balance the power system operations can be considered one of the main functions of RTMs (Wang et al., 2015). Balancing the power system operations, or balance management, includes continuous balancing of supply and demand which ultimately leads to a stabilized power system and secured electricity supply. Balance management is a crucial practice as the total production has to equal the total consumption at each point in time to have a stabilized system frequency. When the grid frequency starts to deviate from its reference value, the system runs out of balance and ultimately the system may collapse. The electricity markets should be designed to deal with this property (KULEnergyInstitute, 2015; van der Veen and Hakvoort, 2016).

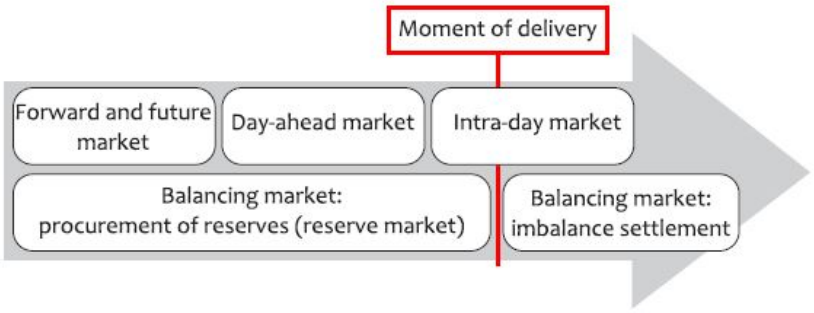

Figure 17: An overview of the different electricity markets and their relation to the actual point of delivery (KULEnergyInstitute, 2015).

Balance management is executed by the Balance Responsible Parties (BRPs) and Balancing Service Providers (BSPs). The physical process that is concerned with the generation and consumption of electricity remains managed by the generators and consumers, respectively. Therefore, the BRP can be described as an administrative entity that is responsible for balancing a portfolio of production and consumption connections, whereas the BSPs are responsible for balancing the imbalances caused by the BRPs and are directly paid for their services by the BRPs (van der Veen et al., 2011; KULEnergyInstitute, 2015). The design of electricity markets is such that it is able to deal with imbalances. There exist different types of electricity markets, of which some start years before the actual delivery, while others end after the actual delivery. An overview of the different electricity markets is given in Figure 17 (KULEnergyInstitute, 2015).

The day-ahead market is the market where is electricity is traded one day before the actual delivery. When trading on the day-ahead market finishes, the market zone has to be in balance. The intra-day market is where the electricity is traded on the day of delivery. It enables market participants to correct for imbalances that occur on the day itself, for example when there is a sudden deviation from the expected electricity production. Finally, the balancing markets take action when there is a real-time imbalance by activating reserves (KULEnergyInstitute, 2015). The current trend of the day-ahead and intra-day market coupling between the countries in Europe enables balancing market integration even further (van der Veen et al., 2011). The EPEX SPOT is the exchange for the power spot markets in Europe and covers a number of countries that are situated in the heart of Europe. In total, these markets represent 50% of the European electricity consumption. A few of these countries that are close to the OG-Windfarm are the UK, The Netherlands and Germany (EPEXSPOT, nd).

Electricity markets that would suit the OG-WindFarm best would display significant fluctuations with peaks, due to the storing potential of the Ocean Grazer and the desired situation where the electricity may be stored when the prices are low and the stored electricity may be sold when the prices are high. In addition, the price market should be close to the chosen location of the OG-WindFarm to limit transportation costs. The Dutch electricity market would be a nearby and suitable choice. The Dutch electricity market can be split into the day-ahead market, the intra-day market and the balancing market, which is the automatic Frequency Restoration Reserves (aFRR) market (Bijl, 2019).

2017	2018	2019
90.5%	89.6%	92.7%

Table 5: The percentages that the prices of the aFRR-up market and aFRR-down market are equal.

For this research it has been decided to select two markets and execute case studies on both of them: one non-balancing market and one balancing market. For the non-balancing markets, there are two options: the day-ahead market and the intra-day market. The Dutch day-ahead market volume in 2018 was 37.5 TWh, while the Dutch intra-day market volume in 2018 was only 2.1 TWh (EPEXSPOT, 2019). Since the day-ahead market displays a much larger share than the intra-day market, the electricity prices, ξ (€/MWh), of the day-ahead market are selected for this research. This data is publicly available and was retrieved from the ENTSOE Transparency Platform (ENTSOE, 2019). In this data set, the electricity prices are given per hour.

The balancing market that is used for this research is the aFRR market. This market consists of the aFRR-up and aFRR-down market. The aFRR-up market is concerned with delivering more power to the network by either consuming less energy or producing more energy, while the aFRR-down market is concerned with extracting power from the network by execution of the exact opposite: consuming more energy or producing less energy (TenneT, 2018). The prices for the aFRR-up and aFRR-down market were retrieved for the years 2017, 2018 and 2019 from the website of TenneT (TenneT, 2019). In this data set, electricity prices are provided per 15 minutes. From this data it was observed that the prices of electricity on the aFRR-up and aFRR-down markets are often equal. Table 5 depicts the percentage of time that the prices of the aFRR-up market and aFRR-down market are exactly the same. From the values of this table it is concluded that the model can be run with either of these price markets without the results deviating significantly from one another. Data has been retrieved from the years 2017, 2018 and 2019 to compare model outcomes from several years and gain more confidence in the resulting revenues. Table 6 depicts the highest, the lowest and the mean price in the data sets retrieved. From this table it can be observed that the prices of the aFRR-up market fluctuate between values that are significantly more extreme than the prices of the day-ahead market. In addition, negative prices occur in the data set, which has the implication that one pays for supplying electricity to the market and receives money when absorbing electricity from the market. The latter may also be potentially interesting for Ocean Grazer BV. Even though balancing efforts are already in a matured state by the network across Europe, prices still fluctuate significantly, showing potential for the Ocean Batteries. In addition, with the increasing amount of renewable energy sources introduced in the market, prices are expected to fluctuate even more due to the intermittent character of renewable energy sources, increasing potential for the Ocean Batteries even further. There are some assumptions regarding the price markets that are applied in this research:

- **Perfect forecasting**: since a historical data set is selected, the assumption exists that prices are perfectly known in advance. For the day-ahead market this is close to reality, since prices are revealed one day in advance. For the aFRR markets this is unrealistic, as prices are determined in real time. However, for this research it is assumed that these prices are also known in advance, as previous research has also taken this approach

Price market	Highest price	Lowest price	Mean price
Day-ahead(2017)	151.07	1.74	39.31
Day-ahead(2018)	175.00	0.55	52.53
Day-ahead(2019)	121.46	-9.02	41.20
aFRR-up(2017)	906.67	-500.00	43.18
aFRR-up(2018)	515.15	-418.64	52.41
aFRR-up(2019)	936.12	-487.65	42.55

Table 6: The highest, lowest and mean prices of the retrieved data sets. All prices are in €/MWh.

(Helseth, 2018; Bijl, 2019). As a result, the model will overestimate the profitability with respect to the aFRR market.

- **Unconstrained production**: for this research it is assumed that there are no constraints regarding the amount of electricity produced. Essentially this means that the production is not restricted by the demand of the market.
- **No selling limitations**: electricity can be sold at each hour and these hours can be decided by the electricity producer.
- **Instant production**: electricity can be produced instantly. The (small) start-up time that a turbine requires to operate at full capacity is disregarded for this research.
- **Positive prices**: from Table 8 it is derived that prices can attain a negative value. When this occurs, the price is set to zero such that the energy is never sold for a negative price.

A requirement for the control is that it is built in such a way that different price market data sets can serve as an input to the control model. It becomes increasingly important in the future to sell the electricity at real time, or close to real time, justifying the assumption that the electricity can be sold at each moment. From now on, the aFRR-up market is referred to as the aFRR market. In this chapter, research question 2, *Which external input is required for the control model?*, was answered.

3 Dynamical model of the Ocean Batteries

Before any control model can be developed, there has to be a model describing the dynamics of the Ocean Batteries. As explained earlier in this chapter, in the ideal situation this model would only be represented by an efficiency describing the losses as a result of the pump and the turbine, which functions are essentially performed by the same device. To find this efficiency, however, there are a number of factors that should be considered. These factors are first considered on a conceptual level before deciding whether or not to include their numerical values in this research. This chapter is dedicated to investigating the effects of these factors and eventually finding the resulting efficiencies.

The technicalities of the Ocean Battery

Before it can be defined which factors influence the efficiency losses of the Ocean Battery, it should be investigated which elements are part of the Ocean Battery design. Figure 18 displays the current design of the Ocean Battery. For this research only the parts that the fluid can move through and therefore lose energy in are of interest. In the case of the Ocean Battery these parts are identified as tubes holding fluid, the flexible storage bladder, pipes through which the fluid flows and a device that acts as a pump and a turbine. As mentioned before, the electricity from wind turbines used to drive the pump of the Ocean Battery could also directly be sold to the electricity grid. It is therefore expected that when it is decided to sell the energy from the storage, the energy from the wind turbines should be sold to the electricity grid as well. Moreover, a decision to store the energy from the wind turbines in this case results in efficiency losses due to the storage process and is therefore undesirable. Based on this reasoning it is decided to continue the research with a PaT instead of a separate pump and turbine. Below the aforementioned elements of the Ocean Grazer storage that result in efficiency losses are explained in more detail.

3.1 Factors affecting the efficiency of the Battery

The identified factors that have an influence of the efficiency of the Ocean Battery are as follows.

1. **Losses due to the efficiency of the PaT**

   These losses consist of the losses due to the pumping function and the losses due to the turbine function of the PaT. The performance of the Ocean Battery largely depends on the type of PaT that is installed: PaT devices are designed for a specific flow rate, available head and pipeline system. Nevertheless, these devices operate across a range of the aforementioned specifications, only at a lower efficiency than the optimum conditions (Morabito and Hendrick, 2019).

   Variable pressure difference

   The design of the Ocean Battery is such that the PaT is subject to a varying pressure difference. This pressure difference occurs through the changing water level in the fluid reservoirs (see tubes in Figure 18). As a result, the pressure that has to be overcome by the PaT to pump the water to the bladder and vice versa changes over time. A change in pressure is equivalent to a change in head, which can be calculated by

   $$H = D - h_f, \tag{6}$$

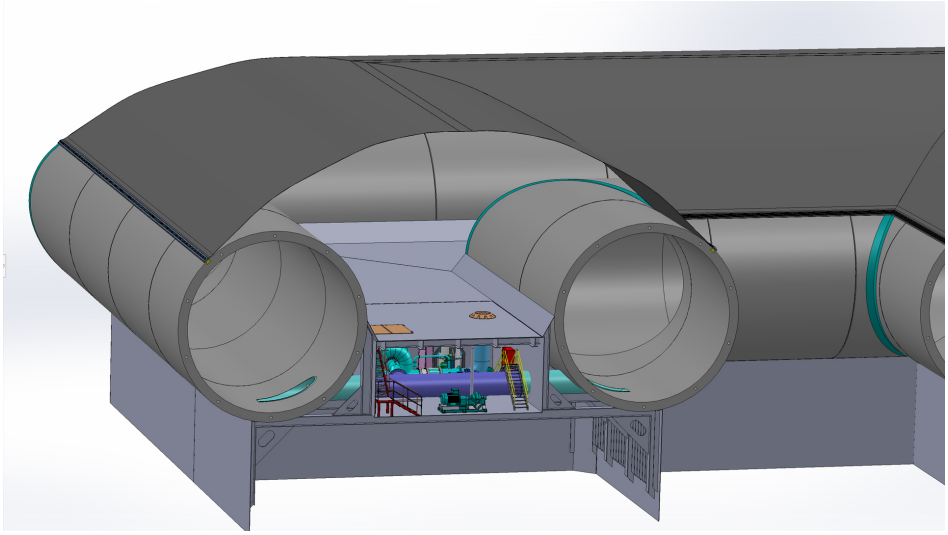

Figure 18: Example of the Ocean Grazer storage system design.

where
H is the head that the pump is subject to in $[m]$,
D is the depth of the Ocean Grazer storage in $[m]$,
h_f is the height of the fluid in the concrete pipes in $[m]$.

The head directly influences the flow rate through the pump according to

$$Q = \frac{P \cdot \eta_p}{\rho \cdot g \cdot H}, \tag{7}$$

where
Q is the flow rate in $[m^3/s]$,
P is the pump power in $[W]$,
η_p is the efficiency of the pump $[-]$,
ρ is the density of the fluid in $[kg/m^3]$,
g is the gravitational acceleration in $[m/s^2]$,
H is the head that the pump is subject to in $[m]$ (Mousavi et al., 2019).

From this equation it can be derived that the flow rate changes over time. This affects the amount of fluid that can be pumped into the bladder and similarly the amount of energy that can be stored. For this research, effects of the variable pressure are excluded.

Another factor to consider regarding the efficiency of the PaT is the start-up time and its corresponding efficiency. As the PaT cannot operate as a pump and turbine simultaneously, the device has to be reversed whenever its function changes. Although relatively small, a certain amount of time is required to reverse the PaT and to reach its full potential again, which is the start-up time (Nicolle et al., 2014). For this research it is assumed that the effects of the start-up efficiency on the results are insignificant and it will therefore not be incorporated. However, the lifetime of a PaT can be optimized

when it is reversed as little as possible and this factor may become important when costs of the system are also considered.

For the level of detail required in this research it is assumed sufficient to assign a constant efficiency to the pump and turbine function of the PaT. From the literature and previous research it was determined that the following are realistic values (Neutrium, 2012; Dijkstra et al., 2016):

- Efficiency of the pump function $\eta_p = 0.9$.
- Efficiency of the turbine function $\eta_t = 0.85$.

2. **Losses in the pipes**: It should also be considered that friction losses occur when the fluid flows through the pipes (Dijkstra et al., 2016).The value of the friction losses depends on the shape and length of the pipes. It requires detailed calculations to find an accurate efficiency value for these losses. Previous research to find this value has been studied in order to make a realistic estimation (van Kessel, 2020). Based on this work, a small but significant value is assumed to represent the losses in the pipes as a single efficiency value as follows:

   - Efficiency of the pipes $\eta_c = 0.9$.

3. **Other losses**: It is plausible that there are other losses due to the displacement of the fluid inside the Ocean Battery. For this research it is assumed that these losses are not significant enough to be incorporated. A detailed study about the efficiency of the Ocean Battery may look at additional losses inside the system.

In this section, the losses in the system have been identified and a number has been assigned that describes the efficiency as a single value that results from the losses. In the next section, the equations that were used for the model of the Ocean Battery dynamics are listed and explained.

3.2 Equations describing the Ocean Battery dynamics

The dynamics of the Ocean Battery can be divided into two parts: the pumping process ('storing') and the turbine process ('draining'). It is required to gain insight in the behavior of the Ocean Battery before designing a controller. Referring back to the goal of this thesis, ultimately the interest is focused on the amount of revenue that is generated by the system. Revenue is generated by multiplying the energy sold by the prices at that specific time. Prices of energy are per MWh of energy sold. Therefore, the behavior of the Ocean Battery is described in terms of how the state of the storage units, which is the storage level, changes over time energy. The change of energy in the storage is calculated by

$$\dot{E}_t = E_{store,t} - E_{drain,t}, \tag{8}$$

where
$\dot{E}$ is the rate of change of energy at time t in $[MWh]$,
E_{store} is the amount of energy stored at time t in $[MWh]$,
E_{drain} is the amount of energy drained at time t in $[MWh]$.

In order to make this equation suitable to be implemented in a model that can be evaluated numerically on a digital computer, the system is discretized using Euler's method by

$$\frac{dx}{dt} = \frac{[x(t_0 + \Delta t) - x(t_0)]}{\Delta t} := \frac{x(k+1) - x(k)}{T_s}, \tag{9}$$

from (Kulakowski et al., 2007).

When applying Euler's method to Equation 8, the change of energy in the system can be displayed by

$$E_{k+1} = E_k + \frac{T_s}{3600}(E_{store,k} - E_{drain,k}), \tag{10}$$

where T_S represents the sampling time in $[s]$.

A suitable sampling time is determined after the storing and draining process are explained in more detail. This is executed below.

Storing process

When the storage is filled, the fluid is pumped from the tube reservoirs to the flexible bladder. Equations describing this process account for the efficiency losses in the system and the available space for energy in the bladder. The available energy is described by

$$E_{av,k+1} = E_{max} - E_k, \tag{11}$$

where
E_{av} is the available space for energy in the bladder $[MWh]$,
E_{max} is the maximum storage level in $[MWh]$.

The potential amount of energy that can be pumped into the bladder is now given by

$$E_{in,k} = \begin{cases} \frac{T_s}{3600} \cdot P_p, & E_{av,k} > \frac{T_s}{3600} \cdot P_p \\ E_{av,k}, & \text{else,} \end{cases} \tag{12}$$

where
E_{in} is the amount of energy that can be pumped into the bladder in $[MWh]$,
E_{av} is the available space for energy in the bladder $[MWh]$,
P_p is the maximum power of the pump in $[MW]$.

The amount of energy that can be stored within one time step can now be calculated by

$$E_{store,k} = E_{in,k} \cdot \eta_P, \tag{13}$$

where
E_{store} is the energy stored at time k in $[MWh]$,
E_{in} is the amount of energy that can be pumped into the bladder in $[MWh]$,
η_P is the efficiency of the pumping mode of the PaT, calculated as $\eta_p \cdot \eta_c$ $[-]$.

Draining process

The steps that have to be undertaken to calculate the amount of energy that can be drained from the bladder at one time step are similar to the steps for the storing process. Small changes are made to the previous equations to finally describe the energy that can be drained from the bladder. First, Equation 11 is substituted by the amount of energy left in the bladder that can be drained to the tube reservoirs. If this amount is not sufficient to use the full capacity of the PaT in turbine mode, the energy has to be adapted. Equation 12 from the storing process is therefore substituted by

$$E_{out,k} = \begin{cases} \frac{T_s}{3600} \cdot P_t, & E_k > \frac{T_s}{3600} \cdot P_t \\ E_k, & \text{else,} \end{cases} \tag{14}$$

where
E_{out} is the amount of energy that can be drained from the bladder in $[MWh]$,
T_s is the sampling time in $[s]$,
P_t is the maximum power of the turbine mode of the PaT in $[MW]$,
E_k is the storage level at the previous time step in $[MWh]$.

The amount of energy that can be drained within one time step can now be calculated by

$$E_{drain,k} = E_{out,k} \cdot \eta_T, \tag{15}$$

where
E_{drain} is the energy drained at time k in $[MWh]$,
E_{out} is the amount of energy drained from the bladder in $[MWh]$,
η_T is the efficiency of the turbine mode of the PaT, calculated as $\eta_t \cdot \eta_c$ $[-]$.

Calculation of the maximum storage capacity

Both the storing process and draining process depend on a variable that has to be calculated, which is the maximum storage capacity of the Ocean Battery. This capacity is dependent on the depth at which the Ocean Battery is situated and can be calculated by using the pressure of the ocean, the pressure of the atmosphere and the maximum volume of the storage as

$$E_{max} = V_{max} \cdot \Delta p. \tag{16}$$

The volume is, contrary to the maximum energy, not dependent on depth. Equation 16 was derived from rewriting Equation 7 into

$$Q = P \cdot \eta_P \cdot \Delta p, \tag{17}$$

by using

$$p = \rho \cdot g \cdot H, \tag{18}$$

where
p is the pressure in $[Pa]$,
ρ is the density of the fluid in $[kg/m^3]$,
g is the gravitational acceleration in $[m/s^2]$,
H is the head that the PaT is subject to in $[m]$.(Neutrium, 2012)

Using $Q = V/t$ and substituting this together with Equation 17 into $E = P \cdot t$ leads to the formula in Equation 16.

3.3 Simulations

A simulation is executed to observe the behavior of the Ocean Battery when storing up to almost full capacity and draining to an almost empty bladder again once. When the full capacity is taken, just slightly before the storage reaches full capacity, the amount of energy that can be pumped in is infinitely small and it therefore takes a long time to fill the storage completely. The same holds for the draining process. The parameters used in this simulation are listed in Table 8. Hereby it is assumed that the Ocean Battery is placed in water with a depth of 40 meters and that the PaT has a maximum power of 1 MW. The PaT operates at this power unless the resources are not sufficient anymore. The maximum volume was calculated from a simplified version of the Ocean Battery design. The calculation of the maximum volume is included in Appendix B.

Parameter	**Value**	**Description [units]**
T_s	900	Sampling time $[s]$
η_p	0.85	Efficiency of the pump mode $[-]$
η_t	0.9	Efficiency of the turbine mode $[-]$
η_k	0.9	Efficiency of the pipes $[-]$
p_{ocean}	400000	Ocean pressure $[Pa]$
p_{atm}	100000	Atmospheric pressure $[Pa]$
V_{max}	25132	Maximum volume of bladder $[m^3]$
P_p	1	Maximum power of the pump mode $[MW]$
P_t	1	Maximum power of the turbine mode $[MW]$

Table 7: Model parameters.

The efficiency results are listed in Table 8. Previous research about the efficiency of the Ocean Battery concluded that the round trip efficiency was close to 56% (van Kessel, 2020), which is a bit lower than the results in this research. This difference can be explained by the amount of simplicity that was introduced in this research, as in this research it was not accounted for changing efficiency as a result of the changing flow rate. Therefore, the model in this research overestimates the efficiency of the system. Nevertheless, the efficiency only deviates a few percent from the efficiency of previous research and the presented model is therefore accepted. One of the main purposes of the simulation was to verify the efficiency

Pump mode efficiency	0.77
Turbine mode efficiency	0.81
Round trip efficiency	0.62

Table 8: Efficiencies of the Ocean Battery.

of the pump mode and turbine mode of the PaT, and the round trip efficiency of the Ocean Grazer storage. The efficiency is calculated by comparing the total energy input and the total energy output, both for the whole process and for the separate pumping and draining processes.

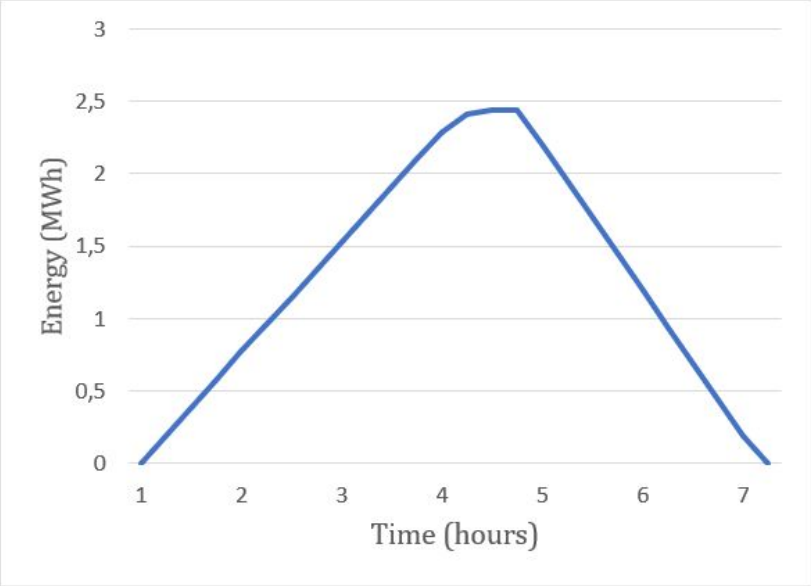

Figure 19: Results change in energy level from filling and draining the bladder once.

Simulation results

The behavior of the Ocean Battery with respect to filling and draining the bladder is depicted in Figure 19. The calculated maximum storage capacity of the Ocean Battery is $E_{max} = 2.44$ MWh. From this figure it can be derived that the model behaves as expected: the energy is stored until the storage is almost full, whereby storing the last bit of energy has a curved shape. Draining the storage happens thereafter until it is almost empty again. From the simulations it is observed that filling and draining the storage once takes approximately 6.5 hours. The efficiencies that resulted from the model by comparing the actual energy output to the energy input are exactly the same as the efficiencies in Table 8. The Python model used for these simulations is included in Appendix C.

3.4 Validation of the dynamical model

An essential part of the development of the model is to validate a model's result and to gain confidence about its correctness (Robinson, 1997; Sargent, 2013). Several techniques can be used to validate a model. To validate the dynamical model of the Ocean Battery, the following quantitative validation techniques are identified as suitable: parameter variability (sensitivity analysis) and analytical calculations.

Parameter variability

Parameter variability, or sensitivity analysis, can for example be executed by changing the value of an input parameter to observe the effect on the model's output. The model is validated when the outcomes display the same relationships as would occur in the real system (Sargent, 2013). For the simulations, a sampling time of $T_s = 900s$ was selected, as previous research has shown this is a suitable time step for simulating the Ocean Battery (Dijkstra et al., 2016). A sensitivity analysis has been executed on the sampling time to find the effects

of changing this parameter. To simulate continuous time, a sampling time of $T_s = 0.01s$ has been selected. This sets a reference value for the other sampling times. When using a larger sampling time, the situation may occur in which the storage is filled to its maximum before the time step has finished. Therefore, the simulation time, which is the time it takes for the Ocean Battery to fill and drain once, is expected to increase when increasing the sampling time.The disadvantage of the longer simulation time is that when the PaT is in pump mode during a time step and the storage reaches its maximum capacity before the end of the time step, there is a certain amount of time that nothing can happen with the energy in the storage. The results of the sensitivity analyses are presented in Table 9. From the table it can be derived that the model behaves according to expectation, as the simulation time increases, and all sampling times still present the same round trip efficiency. Based on these results it is concluded that the Parameter variability validation was successful.

Sampling time [s]	**Simulation time** [s]	**Round trip efficiency**
0.01	20269	0.62
300	21000	0.62
900	22500	0.62
1200	24000	0.62
1800	25200	0.62
3600	36000	0.62

Table 9: Relation between the sampling time and the total simulation time when filling and draining the storage once.

Analytical calculations

Analytical calculations belong to the category of validating a model with the results of other (validated) models. When a model is simple enough, analytical calculations are a suitable method for validation (Sargent, 2013). For the dynamical model of the Ocean Battery, it is calculated analytically how long it would take to fill and drain the storage once. The results of the calculations are depicted in Table 10. The results show that the difference between the total time of the simulation model and the analytical calculations is only 0.1%. This very small difference can be explained by the fact that the once the storage is almost full or almost empty, the PaT cannot operate at full capacity anymore, while for the analytical calculations it was assumed that the PaT could always operate at full capacity. Nevertheless, the difference is small enough to conclude that the dynamical model of the Ocean Battery is valid. The analytical calculations are included in Appendix D.

	Storing time [s]	**Draining time** [s]	**Total time** [s]
Simulation model	11498	8796	20295
Analytical calculations	11485	8784	20269

Table 10: Comparison between the simulation model and analytical calculations.

3.5 Dynamical model for the distributed system

A few changes have to be made to the dynamical model in order to fit the distributed system of Ocean Batteries. First, the amount of energy that is pumped into storage is dependent of energy production from the wind turbines. This factor is added to the model. Second, the dynamical model has to be adapted such that it fits multiple storage units and multiple energy sources. As a result, the control input u consists of all variables necessary to control N Ocean Batteries and wind turbines, which can be explained as follows by identifying which actions influence the state of the system.

- u^{RG} controls the amount of energy that storage i receives from wind turbine j at time step k. As there may be more than one wind turbine that has a connection to storage i, the sum of the energy received by all wind turbines that have a connection to storage i is added to the energy in storage i.
- u^{RS} controls the amount of energy that storage i receives from neighboring storage j at time step k. As again, there may be several storage units connected to storage i, the sum of the energy received from the neighboring storage units is added to the energy in storage i.
- u^{SS} controls the amount of energy sent to neigboring storage j from storage i at time step k. As explained above, the sum is taken of all energy sent to neighboring storage units and this value is subtracted from the energy in storage i.
- u^{SC} controls the amount of energy that is sold from storage i to the electricity grid at time step k. As the electricity grid is a single entity, there can be only one value that is subtracted from the energy in storage i.
- u^{GC} controls the amount of energy that is sold from wind turbine i to the electricity grid. This control variable does not appear in the state of the Ocean Batteries, but does in the revenue calculations.

The dynamical model is expanded such that it calculates the states of all Ocean Batteries in the system. The final equation for calculating the state of individual storage i is formulated as

$$\begin{aligned} E_{i,k+1} = E_{i,k} + \eta_P \sum_{j=1}^{\#G} u^{RG}_{i,j,k} \cdot E^G_{j,k+1} + \eta_T \cdot \eta_P \sum_{j=1, i\neq j}^{\#S} u^{RS}_{i,j,k} \cdot E_{j,k} \\ -\eta_T \cdot E_{i,k} \left[\left(\sum_{j=1, i\neq j}^{\#S} u^{SS}_{i,j,k} \right) + u^{SC}_{i,k} \right], \; i = 1,..,S, \end{aligned} \tag{19}$$

where
E_i is the storage level of storage i in $[MWh]$,
E^G_j is the energy generated by wind turbine j in $[MWh]$,
S is the number of storage units in the system,
G is the number of wind turbines in the system,
$u^{RG}, u^{RS}, u^{SS}, u^{SC}$ are the control variables to be determined by the optimization $[-]$.

Model assumptions

A few assumptions are made for the dynamical model. These assumptions are listed below.

- There are no energy losses inside the cables. This assumption is not realistic, as there are always energy losses in a cable. However, for this research it is out of the scope to include cable lengths. When the cable lengths are within acceptable range, the cable losses are expected to be only a few percent (Commission et al., 2007).
- Electricity can flow through cables in both ways, implying that electricity can go back and forth between the storage units in the system.
- Cables are not restricted by a cable capacity, which means that the amount of electricity that is allowed to flow through a single cable is unlimited.
- The model is linear, implying that the state of the system is not subject to non-linearity with respect to the amount of energy stored or sold.
- The Ocean Batteries and wind turbines have no down-time, which means that they are never out of operation.

By obtaining the dynamical model for the distributed system of Ocean Batteries, sub-question 3, *how can the dynamical model of the Ocean Battery be developed?*, is answered and the development of the dynamical model is finished.

4 The control systems model

The goal of this thesis is to design a control model that ensures that revenues of the distributed system of Ocean Batteries are maximized. Revenues are maximized when the energy is sold from the storage units and the wind turbines when the prices are favorable. Therefore, a control strategy has to be adopted to determine when to sell the energy from the storage units and the wind turbines. The aim is to adopt a control strategy that accomplishes the highest possible performance with the resources available. Before the control strategy is selected, the type of control is specified. In this section, a brief literature review about possible control strategies is conducted. Thereafter a suitable control strategy is selected and the corresponding control model is developed.

4.1 The distributed control system

A Distributed Control System (DCS), is a control system in which each subsystem contains its own control, as opposed to the central control system that controls the actions of all subsystems. The DCS ensures that the subsystem executes the necessary actions that lead to the desired state of the subsystem. Although each DCS has its own autonomous controller, there can still be an operator that controls the state of the whole system centrally.

The aim is to maximize the revenues that can be generated by the system consisting of the Ocean Batteries and the wind turbines as a whole. As the actions of the individual Ocean Batteries affect one another, it seems most promising to adopt a supervisory control that assigns the information on the desired state of the subsystems by means of control variables to the Ocean Batteries and wind turbines. Optimal integration of all subsystems into the whole system studied in this research is ensured when a supervisory control is adopted. Resulting revenues from the chosen control strategy are as high as possible with the given resources from adopting this type of control. Previous research has shown that adopting a supervisory control is a suitable choice for renewable energy systems (Qi et al., 2010, 2011). In literature, the possibility to decentralize the control actions of the subsystems completely has also been investigated. One of the limitations of a central control system, which is the complexity of the computation, can be overcome by decentralizing these control systems, but an optimized state of the system as a whole cannot be ensured (Kumar et al., 2005; Qi et al., 2012). Therefore, for this research it has been decided to adopt a central supervisory control system to inform the distributed controllers of the subsystems about their optimal control variables u.

4.2 Control strategies

For the evaluation of control strategies, the research goal and degree of complexity in the system are considered. To enable maximization of the revenues, a control strategy is selected that can deal with optimization problems. In addition, the control strategy should be able to deal with constraints on the state of the system. If there is a suitable control strategy that has sufficient predictive power to determine when the energy should be stored and sold to the market based on the electricity prices and the weather forecast, this should be the preferred control strategy considering the price peaks and no-production periods that occur in the data sets as described in Chapter 2. From literature it was derived that common control strategies can be categorized as Rule Based Control (RBC) or Model Predictive Control (MPC). RBCs operate at pre-defined set points for the market prices for example to deal with energy systems

efficiently. On the other hand, MPC can predict future states of the system based on input data and optimizes for example the revenues of the system over a sliding horizon that is subject to an objective function (Clauß et al., 2017). In the subsections below both types of control strategies are explained in more detail.

Rule Based Control

Rule Based Controls are a common approach for controlling power systems and are suitable to be implemented for simulations. Other advantages include concept simplicity, broad applicability and these type of controls are known as computationally fast (Lee and El-Sharkawi, 2008; Galus et al., 2010). In addition, updated states can easily be calculated by RBC that uses decision rules to execute this (Clauß et al., 2017). An example of a decision rule in this context is that the energy stored in the Ocean Grazers is sold when the price of electricity exceeds a certain value, set as the threshold price. Although there are many advantages to Rule Based Controls, there is also a major disadvantage as RBCs are not able to optimize the overall system behavior (Lee and El-Sharkawi, 2008; Galus et al., 2010; Clauß et al., 2017).

Model Predictive Control

In short, Model Predictive Control can be described as a strategy that is able to make a forecast on the state of the system. where Rule Based Control is not able to optimize the overall system behavior, MPC is (Meral and Çelík, 2019). MPC guarantees stability of the system for all conditions, which leads to the strategy being assumed one of the advanced control methods (Darabian and Jalilvand, 2017). With MPC, an optimization is conducted by predicting the optimal state of the system now based on the performance of the system over a predefined time horizon (Galus et al., 2010). In order to achieve this, for MPC knowledge is required on the controlled output desired trajectory, or the behavior of the system with respect to for example electricity price (Abdeltawab and Mohamed, 2015). Model Predictive Control is considered one of the most promising developments as it is able to take into account the future weather and electricity price forecast (Clauß et al., 2017), which is precisely what is required of the control strategy. The disadvantages of MPC that are discussed in literature are that MPC is computationally demanding and sensitive to parameter changes (Galus et al., 2010; Bouzid et al., 2015).

Comparison between RBC and MPC

When comparing both control strategies, a trade-off analysis on the advantages and disadvantages of the control strategies has resulting in the following. For this research it is decided that although Model Predictive Control is computationally demanding, it satisfies the requirements specified in 4.1 better than Rule Based Control and is therefore selected as the appropriate control strategy to develop the supervisory control model. In addition, Model Predictive Control has proven its applicability in several comparable studies (Dijkstra et al., 2016; Barradas-Berglind et al., 2016; Alkano, 2016), showing its potential.

Model Predictive Control: the working principle

In this section, the working principle of Model Predictive Control is explained in detail. MPC is generally applied to control the behavior of dynamic systems. In short, MPC uses an

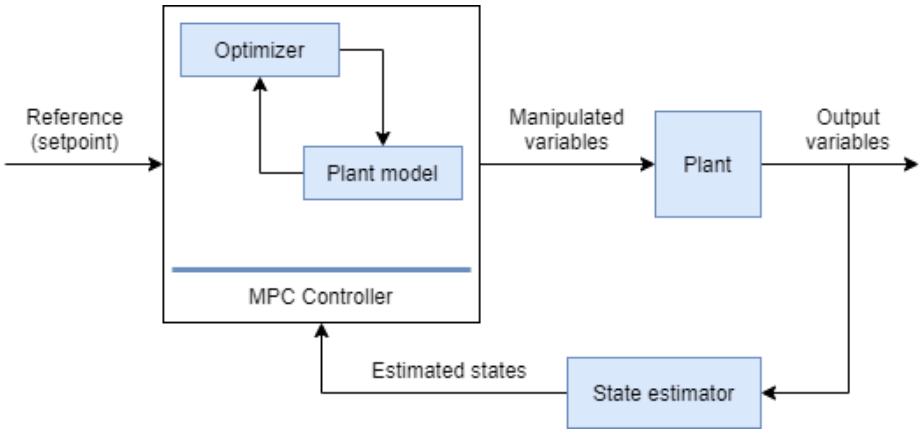

Figure 20: Illustration of the working principle of Model Predictive Control(1)

internal system model to determine which actions in the system give the best performance over a predefined time horizon by solving an optimization problem. A finite horizon is used that consists of N predicted time steps in a receding horizon. In other words, predictions are made at the supervisory controller at each time step to determine the adequate actions of the distributed controllers (Galus et al., 2010). Consequently, an algorithm should be developed that is executed each sampling period, whereby only the first value of the optimal sequence is returned to the system (Vazquez et al., 2014). A schematic representation of the MPC working principle is depicted in Figure 20. The MPC controller is composed of the following:

- **Internal dynamical model**: the internal dynamical model represents the behavior of the studied system. This internal model is identical to the studied system, but is only used within the MPC Controller to make predictions on its future states.
- **Cost function**: a cost function J is used for the optimizer. The cost function is optimized over the receding horizon. In words, the cost function that is used for this research is the sum of the revenues generated by the wind turbines and the Ocean Batteries in the system over the entire prediction horizon.
- **Optimization algorithm**: this algorithm is composed of the cost function and the constraints that the states of the system are subject to. The optimization algorithm ultimately optimizes a control input u.

After the MPC controller has optimized the provided optimization problem, the first value of the optimal sequence is sent to the distributed control systems (the 'plants') in terms of the control variables. Calculations are performed in the distributed control system by implementation of the control variable(s). An output is generated and used for the next computations in the supervisory MPC Controller at the next time step. Another way to illustrate the working principle of MPC is presented in Figure 21. The advantages of MPC are clearly visible in this figure, as the output follows a smooth curve towards the reference trajectory. From the description of MPC, the generic algorithm of Model Predictive Control is as follows, inspired by the algorithm that is presented in (Dijkstra, 2016). The state is in this algorithm described by x and prediction parameters are distinguished from model parameters by adding a hat to the variable.

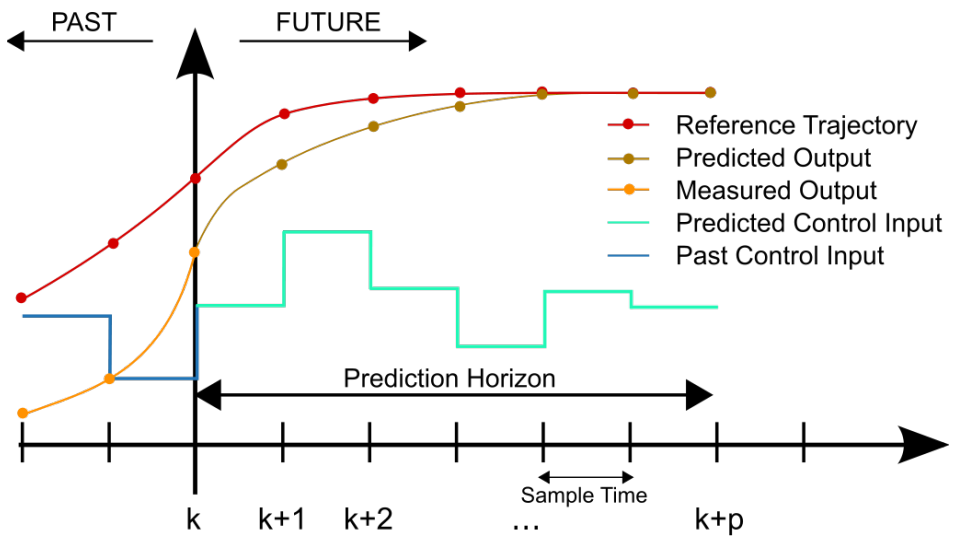

Figure 21: Illustration of the working principle of Model Predictive Control(2)

---

1. Initialize parameters, vectors and time step k
2. Set $\hat{x}_k = x_k$
3. Solve the optimization problem by the model of the system within the MPC controller. The optimization problem is of the form:

$$\max_{\hat{u}} J = \sum_{k=1}^{N} f(\hat{x}_k, \hat{u}_k)$$

subject to constraints including the dynamics of the system, the upper and lower bound of the input and state variables.

4. Take the first value of the optimized control variables and set $u_k = \hat{u}_k$
5. Make system calculations with this control variable
6. Increment k and repeat

This algorithm is used to formulate the algorithm for the control model developed in this research. In Chapter 1, it was mentioned that the control model is developed in Python. Therefore, it is investigated whether there exists a method to apply MPC in Python.

Application of MPC in Python

From literature it was derived that MPC has previously been implemented in Python (Takacs et al., 2015). There is a module available in the Python library for optimization, which is the SciPy package. From this package, the Optimize module contains a solver for many minimization algorithms, including nonlinear optimizations, that is able to deal with constraints (Virtanen et al., 2020; Oliphant, 2007). Within the optimization package, the optimization method has to be specified. The Sequential Least SQuares Programming (SLSQP) method is a suitable choice, as this method is able to deal with bounds on the control variable and constraints on the system (Bouzid et al., 2015).

4.3 Design of the control model

In this section, the design of the control model is explained. From Chapter 4.2 it was derived that for the design of the predictive controller, the elements that have to be designed are the internal dynamical model and the optimization algorithm, which consists of the cost function and the constraints that the states of the system are subject to. All elements are specified in this section.

Internal dynamical model

The internal dynamical model is identical to the dynamical model of the Ocean Battery, which has been developed in Chapter 3. The dynamical model from Equation 19 is transformed to the internal dynamical model of the MPC controller as

$$\begin{aligned}\hat{E}_{i,k+1} = \hat{E}_{i,k} + \eta_P \sum_{j=1}^{\#G} \hat{u}^{RG}_{i,j,k} \cdot \hat{E}^{G}_{j,k+1} + \eta_T \cdot \eta_P \sum_{j=1, i\neq j}^{\#S} \hat{u}^{RS}_{i,j,k} \cdot \hat{E}_{j,k} \\ -\eta_T \cdot \hat{E}_{i,k} \left[\left(\sum_{j=1, i\neq j}^{\#S} \hat{u}^{SS}_{i,j,k} \right) + \hat{u}^{SC}_{i,k} \right], \; i = 1,..,S,\end{aligned} \tag{20}$$

where
$\hat{E}_i$ is the predicted storage level of storage i in $[MWh]$,
$\hat{E}^G_j$ is the predicted energy generated by wind turbine j in $[MWh]$,
$\hat{u}^{RG}, \hat{u}^{RS}, \hat{u}^{SS}, \hat{u}^{SC}$ are the predicted control variables from the optimization $[-]$,
S is the number of storage units in the system,
G is the number of wind turbines in the system,
η_P is the efficiency of the pumping process $[-]$,
η_T is the efficiency of the draining process $[-]$.

The values of $\hat{u}^{RG}, \hat{u}^{RS}, \hat{u}^{SS}$ and $\hat{u}^{SC}$ are not independent of one another. For example, the PaT cannot operate as a pump and turbine simultaneously, implying that a storage can either receive energy or send energy. Whenever there is a dependency between the control variables, a constraint is applied to prevent the control variables from conflicting with one another.

The cost function

Recalling the goal of this thesis, this research aims to maximize the revenues that can be obtained by the distributed system of Ocean Batteries, including wind turbines and the electricity market. The goal has been taken into account for the identification of the cost function J. The cost function relates the states of the system, the storage levels of the Ocean Batteries, to the revenue that can be obtained by the system. Revenues can be obtained in two different ways, as described below. Both types of electricity can be sold for the market price, ξ, in $€/MWh$.

1. By directly selling the electricity generated by the wind turbines in the system. The energy from the wind has already been corrected for the efficiency losses in the wind turbine by the model in Appendix A.

2. By selling the electricity from the storage units. The energy from the storage units is corrected for the efficiency in Equation 20.

The prices of the day-ahead market are provided per hour, while the prices of the aFRR market are provided per 15 minutes. The sampling time is chosen accordingly. The revenue from a storage can be calculated by

$$R_{i,k+1} = \xi_{k+1} \cdot \eta_T \cdot u^{SC}_{i,k} \cdot E_{i,k}, \qquad i = 1,..,S, \tag{21}$$

where
R_i is the revenue from storage i in [€],
ξ is the price of electricity in [€],
η_T, u^{SC}, E_i as defined in (19),

and the revenue from a wind turbine is calculated by

$$R_{i,k} = \xi_k \cdot u^{GC}_{i,k} \cdot E^G_{i,k}, \qquad i = 1,..,G, \tag{22}$$

where
R_i is the revenue from wind turbine i in [€],
u^{GC} is a control variable from the optimization [−],
ξ, E^G_j as defined in (21) and (19), respectively.

The cost function is now defined as the sum of the expected revenues from the storage and the wind turbines over the entire prediction horizon. Mathematically, this can be formulated as

$$\max_{\hat{u}} \; J = \max_{\hat{u}} \sum_{k=1}^{N} (\sum_{i=1}^{\#S} R_i(k) + \sum_{j=1}^{\#G} R_j(k)). \tag{23}$$

4.4 The optimization algorithm

The last element to be specified for the design of the MPC Controller is the optimization algorithm. As mentioned above, the optimization algorithm is composed of the cost function and the constraints that the states of the model are subject to. The cost function has been identified in the previous section and is formulated in Equation 23. In this section, first the constraints and bounds are identified and explained, and mathematically presented. Thereafter, the full optimization problem is depicted. The section is finished with the optimization algorithm that completes the supervisory predictive control model.

Constraints

The model is subject to several constraints. The constraints are listed below and thereafter explained in more detail. Since the model in this research is linear, all constraints appear in the model explicitly.

1. The PaT cannot operate in pump and turbine mode simultaneously.
2. The PaT has a maximum operational capacity.
3. Ocean Batteries have a maximum storage capacity.
4. Ocean Batteries and wind turbines cannot sell more than 100% of their available energy.

1. The PaT cannot operate in pump and turbine mode simultaneously

The implication of this constraint is that either a storage receives energy from another storage or a wind turbine (or both), or a storage sends energy to another storage or the market (or both). The control variables have to be constrained such that either one of the options can happen at one time step. Recalling Equation 20, four types of control variables were identified ($\hat{u}^{RG}_{i,k}, \hat{u}^{RS}_{i,k}, \hat{u}^{SS}_{i,k}, \hat{u}^{SC}_{i,k}$). In this equation, $\hat{u}^{RG}_{i,k}$ and $\hat{u}^{RS}_{i,k}$ control incoming energy from other storage units or wind turbines, and $\hat{u}^{SS}_{i,k}$ and $\hat{u}^{SC}_{i,k}$ control outgoing energy to other storage units or the market. The constraint can now be formulated as

$$(\hat{u}^{RG}_{i,k} + \hat{u}^{RS}_{i,k}) \cdot (\hat{u}^{SS}_{i,k} + \hat{u}^{SC}_{i,k}) = 0, \qquad i = 1,..,S. \tag{24}$$

By multiplying the control variables as in (24), it is ensured that a particular storage is either filling or draining at a time step.

2. The PaT has a maximum operational capacity

The implication of this constraint is that the amount of energy that is either received or sent at a time step, cannot exceed the capacity of the PaT. A constraint is formulated that ensures that the control variable multiplied with the available energy does not exceed the PaT capacity. Since constraint 1 already ensures that a storage does not operate in pump and turbine mode simultaneously, constraint 2 can combine both operations into one constraint as

$$\begin{aligned} TC - \eta_P \sum_{j=1}^{\#G} \hat{u}^{RG}_{i,j,k} \cdot \hat{E}^{G}_{j,k+1} + \eta_T \cdot \eta_P \sum_{j=1, i\neq j}^{\#S} \hat{u}^{RS}_{i,j,k} \cdot \hat{E}_{j,k} \\ -\eta_T \cdot \hat{E}_{i,k} \left[\left(\sum_{j=1, i\neq j}^{\#S} \hat{u}^{SS}_{i,j,k} \right) + \hat{u}^{SC}_{i,k} \right], \qquad i = 1,..,S, \end{aligned} \tag{25}$$

where
TC is the PaT capacity in $[MWh]$,
$\eta_P, \hat{u}^{RG}, \hat{E}^{G}, \eta_T, \hat{u}^{RS}, \hat{E}, \hat{u}^{SS}, \hat{u}^{SC}$ as in (20).

For this research it has been decided that all storage units have the same PaT installed. The PaT capacity is given in $[MW]$. For this constraint, the PaT capacity is corrected for the time step such that it can be defined in $[MWh]$.

3. Ocean Batteries have a maximum storage capacity

The energy inside a storage cannot exceed the maximum capacity of the Ocean Battery. The capacity is dependent on the depth at which the Ocean Battery is located and the dimensions of the Ocean Battery. For the constraint this means that the energy that a storage receives must be less than the available capacity of that storage. All Ocean Batteries in the system have the same maximum capacity. The constraint is formulated as

$$E_{max} - \left(\eta_P \sum_{j=1}^{\#G} \hat{u}^{RG}_{i,j,k} \cdot \hat{E}^{G}_{j,k+1} + \eta_T \cdot \eta_P \sum_{j=1, i\neq j}^{\#S} \hat{u}^{RS}_{i,j,k} \cdot \hat{E}_{j,k} \right) \geq 0, \tag{26}$$

where
E_{max} is the maximum storage capacity in $[MWh]$,
$\eta_P, \hat{u}^{RG}, \hat{E}^{G}, \eta_T, \hat{u}^{RS}, \hat{E}$ as in (20).

4. Ocean Batteries and wind turbines cannot sell more than 100% of their available energy

This constraint is straight-forward but should nevertheless be adopted in the model. It ensures that the sum of the control variables that control the amount of energy that is sent from a storage ($\hat{u}^{SS}, \hat{u}^{SC}$) or a wind turbine ($\hat{u}^{SS}, \hat{u}^{GC}$) does not exceed 1, as it is not possible to sell more than 100% of the available energy. The constraints corresponding to the storage units and the generators are

$$\left[\left(\sum_{j=1,i\neq j}^{\#S} \hat{u}_{i,j,k}^{SS}\right) + \hat{u}_{i,k}^{SC}\right] \leq 1, \qquad i = 1,..,S, \text{ and} \tag{27}$$

$$\left[\left(\sum_{j=1}^{\#S} \hat{u}_{i,j,k}^{SS}\right) + \hat{u}_{i,k}^{GC}\right] \leq 1, \qquad i = 1,..,G, \tag{28}$$

where
$\hat{u}^{SS}, \hat{u}^{SC}$ as in (20) and $\hat{u}^{GC}$ as in (22).

Bounds

As the control variables represent a percentage of available energy that is sent, it is easy to understand that no less than 0% and no more than 100% of the available energy can be moved within the system. The control variables are therefore all bounded as

$$0 \leq \hat{u}^{RG}, \hat{u}^{RS}, \hat{u}^{SS}, \hat{u}^{SC}, \hat{u}^{GC} \leq 1. \tag{29}$$

The optimization problem

The full optimization problem, including the cost function, the constraints and the bounds that the states of the system are subject to, is presented in the statement below.

$$\max_{\hat{u}} \quad J = \sum_{k=1}^{N}(\sum_{i=1}^{\#S} R_i(k) + \sum_{j=1}^{\#G} R_j(k)) \tag{30}$$

$$\begin{aligned}
\text{s.t.:} \quad \hat{E}_{i,k+1} = \hat{E}_{i,k} + \eta_P \sum_{j=1}^{\#G} \hat{u}^{RG}_{i,j,k} \cdot \hat{E}^{G}_{j,k+1} + \eta_T \cdot \eta_P \sum_{j=1,i\neq j}^{\#S} \hat{u}^{RS}_{i,j,k} \cdot \hat{E}_{j,k} \\
-\eta_T \cdot \hat{E}_{i,k} \left[\left(\sum_{j=1,i\neq j}^{\#S} \hat{u}^{SS}_{i,j,k} \right) + \hat{u}^{SC}_{i,k} \right], \qquad i = 1,..,S \\
(\hat{u}^{RG}_{i,k} + \hat{u}^{RS}_{i,k}) \cdot (\hat{u}^{SS}_{i,k} + \hat{u}^{SC}_{i,k}) \quad = 0, \quad i = 1,..,S \\
TC - \eta_P \sum_{j=1}^{\#G} \hat{u}^{RG}_{i,j,k} \cdot \hat{E}^{G}_{j,k+1} + \eta_T \cdot \eta_P \sum_{j=1,i\neq j}^{\#S} \hat{u}^{RS}_{i,j,k} \cdot \hat{E}_{j,k} \\
-\eta_T \cdot \hat{E}_{i,k} \left[\left(\sum_{j=1,i\neq j}^{\#S} \hat{u}^{SS}_{i,j,k} \right) + \hat{u}^{SC}_{i,k} \right] \quad \geq 0, \quad i = 1,..,S \\
E_{max} - \left(\eta_P \sum_{j=1}^{\#G} \hat{u}^{RG}_{i,j,k} \cdot \hat{E}^{G}_{j,k+1} + \eta_T \cdot \eta_P \sum_{j=1,i\neq j}^{\#S} \hat{u}^{RS}_{i,j,k} \cdot \hat{E}_{j,k} \right) \quad \geq 0, \quad i = 1,..,S \\
\left[\left(\sum_{j=1,i\neq j}^{\#S} \hat{u}^{SS}_{i,j,k} \right) + \hat{u}^{SC}_{i,k} \right] \quad \leq 1, \quad i = 1,..,S \\
\left[\left(\sum_{j=1}^{\#S} \hat{u}^{SS}_{i,j,k} \right) + \hat{u}^{GC}_{i,k} \right] \quad \leq 1, \quad i = 1,..,G \\
0 \leq \hat{u}^{RG}, \hat{u}^{RS}, \hat{u}^{SS}, \hat{u}^{SC}, \hat{u}^{GC} \leq 1
\end{aligned}$$

In this optimization problem, R_i and R_j are calculated from (21) and (22), respectively. $\hat{E}^G$ is imported from the wind power production data set.

The optimization algorithm

Now that the MPC Contoller has been designed, the last step is to define optimization algorithm that solves the aforementioned optimization problem. The inputs for the algorithm are related to the design of the system such as the depth, the wind power data and price data, among other parameters related to the Ocean Battery design including the efficiency and capacity of the PaT and the maximum volume of the bladder. Another input that defines the interconnections between the Ocean Batteries and the wind turbines is the adjacency matrix of the system. The optimization algorithm is depicted in the table below, where τ presents the total number of time steps.

Algorithm: Revenue maximizing by MPC
Inputs: ξ, A, E^G, $E_{i,0}$,
Outputs: u, R
1: **for** $k = 0, .., \tau$ **do**
2: **solve** the optimization problem in (30)
3: **return** $\hat{u}_{i,k} = \{\hat{u}_{i,0}, .., \hat{u}_{i,N}\}$, $i = 1, ..S$
4: $u_{i,k} \leftarrow \hat{u}_{i,0} \quad \forall \hat{u}_{i,k}$ in $U = \{\hat{u}^{RG}_{i,k}, \hat{u}^{RS}_{i,k}, \hat{u}^{SS}_{i,k}, \hat{u}^{SC}_{i,k}\}$
5: **calculate** $E_{i,k+1}$ with (19) and $u_{i,k}$
6: **return** $R_{i,k} + R_{j,k}$ from (21) and (22)
7: **end for**

This optimization algorithm is used to determine the most beneficial control actions such that the total revenues of the system, composed of the revenues from the storage units and the revenues from the wind turbines, are maximized. The results from the closed loop implementation of the optimization algorithm are discussed in Chapter 6. From a step-by-step approach, first a One-Storage-One-Generator (1S1G) simulation model, that consists of one storage and one wind turbine, of the optimization problem was developed. Thereafter, a Multiple-Storage-Multiple-Generator (MSMG) simulation model, that can process multiple storage units and multiple generators was developed. Results from both simulation models appear in Chapter 6. In addition, a Rule Based Control model was developed to compare the results from both strategies (RBC and MPC) with respect to the obtained results. The 'rule' that is applied to the RBC model relates to the decision to store or sell based on a threshold price ξ. The simulation models for the 1S1G RBC model, 1S1G MPC model and MSMG MPC model are included in appendices G, F and H, respectively. In the next chapter, the presented control models are validated. In this section, an answer has been provided to sub-question 4, *what would be an suitable control strategy and how can this control strategy be applied to the dynamical model?*, and the corresponding control model has been designed. With the design of the control model, the treatment design phase from the engineering cycle by Wieringa has been finished.

5 Validation of the distributed storage control system

In the development of a prediction model, a validation step is required as it is important that the prediction model provides valid outcome predictions (Steyerberg et al., 2019). In this section, the control models developed in the previous sections are validated. The validation step is executed using the techniques in the article of Sargent (Sargent, 2013). Several quantitative and qualitative techniques are applied to the different control models. At each control model it is discussed which techniques are used and how.

5.1 Validation of the MPC 1S1G model

The MPC 1S1G model is validated using a combination of techniques. Animation and prediction validation are combined for the first validation and sensitivity validation is executed to conclude the validation. Both validation techniques are applied in a qualitative analysis.

Animation and prediction validation

Animation is a qualitative validation technique that uses a graphical representation of how the model evolves over time. Predictive validation makes use of a predicted system behavior and compares this with the model's behavior to see if it displays the same (Sargent, 2013). It can be predicted on a conceptual level how the model is expected to behave. When prices are lower than average, it is expected that the model stores the energy such that it can be sold to the market when the prices are high again, especially considering the lossless storage property of the Ocean Battery. Similarly, when the prices are high, it is expected that the model sells all energy to optimize the revenues obtained during the simulation. For this validation step, the 1S1G model has been simulated for one day such that it is graphically visible how the simulation model behaves. Figure 22 displays this behavior. By placing both the energy storage level and price graphs in the figure directly below each other, it can be observed that the model behaves as expected, as the energy is stored when the prices are low and is sold when the prices are at its peak. In addition, for the highest price peak in the model it would be expected that the Ocean Battery fills completely before this peak and drains fully during the peak. From Figure 22 it is observed that this is indeed the case. It can therefore be concluded that this validation step was successful.

Parameter variability

Parameter variability, or sensitivity analysis, can be used as a qualitative validation technique that consists of changing the input values to the model such that the effects on the model's behavior and output can be studied (Sargent, 2013). For this validation step it has been decided to change the input parameters with respect to the efficiency of the pump and the turbine. This validation technique is again combined with animation to observe the model's behavior. Five different efficiency parameters have been selected to test the validity of the model. One would expect the following: if the efficiency of the Ocean battery is low, only a little amount of energy is stored. When the efficiency increases, more energy is stored. Following all assumptions explained in Chapter 4, the only motivation to store energy is to sell it later for a higher price. This price difference has to overcome the efficiency losses at minimum, which is why it is expected that the higher the efficiency, the more energy is stored over time. From Figure 23 is can be observed that this is indeed the case, concluding that also this validation step was successful. An interesting outcome in this validation step

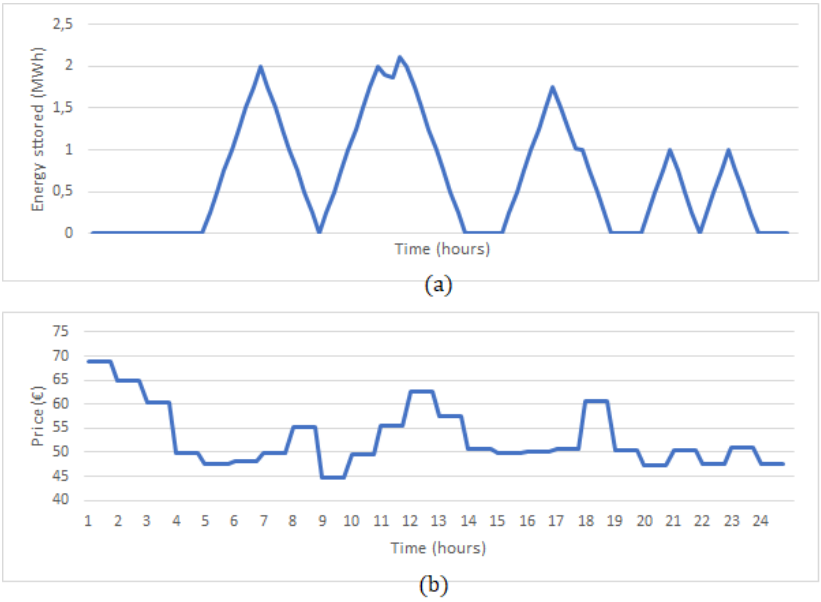

Figure 22: The behavior of the simulation model when simulated for a day in terms of storage level (a) and price (b).

is that at least for the first day of January 2019, when the efficiency parameters are set to a realistic value ($\eta_P = 75\%$ & $\eta_T = 80\%$), no energy is stored at all. This means that the fluctuations in price are not large enough to overcome the efficiency losses. For the purpose of this research an efficiency is selected for the actual simulations that allows the model to store a significant amount of energy. The basic settings for the simulations in this section can be found in Appendix E.

5.2 Validation of the RBC 1S1G model

The RBC 1S1G model is validated using the parameter variability and comparison to other models techniques. Both techniques are applied in a quantitative analysis.

Parameter variability

For the parameter variability validation step of this model, also the efficiency is adapted to observe the model's behavior. This cannot be executed similarly to the previous step, as the decision to store energy is solely based on the threshold price and therefore independent of the efficiency. Another method of determining the validity by changing the efficiency is to compare the total amount of energy sent to the Ocean Battery to the total amount of energy sold from the storage. For this validation step, a piece of code was added to the model that keeps track of these amounts of energy. It is expected that due to fact that a storage fills up to its maximum slower at a lower efficiency, the amount of energy sent to storage is higher in this case. In addition, the total amount of energy sold from the storage is lower when the efficiency is lower. In summary, the lower the efficiency, the more energy sent from the wind turbine to the storage and the less energy sold from the storage to the customer. The results of changing this parameter are listed in Table 11.

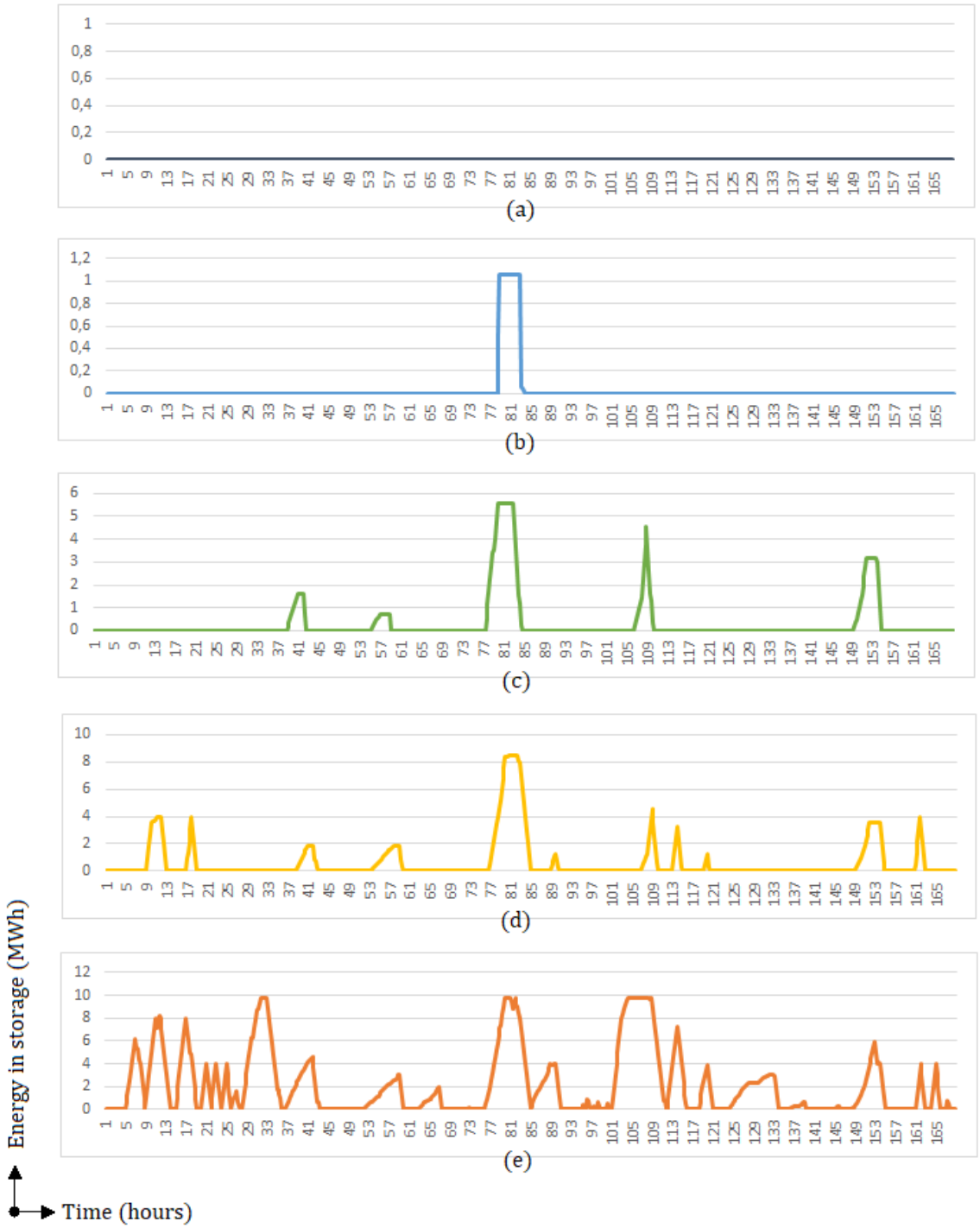

Figure 23: The effect of efficiency on the storage levels with the day-ahead market (2019). The efficiencies are (a) $\eta_P = 0.75, \eta_T = 0.8$; (b) $\eta_P = 0.8, \eta_T = 0.85$; (c) $\eta_P = 0.85, \eta_T = 0.9$; (d) $\eta_P = 0.9, \eta_T = 0.95$; (e) $\eta_P = 1, \eta_T = 1$.

Efficiency	Total energy received [MWh]	Total energy sold [MWh]
$\eta_P = 75\%, \eta_T = 80\%$	6050	3630
$\eta_P = 80\%, \eta_T = 85\%$	5809	3950
$\eta_P = 85\%, \eta_T = 90\%$	5586	4273
$\eta_P = 90\%, \eta_T = 95\%$	5381	4600
$\eta_P = 100\%, \eta_T = 100\%$	5013	5013

Table 11: Effects of changing the efficiency parameters on the amount of energy sent to the storage and sold from the storage.

Comparison to another model

For the second quantitative validation step, the outcomes of the model are compared to another model that was developed in Excel. In this Excel model, the amount of times the price exceeds the mean price of the data set is counted, as the actions of the RBC model are dependent on this value as the threshold price. Also a piece of code is therefore added to the RBC model to count the number of times the decision is made to drain the storage. The data sets from 2017-2019 of the day-ahead market and aFRR market were used for these calculations. The results are depicted in Tables 12 and 13. It can be observed that the results are identical, which concludes that also this validation was successful. All basic settings for the simulations in this section can be found in Appendix E.

Data set	Mean price [€]	Amount of times mean is exceeded
Day-ahead 2017	39.31	13896
Day-ahead 2018	52.53	15844
Day-ahead 2019	41.20	15296
aFRR-up 2017	43.18	6847
aFRR-up 2018	52.41	9712
aFRR-up 2019	42.55	8750

Table 12: The amount of times the mean of the data set is exceeded for various price data sets, by the Excel model.

Data set	Mean price [€]	Amount of times mean is exceeded
Day-ahead 2017	39.31	13896
Day-ahead 2018	52.53	15844
Day-ahead 2019	41.20	15296
aFRR-up 2017	43.18	6847
aFRR-up 2018	52.41	9712
aFRR-up 2019	42.55	8750

Table 13: The amount of times the mean of the data set is exceeded for various price data sets, by the Python model.

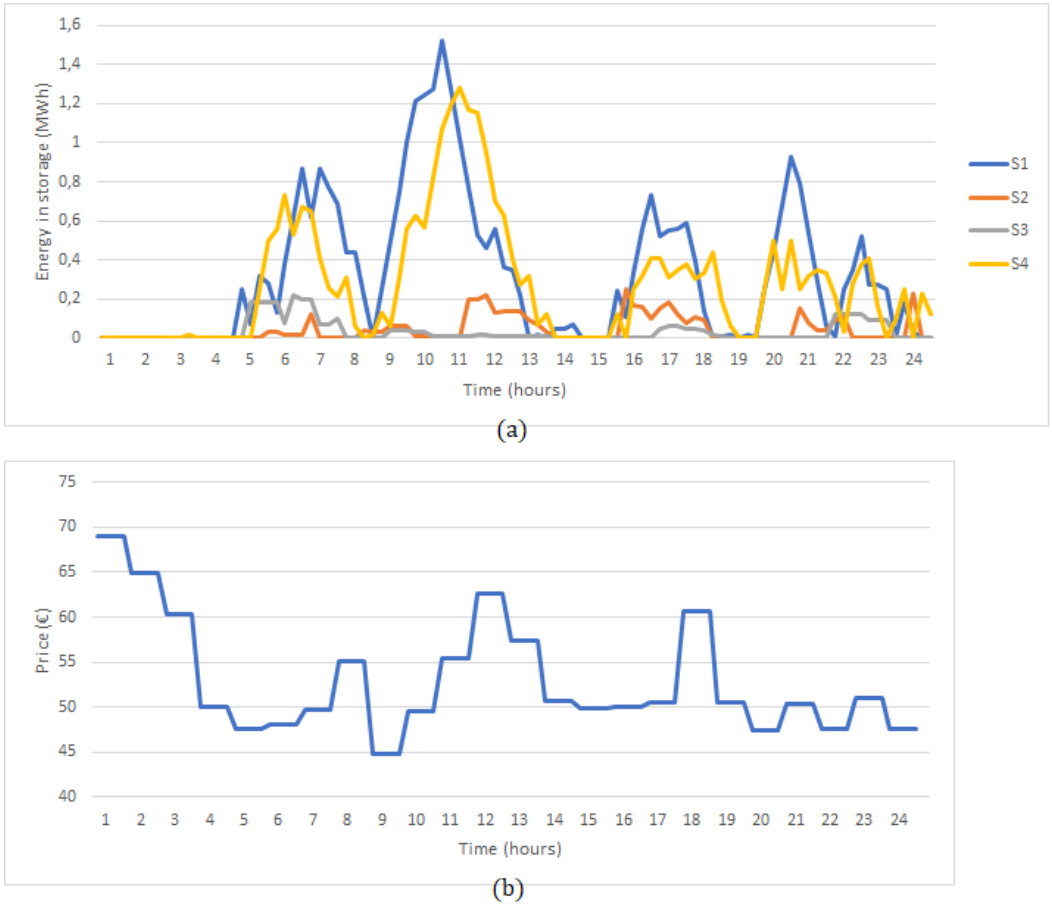

Figure 24: The behavior of the simulation model when simulated for a day in terms of storage levels (a) and price (b).

5.3 Validation of the MSMG model

Finally, to validate the multiple-storage-multiple-generator model two techniques are used that have also been used for the other validations: prediction validation and sensitivity validation. Prediction validation is applied as a qualitative validation again, while the sensitivity validation is applied in a quantitative analysis.

Prediction validation

For the prediction validation, a similar approach has been taken as for the MPC 1S1G model, namely to plot the curve of the energy in storage over time and check this graph with the expectations. An example has been taken of four storage units, of which two are directly connected to a wind turbine and two are not. For this model it is expected that the storage units that are connected to a wind turbine fill up more often and to a higher extent. For the model where it is assumed that a connection can pass a storage system instead of forcing the energy to be stored first before it can be transferred, it is expected that it is more or less random which storage is used. Figures 24 and 25 display these curves according to expectation and it is therefore concluded that the validation was successful.

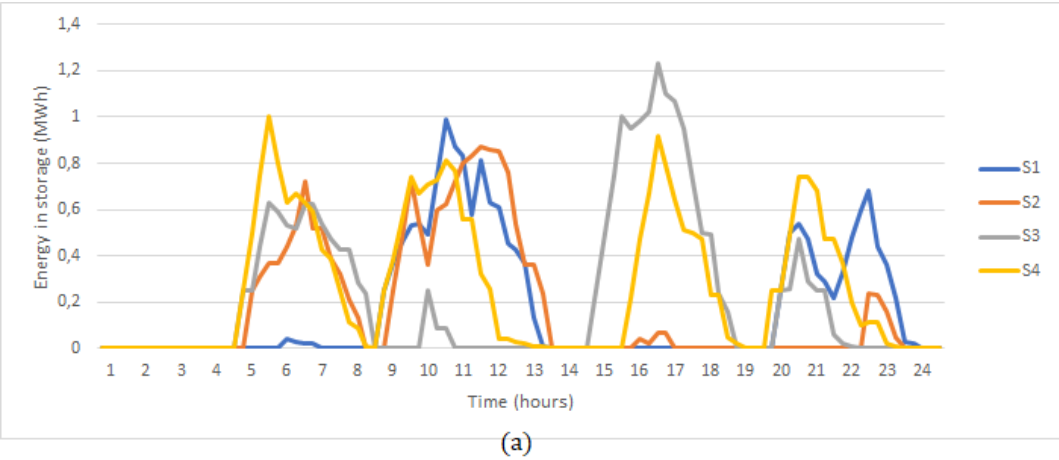

(a)

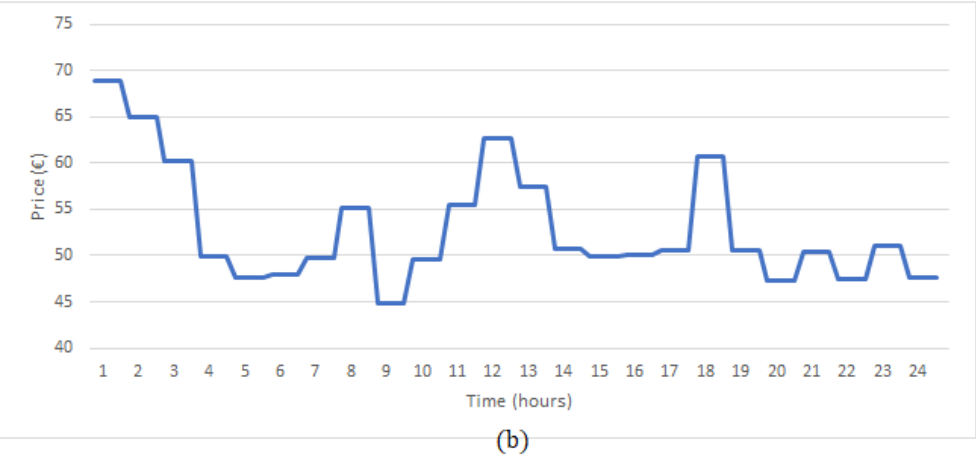

(b)

Figure 25: The behavior of the simulation model when simulated for a day in terms of storage levels (a) and price (b).

Sensitivity validation

Also for the MSMG model, a quantitative analysis has been executed to validate the model by investigating the effects of changing the efficiency of the PaT. Previously in this section it was observed that once the efficiency is increased or decreased, more or less energy is stored in the Ocean Batteries. For this validation step, the same efficiencies as in Figure 23 are tested in the MSMG MPC model. The simulation time is one day and the prediction horizon is set to 3 hours, which is equivalent to 6 time steps. The resulting amounts of energy sent to the storage from the wind turbine are presented in Table 14. From this table it is observed that the higher the efficiency, the more energy stored. In addition, the revenues generated from the model also tend to increase with an increasing efficiency. The fact that revenues can sometimes be slightly less when increasing the efficiency can be explained by that only one simulation for this validation was executed with each combination of efficiencies. The general trend, namely that the amount of energy stored becomes higher once the efficiency is increased, is a trend that is also expected in a real-world situation and it is therefore concluded that this validation was successful. All basic settings for these simulations are included in Appendix E. In this chapter, an answer to sub-question 5, *how can the proposed*

Efficiency	**Total energy received [MWh]**	**Revenue [€]**
$\eta_P = 75\%, \eta_T = 80\%$	23.5	15840
$\eta_P = 80\%, \eta_T = 85\%$	26.2	15804
$\eta_P = 85\%, \eta_T = 90\%$	31.2	16432
$\eta_P = 90\%, \eta_T = 95\%$	30.7	16313
$\eta_P = 100\%, \eta_T = 100\%$	36.1	16847

Table 14: Effects of changing the efficiency parameters on the amount of energy stored from the wind turbine and the revenues generated by the system.

control model be validated? has been provided and the control model has been validated by using these techniques. The successful validation of the control model marks the end of the treatment validation phase of the engineering cycle by Wieringa as explained in Chapter 1. The results can now be generated from the validated control model.

6 Results

In this chapter the results from the simulations are discussed. This chapter is organized as follows. First, the simulation set-up is explained. Second, a reference model is developed that calculates the revenues of the system without the implementation of Ocean Batteries. Thereafter, all results from the 1S1G model simulations are discussed, including the comparison of different price markets and the effects of different PaT efficiencies and prediction horizons. In addition, a comparison is made between the RBC and MPC results. Once insight in these results is provided, the results of the simulations with the MSMG model are discussed. The simulations for the MSMG are executed with a case study model. However, the developed MSMG model is generic, implying that any adjacency matrix of a system can serve as an input to the model to study the effects of changing the interconnections. Again, different price markets are tested, but insight is also provided in the behavior of the individual storage systems. Furthermore, sensitivity analyses are executed on the turbine capacity and the depth of the Ocean Batteries. The chapter is finished with a section that discusses the effects of extending the model with the possibility to buy energy from the market.

6.1 Simulation set-up

Recalling from Chapter 4, the model requires several external inputs. The price and wind power data sets, and the adjacency matrix describing the interconnections between the Ocean Batteries and wind turbines are imported from an Excel file. In Chapter 2 it was found that the prices can become negative, especially for the aFRR market. For this research it is assumed that prices are always positive, i.e. $\xi \geq 0$. All negative prices are therefore set to 0. The practical implication of this measurement is that if a situation occurs that the prices are negative and the storage units are full, electricity from the wind turbine is not sold to the market.

The initial state of the system, $E^{i,0}$, is assumed to be zero for all i, which means that all storage units are empty when the simulations are started. Next to these inputs, there is a number of variables that the model uses for its calculations, such as the depth of the Ocean Batteries, the maximum volume of the bladder and the efficiency and capacity of the PaT. The total simulation time that was selected was 1 year, as seasonal fluctuations in for example price or wind are now incorporated. For the simulation set-up, a distinction is made between the 1S1G set-up and the MSMG set-up. All parameters used for the 1S1G simulations are listed in Table 15 and all parameters used for the MSMG simulations are listed in Table 16. For the MSMG simulations, the number of Ocean Batteries and wind turbines have to be entered by the user of the model in order for it to work. Changes between both set-ups are as follows. First, the sampling time was changed from 900 $[s]$ to 1800 $[s]$ due to the large computational time of the MSMG simulation model. In Chapter 6.3 the effects of changing the sampling time are discussed. In addition, the efficiency of the PaT has been changed for the purpose of the research. The number of storage units in a cluster has also been changed to 3 for the MSMG simulations such that the total storage capacity matches the energy production from the wind turbines. All is explained in more detail in the corresponding sections of this chapter.

Parameter	Value	Description [units]
ST	31536000	Total simulation time $[s]$
T_s	900	Sampling time $[s]$
P	4	Prediction horizon $[hours]$
p_{ocean}	400000	Ocean pressure $[Pa]$
p_{atm}	100000	Maximum volume of the bladder $[m^3]$
η_P	0.75	Efficiency of the pump mode of the PaT $[-]$
η_T	0.8	Efficiency of the turbine mode of the PaT$[-]$
nrS	4	Number of storage units in a cluster $[-]$
TC	1	Capacity of the PaT $[MW]$

Table 15: Parameters used for the 1S1G simulations.

Parameter	Value	Description [units]
ST	31536000	Total simulation time $[s]$
T_s	1800	Sampling time $[s]$
P	3	Prediction horizon $[hours]$
p_{ocean}	400000	Ocean pressure $[Pa]$
p_{atm}	100000	Maximum volume of the bladder $[m^3]$
η_P	0.95	Efficiency of the pump mode of the PaT $[-]$
η_T	0.95	Efficiency of the turbine mode of the PaT$[-]$
nrS	3	Number of storage units in a cluster $[-]$
TC	1	Capacity of the PaT $[MW]$

Table 16: Parameters used for the MSMG simulations.

6.2 Reference model: without storage

A model is developed that sets a reference revenue for all future simulations. In this model, the energy that is generated and the price from two different price markets are an input to the model. The revenues are now calculated by

$$R_{j,k} = \xi_k \cdot E^G_{j,k}, \qquad j = 1,..,G, \tag{31}$$

where R, ξ, E^G are as in (22) and (19).

The resulting revenues are depicted in the graph in Figure 26. In this figure a distinction was made between the revenues for one operating wind turbine and two operating wind turbines. This distinction was made because results are generated for a One-Storage-One-Generator case study, thereby requiring the revenues from one wind turbine as a reference, and for a Multiple-Storage-Multiple-Generator case study, whereby two generators are in operation. Power data has been used from wind turbine 1 and 10 in the OG-WindFarm (see Appendix A). From Figure 26 it was derived that the yearly revenue differs for the three years that the data was retrieved from. The explanation for this is either that the wind turbine production fluctuates over the years or that the prices fluctuate over the years. The Python model and the numbers of the revenues in the graph for the reference model are included in Appendices I and J, respectively.

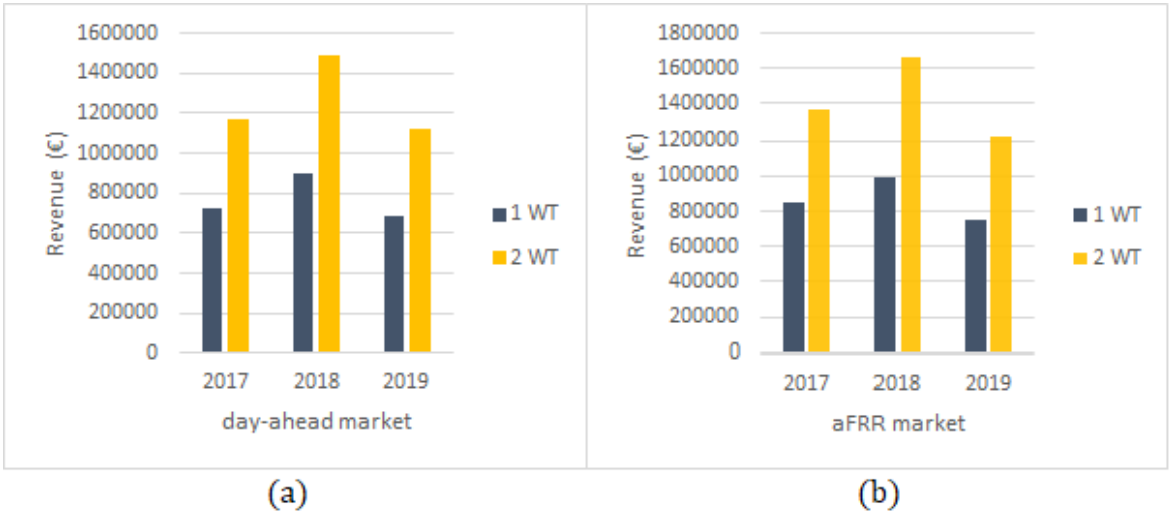

Figure 26: The calculated revenues from the day-ahead market (a) and aFRR market (b).

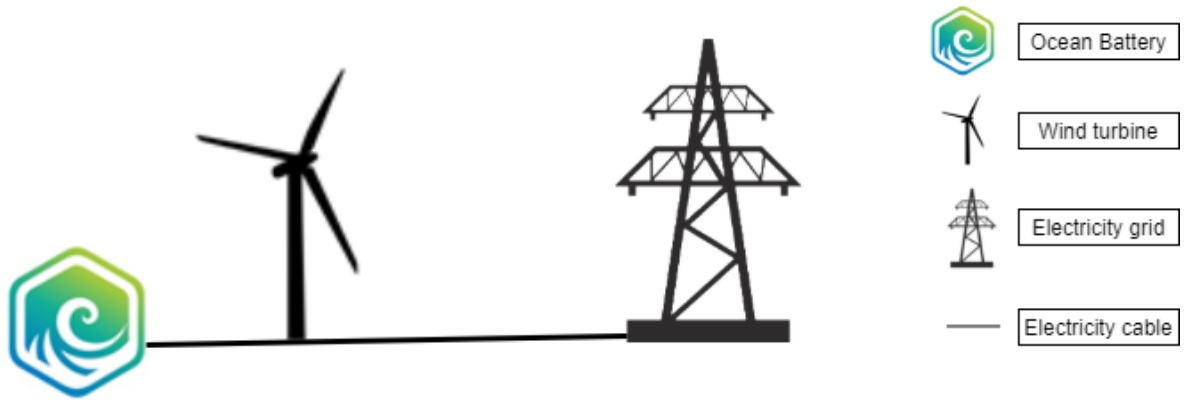

Figure 27: The set-up of the system for the 1S1G case study.

6.3 Results of the simulations: One-Storage-One-Generator

In this section, first the results from the MPC simulations are discussed. Thereafter, the results from the RBC simulations are discussed and finally, a comparison is made between the two control strategies with respect to the reference case built in the previous section. The set-up of the system for the 1S1G case is depicted in Figure 27.

Model Predictive Control results

During the development of the MPC model, it was observed that the SciPy optimizer did not always return feasible results and that this phenomenon was correlated with the initial conditions of the control variable u that is used for the optimizer. In addition, it is also dependent on the initial conditions what the optimizer returns as result of the objective function. This can be considered a limitation to the model, as it is expected that improvement in this area is possible. A part where the model checks if all constraints are satisfied by the outcome of the optimizer was added to the model and the model was run several times

to check how much the final outcome would deviate between runs. It was found that the difference between the individual runs was less than 1%, which is acceptable and it was therefore concluded that the model does not need several iterations to find the best result from the optimizer. For this simulation an efficiency of 100% of the pump and turbine was used. The outcomes of the simulations can be found in Appendix J.

Sensitivity of model parameters

In this section, the sensitivity of different parameters in the system with respect to the resulting revenues and computation time has been investigated, including the sampling time, the number of storage units in a cluster, the prediction horizon and the efficiency of the PaT.

The effects of changing the sampling time to 30 minutes

As one of the issues regarding the implementation of MPC is that computational times can be large, it was tested whether changing the sampling time from 15 to 30 minutes has a large effect on the final results. When the sampling time becomes larger, the situation occurs more often that the storage is full or empty before the time step has finished, which essentially means that the system has to wait until the time step is finished before it can do something else. For executing these tests, the yearly revenues have been calculated from the market prices of the day-ahead market and the aFRR market for the years 2017-2019. Again, an efficiency of 100% was used for the pump and turbine. From these simulations, it was observed that the resulting revenues on average only differed 0.4% in case of the day-ahead market and 5.2% for the aFRR market. The difference between these results can be explained by the following. For the aFRR market, the prices are determined each 15 minutes, which means that if the sampling time increases to 30 minutes, every one out of two data points is skipped by the simulation model. A different approach to this issue could be to take the average of the two data points that fall within the time step. This has not been tested for this research. Apart from the difference in revenue, another interesting aspect of the simulation is the total computation time for both sampling times. The results of this study are listed in Table 17. From this table it was derived that computation times are significantly larger for a sampling time of 15 minutes. As long as the simulation finishes within reasonable time, the sampling time of 15 minutes is preferred. However, from the little deviations in final results of the simulations discussed above, it was concluded that a sampling time of 30 minutes is also sufficient. The resulting revenues are included in Appendix J.

Data set	$T_s = 900$ s	$T_s = 1800$ s
Day-ahead market (2017)	00:36:04	00:05:14
Day-ahead market (2018)	00:38:02	00:05:15
Day-ahead market (2019)	00:35:04	00:04:48
aFRR market (2017)	01:02:58	00:08:48
aFRR market (2018)	00:57:58	00:08:25
aFRR market (2019)	01:01:34	00:08:37

Table 17: Computation times for a yearly simulation with MPC 1S1G code in $hh : mm : ss$.

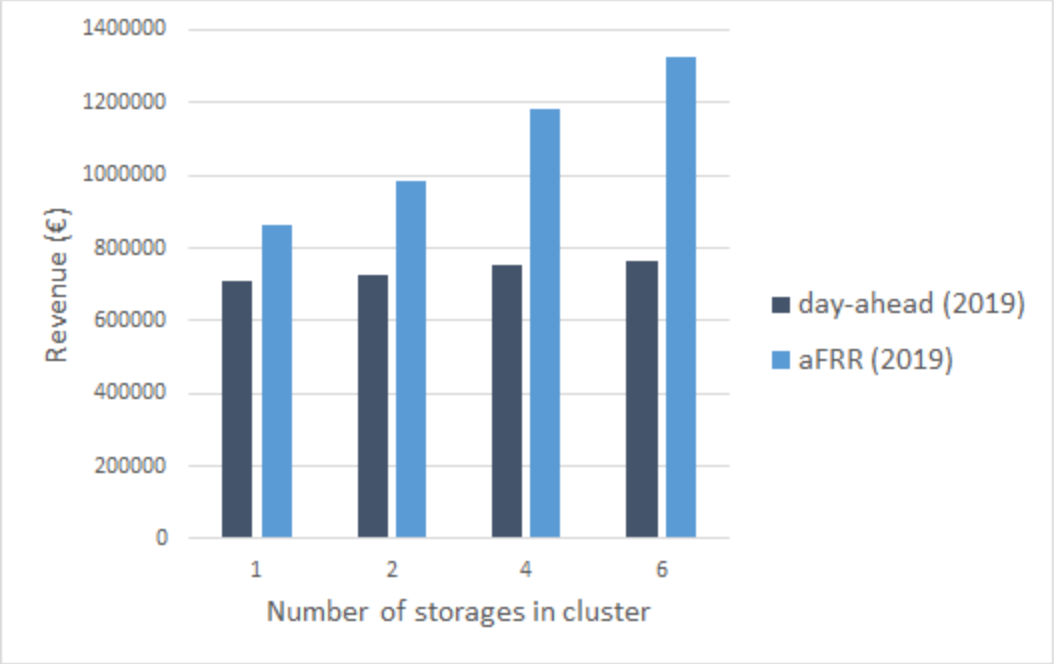

Figure 28: The calculated revenues from a variable number of storage systems in a cluster for the 1S1G MPC model.

The effects of changing the number of storage units in a cluster

The number of Ocean Batteries in a cluster represents N storage units that are always in the same state. The number of Ocean Batteries in a cluster influences the PaT capacity and the total storage capacity of the cluster. The simulations have been executed with the day-ahead (2019) and aFRR (2019) price market, and a PaT efficiency of 100%. The resulting yearly revenues are depicted in Figure 28. From this figure it is observed that the difference in revenues for the day-ahead market are relatively small, while the difference in revenues for the aFRR market with an increasing number of storage systems in a cluster is significant. This difference between the price markets can be explained by the price fluctuations that occur in both price markets: for the aFRR market the price fluctuations are larger and the model would therefore benefit more from a larger capacity when it is operating in this market. The general trend is that revenues increase with an increase in Ocean Batteries in a cluster for the same reason as just mentioned, namely that the capacity is higher for a larger number of Ocean Batteries in a cluster, which results in more revenues whenever the price peaks occur. From now on, the simulations are continued with four Ocean Batteries in a cluster. It should, however, be noted that the optimum number of storage systems in a cluster also depends on the costs of the Ocean Batteries. These costs are not included in this research.

Investigate the effects of changing the prediction horizon

The prediction horizon provides information about how far into the future the prices and wind turbine power can be observed or forecasted. In addition, the revenues over the full prediction horizon are optimized. Simulations have been executed with data from the day-ahead market (2019) and aFRR market (2019). An efficiency of 100% for the PaT was used for these simulations. The resulting yearly revenues are depicted in Figure 29. From

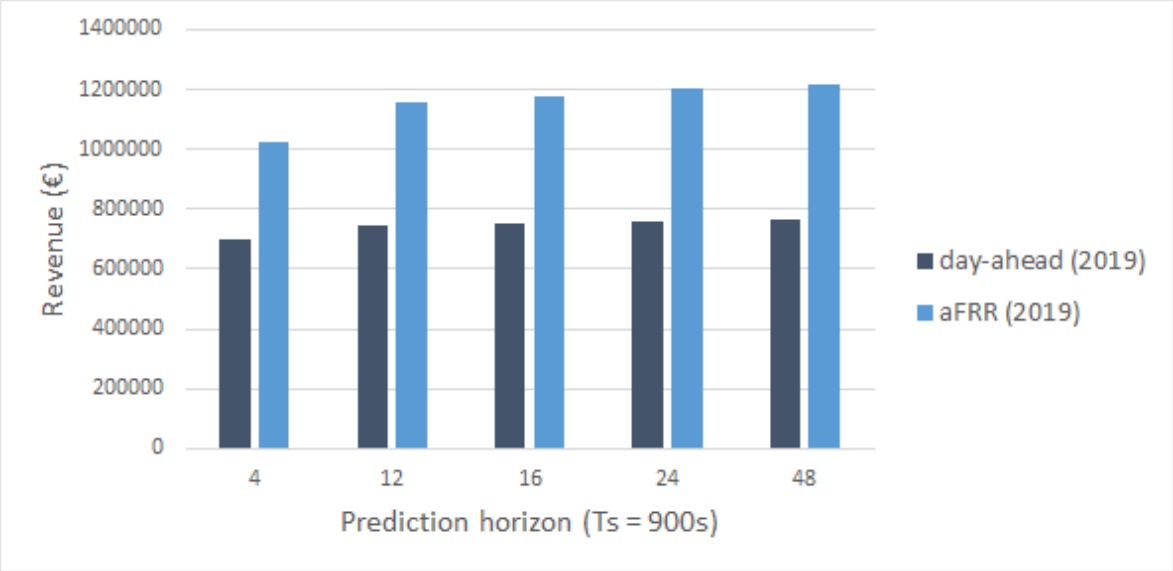

Figure 29: The calculated revenues from different prediction horizons for the 1S1G MPC model.

this figure it can be derived that the revenues increase significantly when the prediction horizon is changed from 4 to 12 time steps. The interpretation of this result is that a better forecast can be made when the model can observe the required input values further into the future. However, this is not a relation that continues forever. Already from Figure 29 it is observed that the revenues do not increase significantly anymore when the prediction horizon is increased from 24 to 48 time steps. The computation time, however, increases exponentially with the increasing prediction horizon as in Figure 30. The data points for the computation times were interpolated to observe the relation between the prediction horizon and the computation time. The computation times for the aFRR market are almost twice as high as the computation times for the day-ahead market. This difference can be explained by the fact that the simulations for the aFRR market have more trouble finding a feasible solution. Based on the results of these simulations, a prediction horizon of 24 time steps has been selected for further simulations. The tables representing the numbers that appear in Figure 29 and 30 are included in Appendix J.

The effects of the efficiency of the PaT

The effects of changing the efficiency of the pump and turbine mode have also been investigated. The starting point was the efficiency that is close to the real efficiency of the Ocean Battery ($\eta_P = 0.75$ & $\eta_T = 0.8$) and from there the efficiency was increased. The resulting revenues are depicted in Figure 31. In this figure it seems the revenues are not highly dependent on the efficiency. However, the difference in resulting revenues between the scenario with the lowest efficiency and the scenario without efficiency losses is more than 20%, which is a large difference. In addition, recalling the reference prices from the case in which there were no Ocean Batteries implemented gives €687603 (day-ahead, 2019) and €751783 (aFRR, 2019). The revenues for the lowest efficiencies are €691004 and €996447 for the day-ahead market and aFRR market, respectively. The general interpretation is that the MPC still

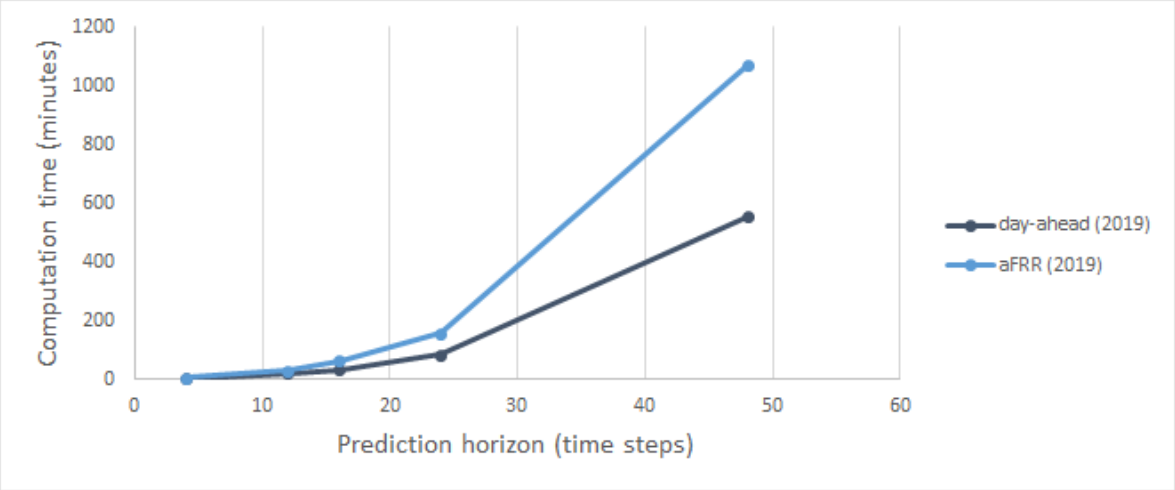

Figure 30: The computation times for different prediction horizons for the 1S1G MPC model.

optimizes the revenues of the system. However, for the day-ahead market this results in a situation where hardly any energy is stored since the difference in revenue is only 0.5%. For the aFRR market, this difference is still more than 30%. Based on these results, the calculations are continued with an efficiency of 85% for the pump mode and 90% for the turbine mode.

Results of the MPC 1S1G simulations

Now that all parameter sensitivities have been investigated and suitable values have been selected, the final MPC 1S1G simulations have been executed. The results have been generated for different price markets and are presented in Table 18. These results are compared to the results from the reference case (without storage) and the results of the RBC strategy at the end of Chapter 6.3. The predictive control ensures that the energy is sold from the wind turbines and storage units when the price is favorable, thereby maximizing the revenue generated by the system from this approach.

Data set	**Revenue [€]**
Day-ahead market (2017)	749756
Day-ahead market (2018)	924766
Day-ahead market (2019)	703323
aFRR market (2017)	1236307
aFRR market (2017)	1323391
aFRR market (2017)	1082613

Table 18: Yearly revenues for the 1S1G MPC strategy.

Rule Based Control results

The Rule Based Control algorithm relies on the rule that above a certain threshold price, energy is always sold from the wind turbine and storage, while below this threshold price, as much energy as possible is stored. For this research, the threshold price is set to the mean of

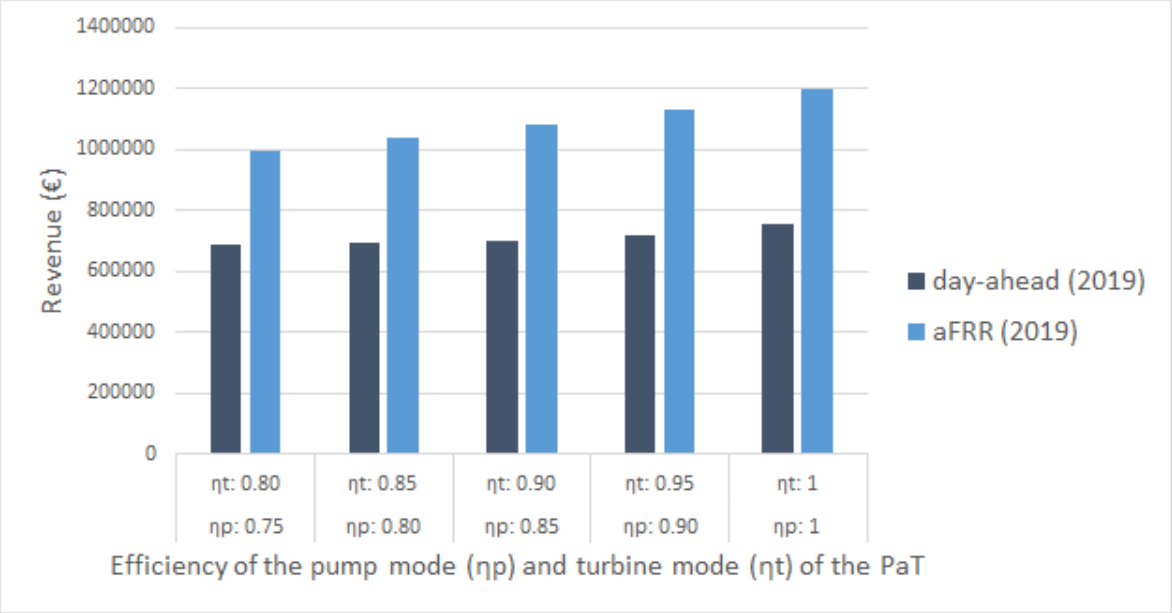

Figure 31: The resulting revenues from varying efficiencies for the pump and turbine mode of the PaT for the 1S1G MPC model.

the price market data set. The remainder of the RBC code is based on heuristics: per time step the state of the system is evaluated and the possible actions based on the previous state of the system are determined. For example, when the storage was almost full at $t-1$ and the market price at t is again below the threshold price, only that part of the energy can be stored that does not exceed the space in the storage. The space in the storage is calculated by

$$SiS_{k+1} = E_{max} - E_k, \tag{32}$$

where
SiS is the available space in the storage in $[MWh]$,
E_{max} is the maximum capacity of the storage in $[MWh]$,
E is the energy already in the storage in $[MWh]$.

Furthermore, the state of the system and the revenues generated by the RBC strategy are calculated by

$$E_{k+1} = E_k + u_k^G \cdot \eta_T \cdot E_{k+1}^G - u_k^S \cdot E_k, \text{ and} \tag{33}$$

$$R_k = \xi_k \cdot ((1 - u_k^G) \cdot E_k^G + u_k^S \cdot \eta_T \cdot E_k \tag{34}$$

where
u_k^G is the variable that controls the wind turbine $[-]$,
u_k^S is the variable that controls the storage $[-]$, and
all other variables as defined before.

The algorithm applied for the RBC strategy is described below.

Algorithm: Revenue by RBC

Inputs: ξ, E^G, E_0,
Outputs: u, R

for $k = 0, .., \tau$ **do**
    calculate the available space in storage from (32)
    if $\xi_k \geq \xi_{TP}$
        let $u_k^G = 1$
        if $E_k \geq TC$
            let $u_k^S = \frac{TC}{E_k}$
        else
            let $u_k^S = 1$
    else
        let $u_k^S = 0$
        calculate SiS_{k+1} from (32)
        if $SiS_k \leq E_k^G$
            let $u_k^G = \frac{SiS_k}{E_k^G}$
        else
            let $u_k^G = 1$
    calculate E_{k+1} with (33) and u_k^G, u_k^S
    return $R(\xi_k, u_k^G, u_k^S, E_k$ from (34)
end for

Also for the RBC strategy the effects of changing the efficiency on the resulting revenues have been investigated before arriving at the final simulations for the different price markets. All other parameters that have been investigated in the previous section that are applicable to the RBC strategy are the same as for the MPC strategy. The results from varying the efficiency of the RBC strategy are discussed below.

The effects of the efficiency of the PaT

The same efficiencies have been investigated for the pump mode and the turbine mode of the PaT as for the MPC strategy. The resulting revenues are depicted in Figure 32. Recalling the reference prices from the case in which there were no Ocean Batteries implemented gives €687603 (day-ahead, 2019) and €751783 (aFRR, 2019). For the RBC strategy, the lowest efficiency result in revenues of €660928 (day-ahead, 2019) and €906916 (aFRR, 2019). It is observed that this means that for the day-ahead market, the lowest efficiencies result in a yearly revenue that is below the reference case and therefore undesirable. Only when the efficiencies are above $\eta_P = 85\%$ and $\eta_T = 90\%$, the RBC strategy is able to generate higher revenues than the reference case, but even then the difference is insignificant (€687603 versus €688466). For the aFRR market, the RBC strategy is still significantly better than the reference case, even for the worst efficiency.

Results for the RBC 1S1G simulations

Also for the RBC strategy, the results for different price markets have been generated. The resulting revenues are presented in Table 19. In the next section, these results are compared

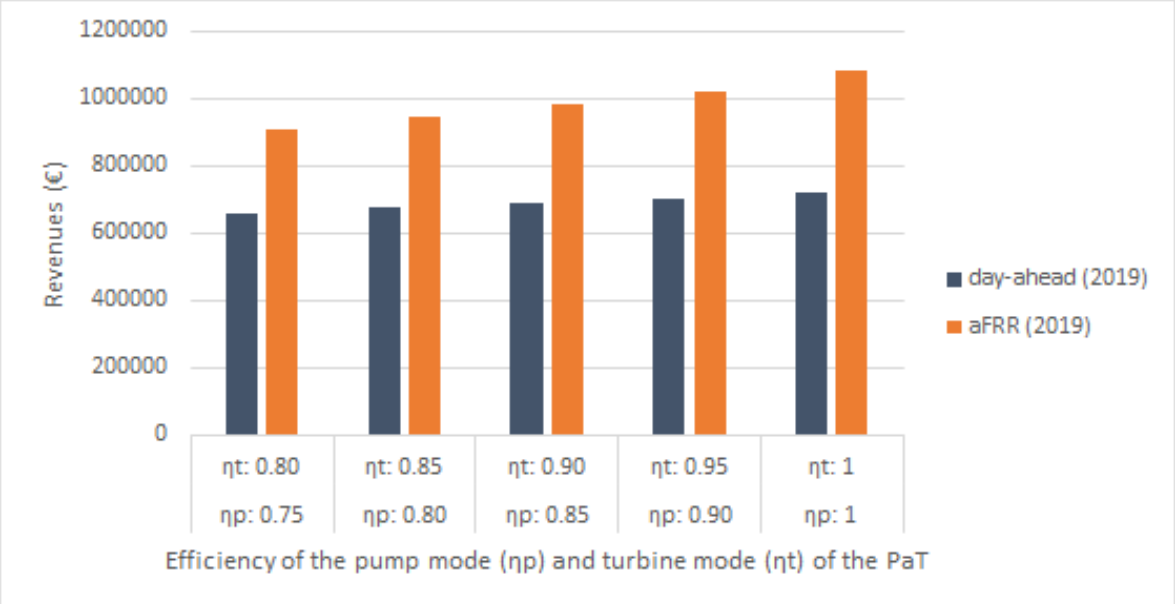

Figure 32: The resulting revenues from varying efficiencies for the pump and turbine mode of the PaT.

to the results from the reference case and the results of the MPC strategy. It should be mentioned that for the simulations of the RBC strategy, the results may be more promising once the sensitivity of the threshold price is investigated and the best value of this parameter is selected. However, this is not executed for this research.

Data set	Mean [€]	Revenue [€]
Day-ahead market (2017)	39.31	730969
Day-ahead market (2018)	52.53	902562
Day-ahead market (2019)	41.20	688466
aFRR market (2017)	43.18	1128840
aFRR market (2017)	52.41	1170752
aFRR market (2017)	42.55	981079

Table 19: Yearly revenues for the RBC strategy.

Comparison between the control strategies

The revenues that were obtained from the simulations in the previous sections have been depicted all-together to visualize the performance of the strategies compared to the reference case. The comparison of the results for the day-ahead market is depicted in Figure 33. From this graph it is observed that the RBC strategy is hardly an improvement to the reference case in terms of yearly revenues. The MPC strategy shows some potential, though relatively small. It could be argued that this can be seen as a 'worst case scenario', as there are other benefits of including storage units in a system. One of these benefits is the ability to guarantee a stable power output from the system or to use the storage units for the purpose of peak shaving.

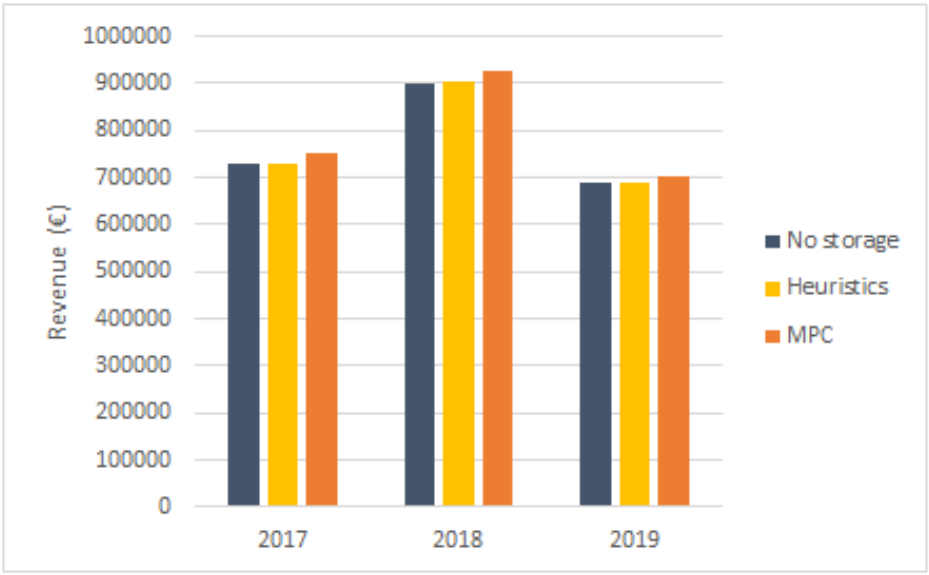

Figure 33: Yearly revenues from the reference case and the RBC and MPC strategies for the day-ahead market.

Another benefit could be that cable capacities can be decreased when adopting storage units in the system, or the impact of storage systems increases when the cable capacity is decreased (de Jonge, 2019). An effect of this would be that cable costs can be significantly reduced when storage units are implemented in the system.

For the aFRR market, however, the results are promising. Applying a RBC strategy improves the revenues with 28% compared to the reference case, while the MPC strategy improves the revenues by more than 41%. This is a very large improvement. However, a limitation to this simulation is that the assumption of perfect price forecast for the aFRR market is unrealistic, since prices are determined in real time and can be known only 15 minutes in advance. This has a large impact on the MPC model, which uses a prediction horizon of 4 hours. For the MSMG model it is investigated what the effects are of changing the prediction horizon to 15 minutes. For the 1S1G model it is observed that the RBC model also performs well for the aFRR market. Therefore, if there would be an excellent determination of the threshold price, for example based on the mean historic price, there is also potential without the need for a predictive model.

Summary of the 1S1G simulation results

A brief summary is given from the results obtained in this section. First of all, the revenues from a reference case in which there are no Ocean Batteries implemented were calculated. Thereafter, the MPC strategy has extensively been evaluated based on parameter sensitivity with respect to the sampling time, number of storage units in a cluster, prediction horizon and efficiency of the PaT before the final results were presented. Similarly, for the RBC model the sensitivity of the efficiency has also been evaluated before presenting the final simulation results. At the end, the different control strategies were compared to each other and to the reference case. From the comparison it can be concluded that the MPC strategy

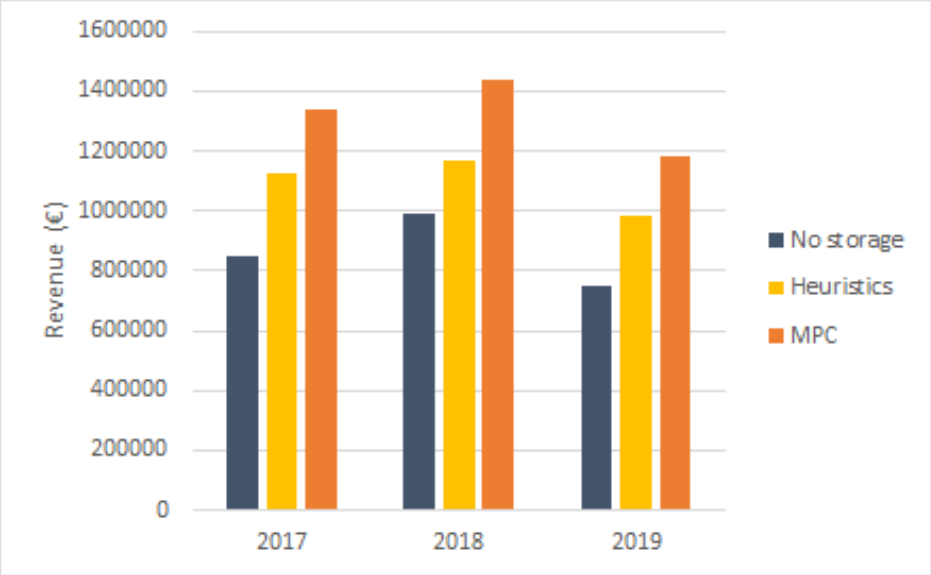

Figure 34: Yearly revenues from the reference case and the RBC and MPC strategies for the aFRR market.

has the largest potential, but the RBC strategy is also better than the reference case. From the results it can also be concluded that operating on the aFRR market is the best choice, as results can be significantly better than the reference case with respect to yearly revenues (28% for the RBC strategy and 41% for the MPC strategy). The results are overestimated for both strategies, as the RBC strategy assumes that the mean price for the full year is known, while the MPC strategy makes use of a larger prediction horizon than is actually possible. Nevertheless, it is expected that there is more potential in operating in this market than in the day-ahead market due to the larger price fluctuations that occur.

6.4 Results of the simulations: Multiple-Storage-Multiple-Generator

In this section, the results from the MSMG simulations are discussed. The MSMG simulations are executed for a specific case study: from the OG-WindFarm two wind turbines have been selected of which the power data serves as an input to the MPC model. Furthermore, four clusters of storage units are present in the system. These clusters of storage units are composed of three individual storage units each. As there are already two clusters of storage units per wind turbine, the number of storage units in a cluster has been reduced. The set-up of the system for the case study is depicted in Figure 35. In this figure, the electricity cables represent the interconnections between the Ocean Batteries, the wind turbines and the electricity grid. Only storage units that have a direct connection to a wind turbine, the 'direct storage units' are allowed to sell their generated electricity to the electricity grid. The so-called 'indirect storage units' have to send their energy to a direct storage first. Essentially, this means that it takes two time steps to sell from an indirect storage to the electricity grid. For the storing process this procedure is reversed. Wind turbines are always allowed to sell their electricity directly to the electricity grid. For the simulations, the results of the 'indirect model' are compared to the results of a 'direct model', where all indirect storage units are allowed to store directly from all neighboring wind turbines and sell directly to the electricity

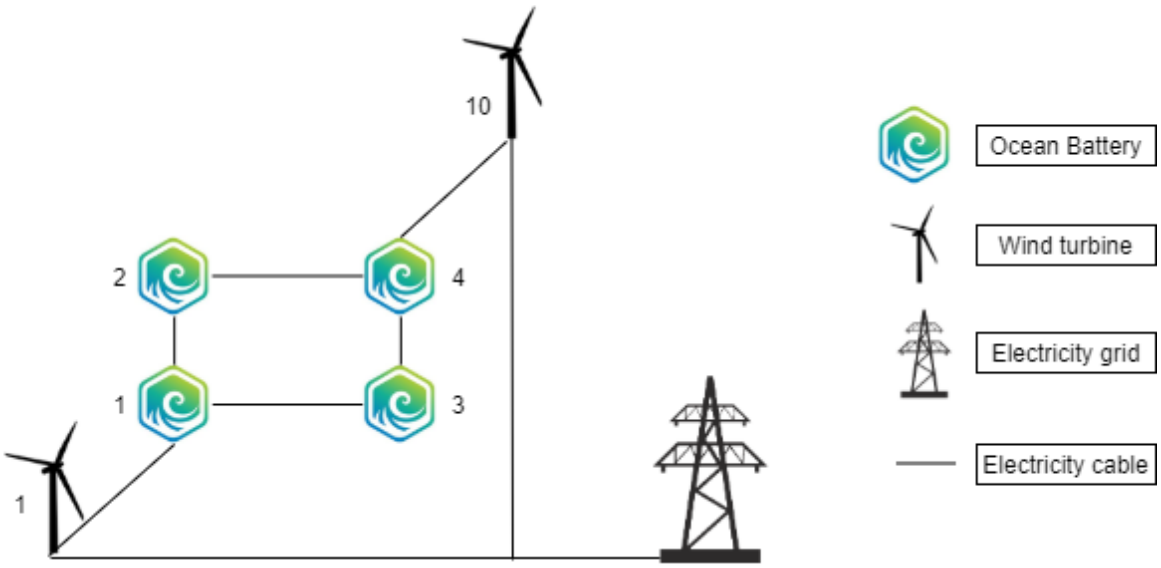

Figure 35: Set-up of the system for the MSMG case study.

grid. Thereafter, the sensitivity of the turbine capacity and the storage capacity in terms of the depth of the Ocean Batteries are analyzed. Furthermore, an extension to the model has been realized to allow the system to buy energy from the electricity grid. The results of this study are also discussed in this section, which is concluded with a comparison of all calculated revenues. Throughout this section, insight is provided into the behavior of the individual Ocean Batteries.

Simulation considerations

In this section, the results of the indirect storing simulations are discussed. First of all, the sampling time has been increased from 15 minutes to 30 minutes, as the simulations require a significant amount of time to finish. The simulations were executed by the University Peregrine cluster on a Intel Xeon E5 2680 processor. The computation times for a yearly simulation of the model for the different price markets is given in Table 20. These computation times hold for a sampling time of 30 minutes and are based on averages of the price markets from 2017-2019 and with a prediction horizon of 3 hours. The efficiency that was used is

Price market	**Indirect model**	**Direct model**
Day-ahead	12:30:00	05:30:00
aFRR	26:00:00	10:00:00

Table 20: The computation times for a yearly simulation of the MSMG MPC model for the different price markets in *hh:mm:ss*.

95% for both the pump and turbine mode of the PaT, since from the simulations it was observed that a relatively small amount of energy was stored in the Ocean Batteries for a lower efficiency. By using a high efficiency the potential of the model can be shown and a comparison can be made between the indirect and direct model. The effects of changing the

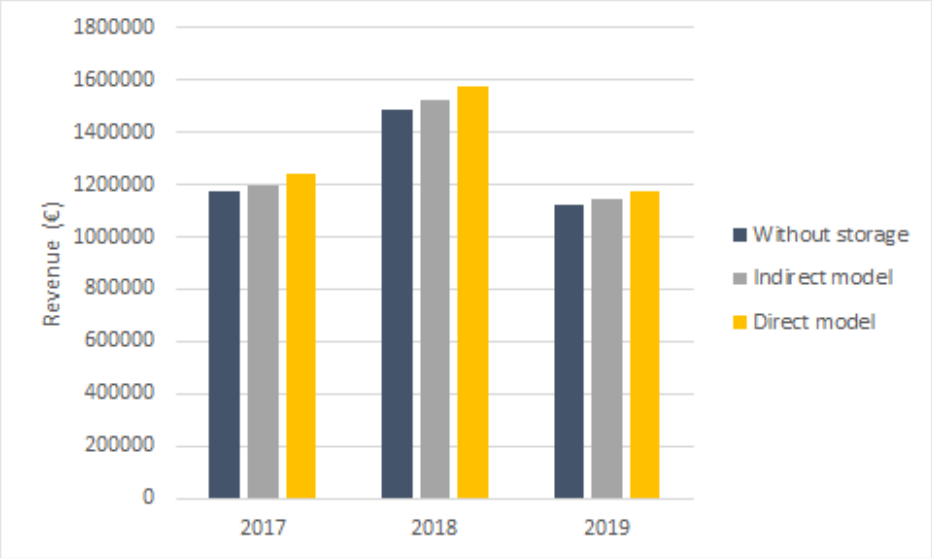

Figure 36: Revenues of the MSMG simulations for the years 2017-2019 of the day-ahead market.

prediction horizon on the computation times for a monthly simulation have also been studied. The results of this study are listed in Table 21. Based on the lengthy computation times of a prediction horizon of 6 hours, a prediction horizon of 3 hours is used for further simulations.

Prediction horizon	**Day-ahead market**	**aFRR market**
1 hour	00:03:36	00:04:16
3 hours	00:58:10	02:06:12
6 hours	09:41:07	> 24:00:00

Table 21: The computation times for a monthly simulation of the MSMG MPC model for a varying prediction horizon in *hh:mm:ss*.

Results of the simulations from the day-ahead market

The revenues resulting from the simulations for the day-ahead price market are depicted in Figure 36. A distinction is made between the resulting revenues from the indirect model and the direct model and the revenues are compared to the reference case. From this figure it is derived that for the day-ahead market, the results are only slightly better than the model without storage. As explained in Chapter 6.3, the situation where a wind turbine can sell an unlimited amount of electricity to the electricity grid at any time is hard to be improved by storage units when the price fluctuations in the market are small. Therefore, the model is considered 'worst case scenario' and many adaptations can be made to limit electricity flows through cables, and thereby reducing cable costs, to increase the positive effect of the MPC strategy.

Yearly revenues do not provide any insight into the behavior of the individual storage units in the system. Therefore, the maximum storage levels and the total amount of energy sent

to each of the storage units have been investigated. The resulting values for the maximum storage level are presented in Table 22. The fact that direct connections exist between wind turbines and all storage units in the direct model becomes clearly visible from this table. For the direct model, all storage units are filled to their maximum at some point. For the indirect model, the indirect storage units S2 and S3 are often not filled to their maximum storage level as it requires two time steps to fill or drain the storage with the accompanying efficiency losses. The fluctuations of the prices of the day-ahead market are apparently not large enough to overcome these drawbacks.

	Storage#	**Max level in 2017** [MWh]	**Max level in 2018** [MWh]	**Max level in 2019** [MWh]
Indirect model	1	6,0	6,3	6,9
	2	1,3	1,4	1,3
	3	1,4	1,4	1,4
	4	6,0	6,0	6,1
Direct model	1	7,3	7,3	7,3
	2	7,3	7,3	7,3
	3	7,3	7,3	7,3
	4	7,3	7,3	7,3

Table 22: Maximum storage levels (day-ahead market) for the MSMG simulations with the MPC strategy.

The total amount of energy sent to each of the storage units is presented in Table 23. From this table it is derived that indirect storage units are barely used for the day-ahead market, whereas the direct storage units are used to a similar extent for both models. The total proportion of energy sent to storage with respect to the total amount of energy produced is presented in Table 24. From this table it can be observed that only a relatively small amount of energy is stored compared to the amount of energy produced. The results for the direct model are significantly better than for the indirect model.

	Storage#	**Stored in 2017** [MWh]	**Stored in 2018** [MWh]	**Stored in 2019** [MWh]
Indirect model	1	1692	1483	1366
	2	19	31	30
	3	26	26	29
	4	1310	1208	1011
Direct model	1	1537	1347	1190
	2	1530	1380	1237
	3	1510	1387	1232
	4	1536	1316	1207

Table 23: Total energy sent to storage (day-ahead market) for the MSMG simulations with the MPC strategy.

	Year	Total production [MWh]	Sent to storage [MWh]	Percentage stored
Indirect model	2017	30170	2962	9.8%
	2018	28967	2639	9.1%
	2019	27876	2323	8.3%
Direct model	2017	30170	6434	21.3%
	2018	28967	5716	19.7%
	2019	27876	5123	18.4%

Table 24: The proportion of energy sent to storage for both models over the years 2017-2019.

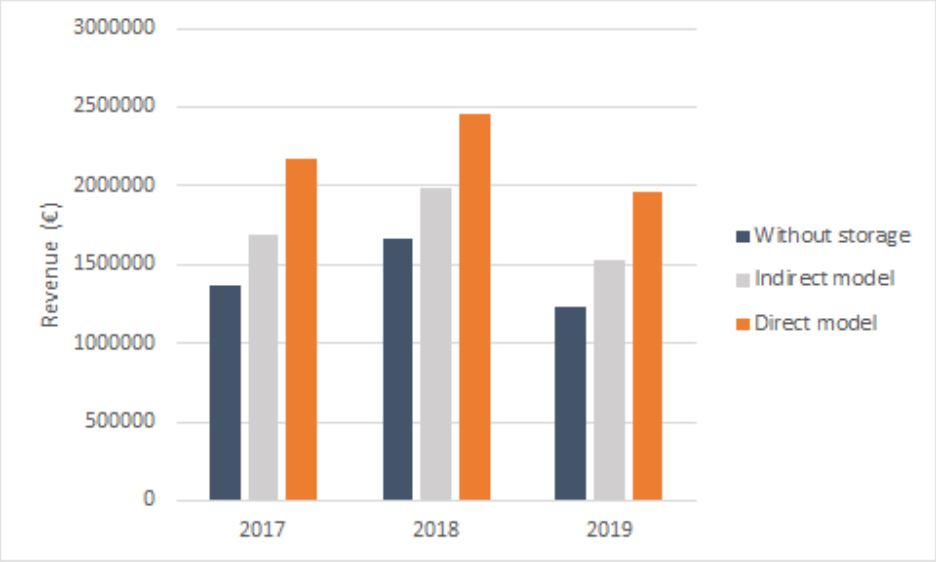

Figure 37: Revenues of the MSMG simulations for the years 2017-2019 of the aFRR market.

Results of the simulations from the aFRR market

Also for the aFRR market, results have been produced. The same format as for the day-ahead market was used for the aFRR market. Resulting revenues from the aFRR market for the years 2017-2019 and for the indirect and direct models are depicted in Figure 37. From this figure it is observed that both the indirect model and the direct model show large potential compared to the day-ahead market, as revenues can increase by around 20% for the indirect model and even close to 50% for the direct model. The results of this model rely heavily on the ability to sell a large amount of energy once the price peaks in the aFRR market occur. When for example the cable capacity would be restricted, it is expected that revenues slightly decrease as a result, though it it likely that more energy is stored.

The maximum storage levels for the individual storage units and the total amount of energy sent to the storage units have also been investigated for the aFRR market. The results are presented in Table 25 and Table 26. Evaluating the numbers in these tables results in that similar behavior is observed as for the day-ahead market. However, it seems that the total amount of energy sent to storage is higher than for the day-ahead market.

	Storage#	Max level in 2017 [MWh]	Max level in 2018 [MWh]	Max level in 2019 [MWh]
Indirect model	1	5,7	6,0	7,1
	2	1,5	1,5	1,5
	3	1,5	1,4	1,7
	4	5,9	6,0	7,3
Direct model	1	6,3	7,3	7,3
	2	6,4	7,3	7,3
	3	7,2	7,3	7,3
	4	6,0	7,3	7,3

Table 25: Maximum storage levels (aFRR market) for the MSMG simulations with the MPC strategy.

	Storage#	2017 [MWh]	2018 [MWh]	2019 [MWh]
Indirect model	1	4438	3954	4222
	2	122	90	113
	3	89	94	103
	4	3472	3243	3297
Direct model	1	3265	2937	3018
	2	3177	2983	3093
	3	3238	3003	3113
	4	3209	3022	3050

Table 26: Total energy sent to storage (aFRR market) for the MSMG simulations with the MPC strategy.

The results from investigating the total amount of energy that is stored relative to the total energy production are presented in Table 27. This confirms the hypothesis that the proportion of energy stored is higher for the aFRR market as compared to the day-ahead market, as the proportion stored is on average 25% for the indirect model and even 45% for the direct model. This indicates great potential for the MPC model to be applied on the aFRR market.

As discussed earlier in this chapter, assuming perfect forecast for the aFRR market is unrealistic. Therefore, simulations have been executed with a sampling time of 15 minutes and a prediction horizon of 2 time steps, which means that both the current price and the price in 15 minutes can be observed by the prediction model, in order to simulate the real-world behavior as close as possible. Resulting revenues and total energy stored are compared to the indirect model with a prediction horizon of 3 hours. The results are depicted in Figure 38 and Table 28. From the figure it is derived that indeed less revenues are obtained when the prediction horizon is set to 15 minutes, but the MPC strategy is still able to improve revenues compared to the reference case by around 25%. The total amount of energy stored is logically also smaller when the prediction horizon is set to 15 minutes. The table learns that roughly 35% less energy is stored. Although using a prediction horizon of 15 minutes decreases the positive effect of the MPC strategy on the total revenues, these results are still

	Year	Total production [MWh]	Sent to storage [MWh]	Percentage stored
Indirect model	2017	30170	7720	25.6%
	2018	28967	7031	24.3%
	2019	27876	7324	26.3%
Direct model	2017	30170	13567	45,0%
	2018	28967	12574	43.4%
	2019	27876	12921	46.4%

Table 27: The proportion of energy sent to storage for both models over the years 2017-2019.

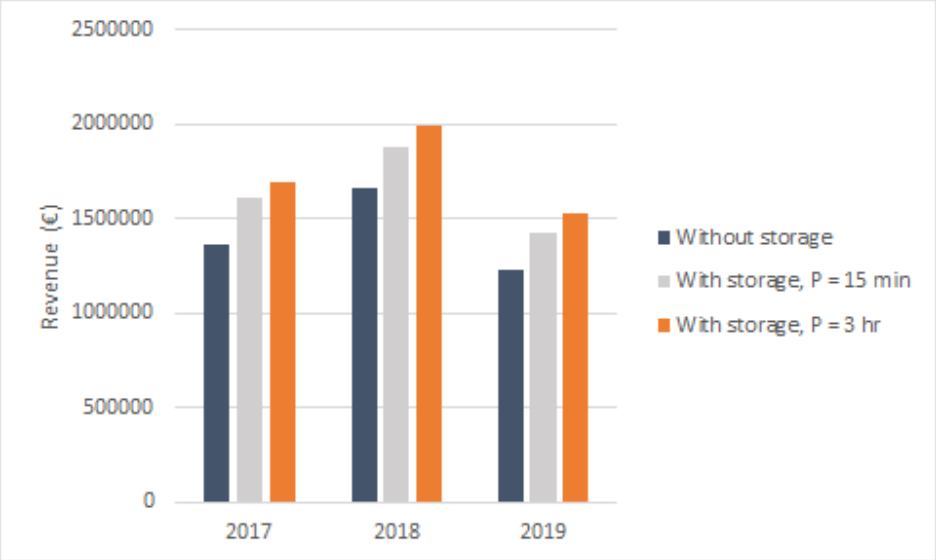

Figure 38: Revenues of the MSMG simulations for the years 2017-2019 with varying prediction horizons.

considered promising.

Summary of the results

For both the day-ahead and the aFRR market, the resulting revenues have been evaluated for an indirect model and a direct model and both have been compared to the reference case. For the day-ahead market, the results show little potential, as resulting revenues are only slightly better than the reference case and the total amount of energy stored is only around 10% for the indirect model and around 20% for the direct model. In addition, for the indirect model the Ocean Batteries are not filled to their maximum at any point in time. For the direct model this is the case and therefore this model may benefit from a greater depth of the Ocean Batteries.

For the aFRR market, the results show large potential, as around 20% higher revenues are obtained from the indirect model and even 50% for the direct model. In addition, the total amount of energy stored is higher than for the day-ahead market, namely 25% for the indirect

	Year	Total production [MWh]	Sent to storage [MWh]	Percentage stored
Indirect model (P = 3 hr)	2017	30170	7720	25.6%
	2018	28967	7031	24.3%
	2019	27876	7324	26.3%
Indirect model (P = 15 min)	2017	30170	5102	16.9%
	2018	28967	4576	15.8%
	2019	27876	4779	17,1%

Table 28: The proportion of energy sent to storage for both prediction horizons over the years 2017-2019.

model and 45% for the direct model. Even when the prediction horizon is reduced to a realistic value, the revenues are about 15% higher than the reference case and around 18% of the energy is stored. These results are still significantly better than for the day-ahead market. In this section, an answer has been provided to sub-question 6: *what are the revenues obtained by the control model in comparison with a no storage system for a predefined case study?*.

6.5 Sensitivity analyses

In this section, a sensitivity analysis is executed with respect to the turbine capacity and the depth at which the Ocean Batteries are placed such that the total storage capacity increases.

Results from the turbine capacity sensitivity analysis

When the turbine capacity is increased, more energy may be stored or drained at a specific time step, thereby opening the possibility to sell more energy when the price peaks occur. The sensitivity has been investigated for both the day-ahead and the aFRR market. The resulting revenues are depicted in Figure 39. From this figure it is derived that the revenues of the day-ahead market are not significantly affected by increasing the turbine capacity, while the revenues of the aFRR market can benefit from this up to an increase in revenue of 15% for a turbine capacity of 4 MW. However, considering the fact that turbines are usually expensive, it should be investigated whether the net present value of the turbine can be positive.

The total energy stored from different turbine capacities is depicted in Table 29. It is observed that the amount of energy stored in the Ocean Batteries increases significantly for the aFRR market, as opposed to the day-ahead market. The table is in line with the results from Figure 39. From both figures it is observed that the largest gain can be obtained by increasing the turbine capacity from 1 MW to 2 MW. This option should therefore carefully be considered once the final design is specified.

Results from the depth sensitivity analysis

Also a study to the sensitivity of the storage capacity has been executed. The depth is varied from 40 meters until 70 meters, thereby increasing the total storage capacity from 7.33 MWh to 13.61 MWh. Although one of the storage units was filled to its maximum for the aFRR market, changing the depth of the system has little to no impact on the yearly revenues

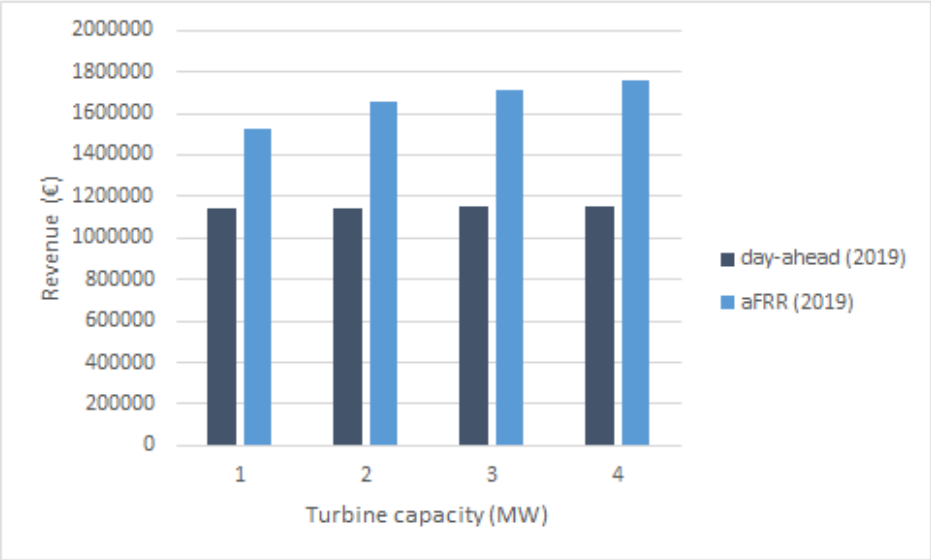

Figure 39: Revenues of the sensitivity of the turbine capacity with the MSMG simulations.

Turbine capacity [MW]	**Energy stored** [Mwh] day-ahead (2019)	**Energy stored** [MWh] aFRR (2019)
1	2323	7324
2	2993	9679
3	3338	10780
4	3364	11304

Table 29: Total amount of energy stored as a result of increasing the turbine capacity with the MSMG simulations.

resulting from the MPC strategy. The revenues obtained by these simulations are presented in Table 30 and the total amount of energy stored is presented in Table 31. Both of these tables indicate that increasing the depth for the Ocean Batteries would not result in higher revenues or more energy stored with its current design.

Summary of the results

From the sensitivity analyses for the turbine capacity and the depth of the Ocean Batteries, the following can be concluded. Increasing the turbine capacity has a positive effect on the yearly revenues, but it should be investigated whether the increased revenues are high enough to cover the costs of a turbine with a larger capacity. Especially increasing the turbine capacity from 1 MW to 2 MW seems a promising modification to the storage design. Increasing the depth of the Ocean Batteries, however, has little to no effect on the yearly revenues or the amount of energy stored. This outcome may be due to the current design of the Ocean Battery. If the design is changed in the future, another analysis can be executed to observe the effects of changing the depth for the new design. In this section, sub-question 7, *how are the storage capacity and turbine capacity related to the generated revenue?*, is answered.

Depth [m]	**Revenue [€]** day-ahead (2019)	**Revenue [€]** aFRR (2019)
40	1142382	1527080
50	1142414	1532689
60	1142044	1531546
70	1141822	1534316

Table 30: Yearly revenues from the sensitivity analysis to the depth of the Ocean Batteries.

Depth [m]	**Energy stored [MWh]** day-ahead (2019)	**Energy stored [MWh]** aFRR (2019)
40	2323	7324
50	2296	7340
60	2290	7352
70	2289	7345

Table 31: Total amount of energy stored as a result of increasing the depth of the Ocean Batteries with the MSMG simulations.

6.6 Model extension: possibility to buy from the market

For the purpose of this research, the model has been extended with the possibility to buy electricity from the market to fill the storage units. A few assumptions are made for this addition. These assumptions are as follows.

- Electricity can be bought from the market for the price at which the electricity can also be sold at that time.
- Electricity from the market is always available and unlimited.

In addition to these assumptions, a modification to the model is that negative prices are no longer set to zero. This essentially means that a situation may occur in which electricity is bought from the market for a negative price, which increases revenues of the system when it absorbs electricity. On the other hand, it is still not allowed that electricity is sold to the market for a negative price. A few situations are identified as possibly interesting for the extension of buying energy from the market.

1. The wind turbines are not producing (enough) energy to be stored when a price peak is approaching.
2. Negative prices occur often and revenues of the system increase when it absorbs electricity.

To investigate whether both situations occur in the price markets and production, it has been studied what the percentage of occurrence of both situations is.

Does it occur that wind turbines are not producing energy for a significant amount of time?

For all data sets from 2017-2019 with the wind power production the percentage of time steps that the wind turbine is producing less than 2 MW on average over an hour, which

is only 25% of its rated power, has been calculated. The results are presented in Table 32. These results show that almost one-third of the time the wind turbine is producing little to no electricity. Results from an analysis with this extension are therefore possibly interesting.

Year	2017	2018	2019
% no production	28.2%	34.4%	30.8%

Table 32: The percentage of time that the wind production is lower than 2 MW.

Do negative prices occur often?
For both the day-ahead market and the aFRR market the percentage of time that negative prices occur has been studied. The results are presented in Table 33. The answer to the

Price market	**Year**	**% negative prices**
Day-ahead	2017	0.0%
Day-ahead	2018	0.0%
Day-ahead	2019	0.03%
aFRR	2017	5.5%
aFRR	2018	4.5%
aFRR	2019	3.7%

Table 33: The percentage of time that prices are negative.

question heading this subsection is therefore that in the day-ahead market, negative prices hardly ever occur, while for the aFRR market, prices are less uncommon. From this result it was decided to continue this analysis only with the aFRR market. Before simulations could be executed, a few small adaptations to the model are made. First, an additional control variable is introduced.

- u^{RC} controls the amount of energy that is bought from the market and stored in storage i at time step k. The electricity grid is a single entity, which means that there is only one value that has to be added to the energy in storage i.

Then, the energy that is bought from the market has to be added to Equation 20. The formula now reads as

$$\begin{aligned}\hat{E}_{i,k+1} = \hat{E}_{i,k} + \eta_P \sum_{j=1}^{\#G} \hat{u}^{RG}_{i,j,k} \cdot \hat{E}^{G}_{j,k+1} + \eta_T \cdot \eta_P \sum_{j=1, i\neq j}^{\#S} \hat{u}^{RS}_{i,j,k} \cdot \hat{E}_{j,k} + \eta_P \cdot \hat{u}^{RC}_{i,k} \cdot E^M \\ -\eta_T \cdot \hat{E}_{i,k} \left[\left(\sum_{j=1, i\neq j}^{\#S} \hat{u}^{SS}_{i,j,k} \right) + \hat{u}^{SC}_{i,k} \right],\ i = 1,..,S,\end{aligned} \tag{35}$$

where
$\hat{E}_i$ is the predicted storage level of storage i in $[MWh]$,
$\hat{E}^G_j$ is the predicted energy generated by wind turbine j in $[MWh]$,
E^M is the available energy from the market in $[MWh]$,

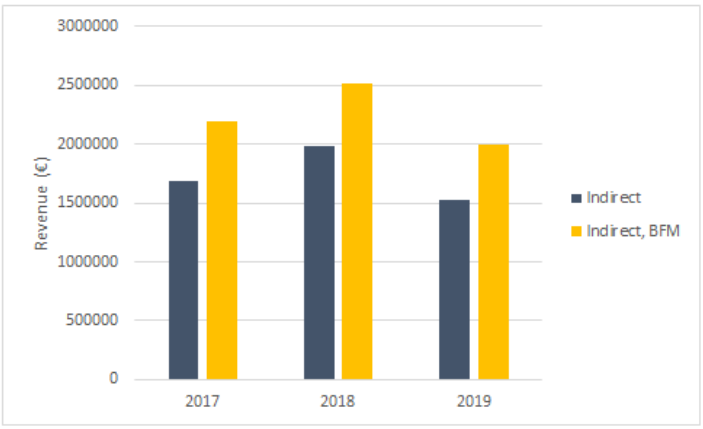

Figure 40: Revenues of the possibility to buy energy from the market from the MSMG simulations.

$\hat{u}^{RG}, \hat{u}^{RS}, \hat{u}^{SS}, \hat{u}^{SC}, \hat{u}^{RC}$ are the predicted control variables from the optimization $[-]$,
η_p is the efficiency of the pumping process $[-]$,
η_t is the efficiency of the draining process $[-]$.

Finally, the costs of electricity bought from the market should be subtracted from the revenues that are obtained by the storage units. The formula for the revenues now reads as

$$R_{i,k+1} = \xi_k \left(\eta_T \cdot u_{i,k}^{SC} \cdot E_{i,k} - u_{i,k}^{RC} \cdot E^M \right), \qquad i = 1,..,S, \tag{36}$$

where
R_i is the revenue from storage i in $[€]$,
ξ is the price of electricity in $[€]$,
$\eta_T, u^{SC}, u^{RC}, E_i, E^M$ as defined in (35).

The optimization problem in (43) is adapted accordingly and included in Appendix K. With the adaptions made to the models, simulations were executed. The results are analyzed in a similar way as in Chapter 6.4. The results are generated for the indirect model. The yearly revenues for this model over the years 2017-2019 with the aFRR market is depicted in Figure 40. From this figure it is derived that the indirect model benefits largely from the possibility to buy energy from the market. Revenues increase by around 30% compared to the situation in which this possibility was not there.

Year	**Stored from wind turbine** [MWh]	**Bought from market** [MWh]
2017	1086	15829
2018	1008	15392
2019	1015	16088

Table 34: The amount of energy stored from the wind turbine and bought from the market for 2017-2019.

It has been investigated much energy is actually bought from the market. The results are presented in Table 34. With these promising results, an answer has been provided to sub-question 8: *what are the effects of introducing the possibility to store energy that is bought from the market?* From this table it is observed that a much larger share that is sent to storage is originating from the market. Recalling the amount of energy stored from the wind turbine from Chapter 6.4, the amount of energy stored from a wind turbine when there is no possibility to buy from the market (around 7500 MWh) is significantly larger than when there is a possibility to buy energy from the market (around 1000 MWh). This difference can be explained by the fact that the model makes no distinction between buying energy from the market and storing energy from wind turbines: both result in equal revenues. Investigating the consequences gives that in real-life it is undesirable that the storage is not particularly used for the wind turbines, but rather for excess energy of the market. The model should be adapted such that it chooses storing energy from the wind turbines over storing energy from the market. Nevertheless, the total amount of energy stored when there is a possibility to buy from the market (around 17000 MWh) is more than twice the value of without this possibility and it is therefore considered to be a valuable extension to the model.

7 Discussion

The discussion is organized as follows. First, a brief summary is provided of the research steps that have been undertaken and the relevance of the developed distributed control model has been analyzed. Thereafter, the limitations of this research are discussed in relation to the assumptions made in this research. Finally, the possibilities for further research are listed and explained to finalize the discussion.

7.1 Summary of the research

The goal of this thesis was to *"develop a control model that ensures higher revenues of the distributed system of Ocean Batteries compared to a system without storage."* In order to achieve this goal, a number of research questions has been formulated. Throughout this report, answers were provided to these research questions, which were used to eventually develop the control model. The developed control model needs several inputs, such as the forecasted prices of the market and forecasted electricity production by the power source that activates the Ocean Batteries. After the strategy to retrieve these inputs was defined, the dynamical model of the Ocean Batteries was developed. To incorporate the full design of the system, the power source – for this research being wind turbines – and the interconnections between the Ocean Batteries, the wind turbines and the electricity grid have been studied and added to the model.

Different control strategies have been evaluated and applied to the model to develop the final control model. It has been decided to adopt a distributed control model with a supervisory MPC controller that decides on the actions of the distributed subsystems in the system. The proposed distributed control model has been validated and an extensive research to the results has been reported, including an analysis of parameter variability *(which values should be selected for the parameters of the model?)* for a simplified version of the model in which there is only one turbine and one storage in the system. In addition, a case study was performed that researched the revenues that could be obtained by the system in comparison to the revenues obtained by the reference case – in which there were no Ocean Batteries implemented. A sensitivity analysis has been executed for the turbine capacity and the depth of the Ocean Batteries in the system. Lastly, the proposed control model was extended with the possibility to buy electricity from the market.

In the developed control model, Ocean Batteries are used solely to store energy that can be sold for a higher price at a later time. However, in practice storage units are not implemented in a system solely to generate revenues. There are other interesting purposes that require storage units, especially as an addition to renewable energy systems. The purposes can be for example to ensure a stable energy supply from the wind turbines, to minimize the cable capacities in the system – thereby reducing costs – or for the purpose of peak shaving. Delivering a stable supply can be a useful purpose as this opens the possibility to sign contracts for a fixed and favorable price of electricity by a grid operator. It is therefore derived that the control model developed in this research can be considered a basis for extending the model with the purposes mentioned. It is expected that more energy is stored in the system as a result. For this research, the amount of energy stored in the Ocean Batteries was slightly disappointing, especially for the day-ahead market. However, taking into account the

efficiency losses of the Ocean Battery and the current purpose of the model it makes sense that for a price market that has little fluctuations, also a little amount of energy is stored.

In Chapter 1, the expected business context and technological aspects were mentioned. Evaluation of these aspects results in the following. The developed control model is able to increase revenues of the system compared to a system in which there are no Ocean Batteries involved, thereby contributing to the business context that Ocean Grazer BV is mainly concerned with. The developed distributed control model is considered an interesting tool that can be applied for further analyses of deep-sea storage systems. From the structure of the developed control model and the possibilities to apply the model on various designs of the system, with different parameters, it was derived that the technological aspects are present to a sufficient extent. A contribution is made to the industrial context by providing insight in the behavior of individual storage units in a distributed control system.

7.2 Limitations

There are some limitations to this research that have to be mentioned. These limitations refer to the assumptions made for the development of the control model and to the risk analysis provided in Chapter 1. First, some of the assumptions are highlighted and their limitations are discussed. Thereafter, the limitations related to the risks of the research are discussed.

1. Perfect forecasting

In this research, perfect forecasting of prices and energy production has been assumed. Although already discussed throughout the research, it should still be mentioned that perfect forecasting is unrealistic for the aFRR market and the developed MPC model therefore overestimates the revenues that can be obtained for this situation.

2. Unconstrained production & no selling limitations

For this research it was assumed that the demand of the market is unlimited, which is not the case in a real-world setting. However, the demand of the market is dependent on many other factors and could therefore not realistically be estimated for this research. If further research is conducted in this area, it may be worth investigating the demand of electricity.

3. Exclusion of cable design

Not only is it unrealistic to assume no energy losses inside the cable, there is also always a certain cable capacity constraining the flow of electricity. Cable lengths and capacities have not been taken into account for this research. This means that the model allows the energy to travel over large distances without any form of penalty, which should be incorporated into the control model to account for real-world behavior.

4. Instant production

The effects of the start-up time and reverse time of the PaT have been disregarded in this research. However, it should be investigated whether its effects are indeed as small as assumed in this research. More information on this topic is provided in the section with further research.

5. No down-time

Down-time of the Ocean Batteries or wind turbines caused by for example maintenance or failures has not been modelled. However, to resemble a real-world situation, the effects can be included as a percentage for testing the control model, for example. If the control model is applied in a real-world situation, the measured states of the subsystems are an input to the supervisory MPC controller, which should take adequate control actions once it observes that a subsystem is out of operation. This is necessary to account for a reduction in total capacity for example.

A limitation related to the risks associated to this research is the fact that power production from the wind turbines has been calculated rather than using an actual power production data set. The results may therefore deviate from the values in this research when the actual power production appears to be different. Once the model would be applied in a real-world situation, however, it receives (forecasted) power from the power source and the model can still function as in this research.

Furthermore, only one case study was executed in this research, which means that the effects of changing the interconnections between the storage units and the wind turbines could not be investigated. This limitation was caused by time constraints, and by the fact that the distributed control model was computationally very demanding. A solution to the latter problem is that part of the code - the iterations of optimization before a feasible solution is obtained - may be parallelized. However, it is not possible to parallelize the full code, as the iterations of the time steps are dependent of one another.

Related to the issue of the model requiring several iterations to find a feasible optimized result, it is worth mentioning that it was observed that the SciPy optimizer did not always return the optimum result. Although it never returned a value deviating significantly from the optimum, it must be noted that in theory the SciPy SLSQP minimizer is a local minimizer, which finds the local optimum instead of the global optimum. It may be investigated whether another method can be applied that ensures the global optimum is found by the optimizer.

The last limitation to this research is related to the lack of time for this research project to execute a full and complete analysis of the system. Nothing can be concluded on the profitability of the distributed system of Ocean Batteries without including the costs of the system, which has not been executed for this research. This is also an interesting direction for further research.

7.3 Further research

There are several possibilities identified for future research. It is believed that the developed distributed control mode with the supervisory MPC controller serves as a basis for the future research mentioned below.

Extensions of the model with the aforementioned purposes

In the summary of the research it was stated that the distributed control model developed is considered a basis for the following purposes of the model: to ensure a stable energy supply from the wind turbines, for the purpose of peak shaving or to minimize the cable capacities

in the system. The latter application is discussed below. These purposes can be added to the model, possibly with adaptation of the objective function and are therefore recommended as further research.

Cable optimization study

Large potential is expected when incorporating the cables between the Ocean Batteries and the wind turbines into an optimization study in which costs are included. It may for example be penalized when energy travels over a large distance. Distances between the Ocean Batteries, wind turbines and the electricity grid should be provided to the model. In this study, the losses of the cables can be incorporated and the optimum arrangement of Ocean Batteries inside a wind farm can be determined.

PaT optimization study

Many assumptions have been made in this research with respect to the PaT implemented in the Ocean Batteries as discussed in the section above. There are many design considerations with respect to the PaT that can be incorporated into a optimization study. Again, it is important that costs are also included in this study. Examples of the design considerations of the PaT are the type of turbine and its capacity. The type of PaT determines the effects of the start-up and reversing process of the PaT in terms of time and efficiency, but also the lifetime expectation of the PaT as a function of the switches made between pumping mode and turbine mode. The turbine capacity determines how much energy can be stored or sold at a specific time step. An interesting thought is that when the number of switches of the PaT is minimized, a situation may occur that a storage is empty and the system cannot deliver full capacity. A higher turbine capacity may account for this. The model should eventually determine, based on the profits that can be obtained by the system, whether it is beneficial to keep all storage units in operation at any time or whether it allows storage units to fully drain. The trade-off between costs and revenues is key in this study. In addition to the discussed considerations with respect to the PaT, previously in this research it was also mentioned that incorporation of a variable speed PaT allows the device to operate closer to its optimum efficiency, which can be an interesting factor to take into account for the PaT optimization study.

Floating wind turbines

Without diving into this topic, in Chapter 1 it was mentioned that the Ocean Batteries may be applied as anchors for floating wind turbines. Once this becomes an idea that is expected to be realized in the nearby future, optimization with respect to this design of the system can be executed. The control model developed in this research serves as an excellent basis for this study.

8 Conclusion

Concluding remarks on the research presented are made in this section. A two-stage analysis has been presented in Chapter 6. The first stage consisted of analyzing the system when there was only one Ocean Battery and one wind turbine incorporated. The different design choices for the model have been investigated in this stage and a comparison between two control strategies has been made. Only the best-performing control strategy, MPC, was implemented in the final control model. The second stage consisted of analyzing the system in which there were more Ocean Batteries and more than one wind turbine incorporated through a case study including four Ocean Batteries and two wind turbines. The conclusions from both stages are as follows.

Stage 1: One-Storage-One-Generator

First of all, the different design choices for the model have been analyzed. Conclusions from this analysis include the following.

- A sampling time of 30 minutes is a suitable choice for the model.
- The higher the number of storage units in a cluster, the more revenue can be generated. However, only for the aFRR market this increase is significant.
- A prediction horizon larger than 3 hours is a suitable choice for the model when making a trade-off between the predictive power of the model and the computation time.
- With the current numbers of efficiency of the Ocean Battery, little energy generated by the wind turbines is actually stored. The higher the efficiency, the more the Ocean Batteries are used.

Furthermore, the MPC strategy has been compared to the RBC strategy and the reference case with respect to revenues. When the efficiency is chosen higher than the current value, but lower than the ambitions for the future, namely $\eta_P = 85\%$ and $\eta_T = 90\%$, the RBC strategy is hardly an improvement to the reference case in terms of yearly revenues for the day-ahead market. However, the threshold price that determines whether the Ocean Batteries sell their energy can be optimized, which can possibly result in higher revenues. The MPC strategy can improve revenues by approximately 3%, which is also really small. The interpretation is that little energy is stored.

More promising results have been obtained for the aFRR market, where even the RBC strategy is able to improve revenues with 28% and the MPC strategy is able to improve revenues by more than 40%, both with respect to the reference case. The results of both strategies are overestimated as the RBC strategy assumes that the mean price for the full year is known, while the MPC strategy makes use of a larger prediction horizon than is actually possible. Nevertheless, it is expected that there is more potential in operating in this market than in the day-ahead market due to the larger price fluctuations that occur.

Stage 2: Multiple-Storage-Multiple-Generator

Results from the case study of the MSMG model are presented in this stage. Two models have been developed, an 'indirect' model and a 'direct' model, of which the latter assumes connections exist between all Ocean Batteries and wind turbines in the system, while for the

indirect model this is not the case and sometimes two time steps are required to transfer energy from a wind turbine to an indirect storage. Similar results from the day-ahead market have been obtained as for the 1S1G model: resulting revenues are only slightly better than the reference case and the total amount of energy stored is only around 10% for the indirect model and around 20% for the direct model. In addition, for the indirect model the Ocean Batteries are not filled to their maximum at any point in time. For the direct model this is the case and therefore this model may benefit from a greater depth of the Ocean Batteries.

For the aFRR market, the results show large potential, as around 20% higher revenues are obtained from the indirect model and even 50% for the direct model compared to the reference case. In addition, the total amount of energy stored is higher than for the day-ahead market, namely 25% for the indirect model and 45% for the direct model. Even when the prediction horizon is reduced to a realistic value, the revenues are about 15% higher than the reference case and around 18% of the energy is stored. These results are still significantly better than for the day-ahead market.

From the sensitivity analysis to the turbine capacity and the depth of the Ocean Batteries, the following can be concluded. Increasing the turbine efficiency has a positive effect on the yearly revenues, but it should be investigated whether the increased revenues are high enough to cover the costs of a turbine with a larger capacity. Especially increasing the turbine capacity from 1MW to 2MW seems a promising modification to the storage design. Increasing the depth of the Ocean Batteries, however, has little to no effect on the yearly revenues or the amount of energy stored. This outcome may be due to the current design of the Ocean Battery. If the design is changed in the future, another analysis can be executed to observe the effects of changing the depth for the new design.

The results from extending the model with the possibility to buy energy from the market are very promising: twice as much energy is stored in the Ocean Batteries and revenues increase by approximately 30% compared to the system without this option. It should be noted, however, that sometimes the model buys energy from the market and sells energy from the wind turbines simultaneously instead of storing the energy from the wind turbines since it makes no difference from a revenue perspective. Not only is this physically impossible, it is also undesirable and should be penalized in further analyses.

The main research question that served as a basis throughout this research, *how should the distributed system of Ocean Batteries be controlled?*, can finally be answered. From a revenue maximization point of view, it is advised to adopt a distributed control system consisting of the distributed controls of the subsystems and a supervisory MPC controller that determines the optimum actions of the system as a whole. It has been proven that revenues obtained can be higher than for the reference case without Ocean Batteries. Although many extensions to the presented control model have not been included due to time restrictions of this research, it is nevertheless concluded that the goal of this research is achieved.

References

Abdeltawab, H. H. and Mohamed, Y. A.-R. I. (2015). Market-oriented energy management of a hybrid wind-battery energy storage system via model predictive control with constraint optimizer. *IEEE Transactions on Industrial Electronics*, 62(11):6658–6670.

Adaramola, M. and Krogstad, P.-Å. (2011). Experimental investigation of wake effects on wind turbine performance. *Renewable Energy*, 36(8):2078–2086.

Alagappan, L., Orans, R., and Woo, C.-K. (2011). What drives renewable energy development? *Energy policy*, 39(9):5099–5104.

Alkano, D. (2016). *Two-layer distributed optimal control for energy system integration*. PhD thesis, Ph. D. dissertation, University of Groningen, Netherlands.

Barbour, E., Wilson, I. G., Radcliffe, J., Ding, Y., and Li, Y. (2016). A review of pumped hydro energy storage development in significant international electricity markets. *Renewable and Sustainable Energy Reviews*, 61:421–432.

Barradas-Berglind, J., Meijer, H., van Rooij, M., Clemente-Pinol, S., Galvan-Garcia, B., Prins, W., Vakis, A., and Jayawardhana, B. (2016). Energy capture optimization for an adaptive wave energy converter. In *Proc. of the RENEW2016 Conference*, pages 171–178.

Barthelmie, R. J., Pryor, S. C., Frandsen, S. T., Hansen, K. S., Schepers, J., Rados, K., Schlez, W., Neubert, A., Jensen, L., and Neckelmann, S. (2010). Quantifying the impact of wind turbine wakes on power output at offshore wind farms. *Journal of Atmospheric and Oceanic Technology*, 27(8):1302–1317.

Bijl, H. (2019). Techno-economic analysis of energy storage systems for offshore wind farms. *Master thesis IEM, University of Groningen*.

Bouzid, A. M., Guerrero, J. M., Cheriti, A., Bouhamida, M., Sicard, P., and Benghanem, M. (2015). A survey on control of electric power distributed generation systems for microgrid applications. *Renewable and Sustainable Energy Reviews*, 44:751–766.

Castellani, F., Astolfi, D., Garinei, A., Proietti, S., Sdringola, P., Terzi, L., and Desideri, U. (2015). How wind turbines alignment to wind direction affects efficiency? a case study through scada data mining. *Energy Procedia*, 75:697–703.

Chen, C.-L. (2008). Optimal wind–thermal generating unit commitment. *IEEE transactions on energy conversion*, 23(1):273–280.

Clauß, J., Finck, C., Vogler-Finck, P., and Beagon, P. (2017). Control strategies for building energy systems to unlock demand side flexibility–a review. In *IBPSA Building Simulation 2017, San Francisco, 7-9 August 2017*. IBPSA.

Commission, I. E. et al. (2007). Efficient electrical energy transmission and distribution. *Switzerland, IEC*.

Darabian, M. and Jalilvand, A. (2017). A power control strategy to improve power system stability in the presence of wind farms using facts devices and predictive control. *International Journal of Electrical Power & Energy Systems*, 85:50–66.

de Jonge, J. (2019). Energy storage as a partial substitute for transmission network capacity for offshore energy production. *Bachelor thesis IEM, University of Groningen*.

Deane, J. P., Gallachóir, B. Ó., and McKeogh, E. (2010). Techno-economic review of existing and new pumped hydro energy storage plant. *Renewable and Sustainable Energy Reviews*, 14(4):1293–1302.

Dijkstra, H., Barradas-Berglind, J., Meijer, H., van Rooij, M., Prins, W., Vakis, A., and Jayawardhana, B. (2016). Revenue optimization for the ocean grazer wave energy converter through storage utilization. In *Proc. of the 2nd Int. Conf. on Renewable Energies Offshore-RENEW*, pages 207–213.

Dijkstra, T. (2016). Maximizing revenue of electricity generated by the ocean grazer. *Master thesis IEM, University of Groningen*.

Dincer, I. (2000). Renewable energy and sustainable development: a crucial review. *Renewable and sustainable energy reviews*, 4(2):157–175.

Drew, B., Plummer, A. R., and Sahinkaya, M. N. (2009). A review of wave energy converter technology.

ENTSOE (2019). Data view. `https://transparency.entsoe.eu/transmission-domain/r2/dayAheadPrices/show?name=&defaultValue=false&viewType=GRAPH&areaType=BZN&atch=false&dateTime.dateTime=05.11.2019+00:00|CET|DAY&biddingZone.values=CTY|10YNL----------L!BZN|10YNL----------L&dateTime.timezone=CET_CEST&dateTime.timezone_input=CET+(UTC+1)+/+CEST+(UTC+2)#`. (Accessed on 05/11/2019).

EPEXSPOT (2019). Epex spot se: Details. `https://www.epexspot.com/en/press-media/press/details/press/Traded_volumes_soar_to_an_all-time_high_in_2018`. (Accessed on 05/11/2019).

EPEXSPOT (n.d.). Epex spot se: About epex spot. `http://www.epexspot.com/en/company-info/about_epex_spot`. (Accessed on 04/11/2019).

Farhangi, H. (2009). The path of the smart grid. *IEEE power and energy magazine*, 8(1):18–28.

Galus, M. D., La Fauci, R., and Andersson, G. (2010). Investigating phev wind balancing capabilities using heuristics and model predictive control. In *IEEE PES general meeting*, pages 1–8. IEEE.

Garcia-Rosa, P. B., Cunha, J. P. V. S., Lizarralde, F., Estefen, S. F., Machado, I. R., and Watanabe, E. H. (2013). Wave-to-wire model and energy storage analysis of an ocean wave energy hyperbaric converter. *IEEE Journal of Oceanic Engineering*, 39(2):386–397.

Gebraad, P., Thomas, J. J., Ning, A., Fleming, P., and Dykes, K. (2017). Maximization of the annual energy production of wind power plants by optimization of layout and yaw-based wake control. *Wind Energy*, 20(1):97–107.

Gebraad, P. M., Teeuwisse, F., Van Wingerden, J., Fleming, P. A., Ruben, S., Marden, J., and Pao, L. (2016). Wind plant power optimization through yaw control using a parametric model for wake effects—a cfd simulation study. *Wind Energy*, 19(1):95–114.

Gowrisankaran, G., Reynolds, S. S., and Samano, M. (2016). Intermittency and the value of renewable energy. *Journal of Political Economy*, 124(4):1187–1234.

Grauers, A. (1996). Efficiency of three wind energy generator systems. *IEEE Transactions on Energy Conversion*, 11(3):650–657.

Guo, Y., Ru, P., Su, J., and Anadon, L. D. (2015). Not in my backyard, but not far away from me: Local acceptance of wind power in china. *Energy*, 82:722–733.

Hansen, M. O. (2015). *Aerodynamics of wind turbines*. Routledge.

Helseth, A. (2018). *Proceedings of the 6th International Workshop on Hydro Scheduling in Competitive Electricity Markets*. Springer.

IRENA (2014). Irena's global renewable energy roadmap, remap 2030: Summary of findings. `https://www.irena.org/-/media/Files/IRENA/Agency/Publication/2014/IRENA_REmap_summary_findings_2014.pdf`. (Accessed on 10/16/2019).

Karger, C. R. and Hennings, W. (2009). Sustainability evaluation of decentralized electricity generation. *Renewable and Sustainable Energy Reviews*, 13(3):583–593.

Kiener, E. (2006). Analysis of balancing markets of electricity in europe. `http://www.diva-portal.org/smash/get/diva2:614429/FULLTEXT01.pdf`.

KNMI (2019). Knmi - uurgegevens van noordzee stations. `https://www.knmi.nl/nederland-nu/klimatologie/uurgegevens_Noordzee`. (Accessed on 11/01/2019).

Koo, B. J., Goupee, A. J., Kimball, R. W., and Lambrakos, K. F. (2014). Model tests for a floating wind turbine on three different floaters. *Journal of Offshore Mechanics and Arctic Engineering*, 136(2):020907.

Kulakowski, B. T., Gardner, J. F., and Shearer, J. L. (2007). *Dynamic modeling and control of engineering systems*. Cambridge University Press.

KULEnergyInstitute (2015). The current electricity market design in europe.

Kumar, P., Kothari, D. P., et al. (2005). Recent philosophies of automatic generation control strategies in power systems. *IEEE transactions on power systems*, 20(1):346–357.

Kusiak, A. and Song, Z. (2010). Design of wind farm layout for maximum wind energy capture. *Renewable energy*, 35(3):685–694.

Ladenburg, J. (2008). Attitudes towards on-land and offshore wind power development in denmark; choice of development strategy. *Renewable Energy*, 33(1):111–118.

Lakshmi, K. and Vasantharathna, S. (2014). Gencos wind–thermal scheduling problem using artificial immune system algorithm. *International Journal of Electrical Power & Energy Systems*, 54:112–122.

Lee, K. Y. and El-Sharkawi, M. A. (2008). *Modern heuristic optimization techniques: theory and applications to power systems*, volume 39. John Wiley & Sons.

Meral, M. E. and Çelík, D. (2019). A comprehensive survey on control strategies of distributed generation power systems under normal and abnormal conditions. *Annual Reviews in Control*, 47:112–132.

Morabito, A. and Hendrick, P. (2019). Pump as turbine applied to micro energy storage and smart water grids: A case study. *Applied energy*, 241:567–579.

Moskalenko, N., Rudion, K., and Orths, A. (2010). Study of wake effects for offshore wind farm planning. In *2010 Modern Electric Power Systems*, pages 1–7. IEEE.

Mousavi, N., Kothapalli, G., Habibi, D., Khiadani, M., and Das, C. K. (2019). An improved mathematical model for a pumped hydro storage system considering electrical, mechanical, and hydraulic losses. *Applied energy*, 247:228–236.

Nautiyal, H., Kumar, A., et al. (2010). Reverse running pumps analytical, experimental and computational study: A review. *Renewable and Sustainable Energy Reviews*, 14(7):2059–2067.

Neutrium (2012). Pump power calculation – neutrium. `https://neutrium.net/equipment/pump-power-calculation/`. (Accessed on 02/09/2020).

Nicolle, J., Giroux, A., and Morissette, J. (2014). Cfd configurations for hydraulic turbine startup. In *IOP conference series: earth and environmental science*, volume 22, page 032021. IOP Publishing.

Oliphant, T. E. (2007). Python for scientific computing. *Computing in Science & Engineering*, 9(3):10–20.

Origins, I. (2019). Start-up of the day: 'we've got to make better use of wind farms'. `https://innovationorigins.com/start-up-of-the-day-weve-got-to-make-better-use-of-wind-farms/`. (Accessed on 10/25/2019).

Perveen, R., Kishor, N., and Mohanty, S. R. (2014). Off-shore wind farm development: Present status and challenges. *Renewable and Sustainable Energy Reviews*, 29:780–792.

Porté-Agel, F., Wu, Y.-T., and Chen, C.-H. (2013). A numerical study of the effects of wind direction on turbine wakes and power losses in a large wind farm. *Energies*, 6(10):5297–5313.

Qi, W., Liu, J., Chen, X., and Christofides, P. D. (2010). Supervisory predictive control of standalone wind/solar energy generation systems. *IEEE transactions on control systems technology*, 19(1):199–207.

Qi, W., Liu, J., and Christofides, P. D. (2011). Supervisory predictive control for long-term scheduling of an integrated wind/solar energy generation and water desalination system. *IEEE transactions on control systems technology*, 20(2):504–512.

Qi, W., Liu, J., and Christofides, P. D. (2012). Distributed supervisory predictive control of distributed wind and solar energy systems. *IEEE Transactions on Control Systems Technology*, 21(2):504–512.

Ragheb, M. and Ragheb, A. M. (2011). Wind turbines theory-the betz equation and optimal rotor tip speed ratio. *Fundamental and advanced topics in wind power*, 1(1):19–38.

Rehman, S., Al-Hadhrami, L. M., and Alam, M. M. (2015). Pumped hydro energy storage system: A technological review. *Renewable and Sustainable Energy Reviews*, 44:586–598.

REN21 (2019). Renewables 2019 global status report. `https://www.ren21.net/gsr-2019/chapters/chapter_01/chapter_01/`. (Accessed on 10/16/2019).

Rijksoverheid (2015). White paper on offshore wind energy - google zoeken. `https://www.google.com/search?q=White+paper+on+offshore+wind+energy&oq=White+paper+on+offshore+wind+energy&aqs=chrome..69i57j69i60l3.167j0j7&sourceid=chrome&ie=UTF-8`. (Accessed on 10/16/2019).

Rijksoverheid (2016). Energieagenda: naar een co_2-arme energievoorziening — rapport — rijksoverheid.nl. `https://www.rijksoverheid.nl/onderwerpen/duurzame-energie/documenten/rapporten/2016/12/07/ea`. (Accessed on 10/16/2019).

Robinson, S. (1997). Simulation model verification and validation: increasing the users' confidence. In *Proceedings of the 29th conference on Winter simulation*, pages 53–59.

Rodrigues, S., Restrepo, C., Kontos, E., Pinto, R. T., and Bauer, P. (2015). Trends of offshore wind projects. *Renewable and Sustainable Energy Reviews*, 49:1114–1135.

Rudion, K., Styczynski, Z. A., Orths, A., and Ruhle, O. (2008). Mawind-tool for the aggregation of wind farm models. In *2008 IEEE Power and Energy Society General Meeting-Conversion and Delivery of Electrical Energy in the 21st Century*, pages 1–8. IEEE.

Sargent, R. G. (2013). Verification and validation of simulation models. *Journal of simulation*, 7(1):12–24.

Sarkar, A. and Behera, D. K. (2012). Wind turbine blade efficiency and power calculation with electrical analogy. *International Journal of Scientific and Research Publications*, 2(2):1–5.

Siahkali, H. and Vakilian, M. (2010). Stochastic unit commitment of wind farms integrated in power system. *Electric Power Systems Research*, 80(9):1006–1017.

Singh, B. and Singh, S. (2009). Wind power interconnection into the power system: A review of grid code requirements. *The Electricity Journal*, 22(5):54–63.

Smith, J. C. (2017). A major player: Renewables are now mainstream [guest editorial]. *IEEE Power and Energy Magazine*, 15(6):16–21.

Steyerberg, E. W. et al. (2019). *Clinical prediction models*. Springer.

Suberu, M. Y., Mustafa, M. W., and Bashir, N. (2014). Energy storage systems for renewable energy power sector integration and mitigation of intermittency. *Renewable and Sustainable Energy Reviews*, 35:499–514.

Takacs, B., Holaza, J., Števek, J., and Kvasnica, M. (2015). Export of explicit model predictive control to python. In *2015 20th International Conference on Process Control (PC)*, pages 78–83. IEEE.

TenneT (2018). Product information automatic frequency restoration reserve. https://www.tennet.eu/fileadmin/user_upload/SO_NL/Product_information_aFRR_2018-12-18.pdf. (Accessed on 16/02/2020).

TenneT (2019). Tennet - exporteer data. https://www.tennet.org/bedrijfsvoering/ExporteerData.aspx. (Accessed on 02/16/2020).

turbine models.com, W. (2016). Mhi vestas offshore v164-8.0 mw - 8,00 mw - wind turbine. https://en.wind-turbine-models.com/turbines/1419-mhi-vestas-offshore-v164-8.0-mw#powercurve. (Accessed on 10/30/2019).

van der Veen, R. A., Abbasy, A., and Hakvoort, R. A. (2011). Analysis of the impact of cross-border balancing arrangements for northern europe. In *2011 8th International Conference on the European Energy Market (EEM)*, pages 653–658. IEEE.

van der Veen, R. A. and Hakvoort, R. A. (2016). The electricity balancing market: Exploring the design challenge. *Utilities Policy*, 43:186–194.

van Kessel, T. (2020). Simulation of the energy flow of an offshore energy storage system. *Bachelor thesis IEM, University of Groningen*.

van Rooij, M., Meijer, H., Prins, W., and Vakis, A. (2015). Experimental performance evaluation and validation of dynamical contact models of the ocean grazer. In *OCEANS 2015-Genova*, pages 1–6. IEEE.

Vazquez, S., Leon, J. I., Franquelo, L. G., Rodriguez, J., Young, H. A., Marquez, A., and Zanchetta, P. (2014). Model predictive control: A review of its applications in power electronics. *IEEE industrial electronics magazine*, 8(1):16–31.

Virtanen, P., Gommers, R., Oliphant, T. E., Haberland, M., Reddy, T., Cournapeau, D., Burovski, E., Peterson, P., Weckesser, W., Bright, J., et al. (2020). Scipy 1.0: fundamental algorithms for scientific computing in python. *Nature Methods*, pages 1–12.

Wang, Q., Zhang, C., Ding, Y., Xydis, G., Wang, J., and Østergaard, J. (2015). Review of real-time electricity markets for integrating distributed energy resources and demand response. *Applied Energy*, 138:695–706.

Wei, Y., Bechlenberg, A., van Rooij, M., Jayawardhana, B., and Vakis, A. (2019). Modelling of a wave energy converter array with a nonlinear power take-off system in the frequency domain. *Applied Ocean Research*, 90:101824.

Wieringa, R. J. (2014). *Design science methodology for information systems and software engineering*. Springer.

Wu, Y.-T. and Porté-Agel, F. (2015). Modeling turbine wakes and power losses within a wind farm using les: An application to the horns rev offshore wind farm. *Renewable Energy*, 75:945–955.

Appendices

A Generation of wind data set

For generating the wind data set, the wind directions and velocities were taken from the KNMI data set. The wind directions were categorized into four categories that were described in the chapter. For example: when the wind was blowing from North-East to South-East, between 45°and 135°, the wind direction was classified as East. The same method applies for the other wind directions. The distribution of the wind directions in the obtained data set and the average wind speed per wind direction is as in Figure 41. From the figure it can be derived that the wind is blowing from the South or West for more than half of the time, with West as the dominant wind direction. It would therefore be expected that the turbines facing West would perform best in terms of their power output. In addition, wind from the West is also stronger, which enables a higher power output and strengthens the hypothesis that wind turbines facing West will produce a higher power output.

The Python code that was used to generate the wind power output is included on the next page. It is a simple peace of code that inputs a data set, does some calculations on its values and outputs the power data set. The allocation of the turbines from $T_1 ... T_{64}$ is depicted in Figure 42. The resulting power outputs for the 64 wind turbines in the OG-WindFarm is depicted in the graph in Figure 43. In this graph there are some major peaks shown. These peaks correspond to the rows facing the West direction, which is according to expectation. The other rows that are in the first row for any of the wind direction also perform better than the rows in the middle, which is in line with expectation.

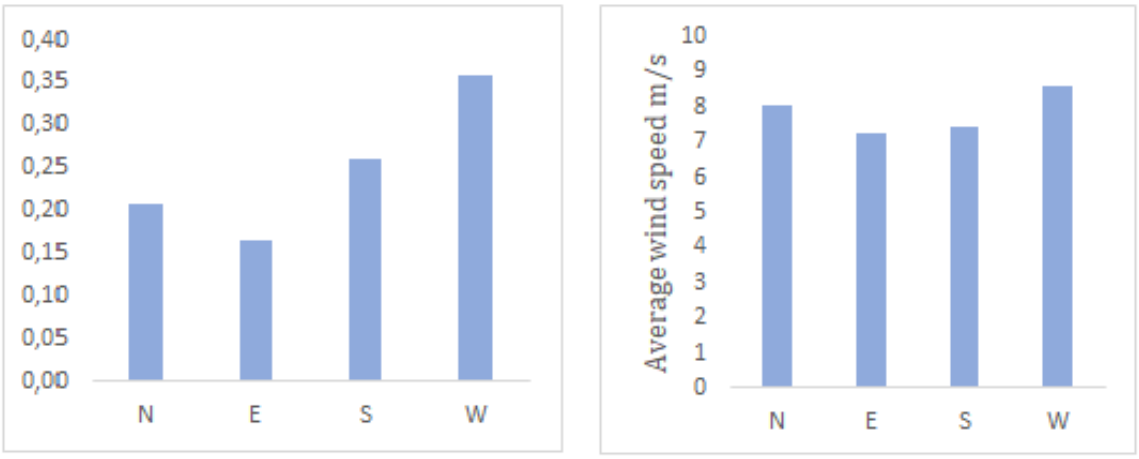

Figure 41: Distribution of the wind directions in the data set (left) and average wind speed per wind direction (right).

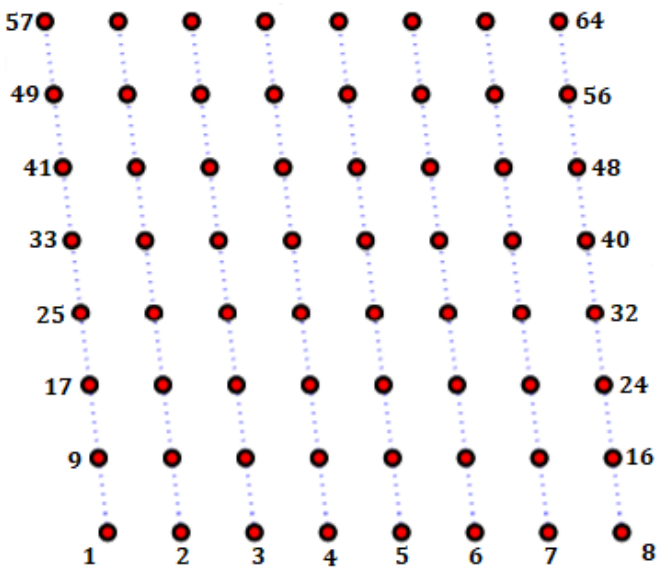

Figure 42: Configuration and allocation of turbines in the grid.

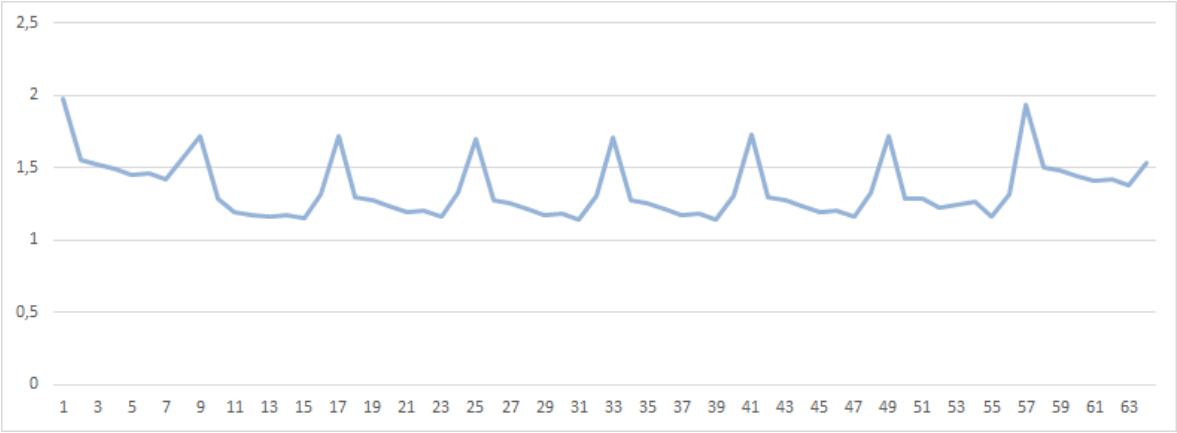

Figure 43: Power output per wind turbine produced with the wind data set.

Python code

```
import xlrd
import os
import openpyxl
Wind_Data = xlrd.open_workbook("Wind_month.xlsx")
sheet = Wind_Data.sheet_by_index(0)


# Create a new blank Workbook to store the powers
wb = openpyxl.Workbook()
sheet2 = wb.active


# Insert variables
PR = 8 # Rated power in MW
VI = 4.0 # Cut-in speed in m/s
VR = 13.0 # Rated wind speed in m/s
VO = 25.0 # Cut-out wind speed in m/s
Rho = 1.225 # Density of air in kg/m3
Eta = 0.2809 # Efficiency of the turbine + generator
A = 21164 # Swept area in m2


for i in range(3, sheet.ncols):
    for j in range(1, sheet.nrows):
    V = sheet.cell_value(j, i)
        if (V >= VI and V < VR):
            Power = (0.5 * A * Rho * Eta * (V**3))/(10**6)
        elif (V >= VR and V < VO):
            Power = PR
        else:
            Power = 0
        Powerdata = sheet2.cell(row = j+1, column = i+1)
        Powerdata.value = Power


wb.save("Powerdatas.xlsx")
```

B Calculation of the volume of the Ocean Grazer storage

The volume of the Ocean Grazer storage is approximated by calculating the volume of the concrete pipes. For this approximation it was assumed that the inner diameter of the pipes is 10 meters and that the space between the two concrete pipes is also 10 meters. A top-view of the Ocean Grazer is depicted in Figure 44.

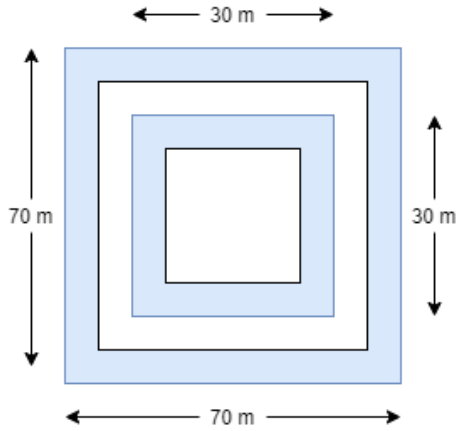

Figure 44: Top-view of the Ocean Grazer.

The volume of a pipe is calculated by Equation 37 and the parameters used for the calculations are listed in Table 35. The area is calculated by $\pi \cdot r^2$. The length of the pipes is calculated by subtracting the length of the corners from the total circumference of the pipes. The resulting volumes are depicted in Table 36

$$V = A \cdot L \tag{37}$$

Where
V is the volume of the pipe in $[m^3]$
A is the cross-sectional area of the pipe in $[m^2]$
L is the length of the pipe in $[m]$

Parameter	A_{out}	A_{in}	L_{out}	L_{in}
Value	$25\pi\ m^2$	$25\pi\ m^2$	$240\ m$	$80\ m$

Table 35: Parameters for the calculation of the volume of the Ocean Grazer.

V_{out}	$18849\ m^3$
V_{in}	$6283\ m^3$
V_{total}	$25132\ m^3$

Table 36: Volume of the Ocean Grazer storage.

C Dynamical model of the Ocean Grazer storage

```
import time
from scipy.optimize
import minimize
from matplotlib.pyplot import plot,show,figure,subplot,title,ylabel
import numpy as np
from numpy import *

# set printoptions: print values up to 2 decimals
np.set_printoptions(formatter='float': lambda x: "0:0.2f".format(x))

# initialize parameters
ts = 3600 # sampling time [s]
N = 40000000 # take large number for creating vectors of unknown length
Eta_p = 0.85 # pump efficiency [-]
Eta_l = 0.9 # loss efficiency [-]
Eta_t = 0.9 # turbine efficiency [-]
Eta_pump = Eta_p*Eta_l # total efficiency pumping process [-]
Eta_turbine = Eta_t*Eta_l # total efficiency turbine process [-]
p1 = 400000 # ocean pressure [Pa]
p2 = 100000 # atmospheric pressure [Pa]
V_max = 25132 # maximum volume of the tubes [m3]
PP = 1 # rated power of the pump [MW]
PT = 1 # rated power of the turbine [MW]

# initialize vectors  variables
ES = np.zeros(N) # energy in storage [MWh]
E_in = np.zeros(N) # energy to storage [MWh]
E_out = np.zeros(N) # energy from storage [MWh]
V = np.zeros(N) # volume of storage [m3]
Energy_in = 0 # total energy to storage [MWh]
Energy_out = 0 # total energy from storage [MWh]
Energy_in_act = 0 # total energy in bladder [MWh]
Energy_out_pot = 0 # total energy from bladder [MWh]

# calculate the maximum storage capacity [MWh]
dPav = p1 - (p2/2)
E_max = ((V_max*dPav)/3600)/10**6
print(f'Maximum storage level = {E_max} MWh)

u = 0 # u = 0: store, u = 1: drain
i = 1 # count the time steps
st = 0 # count the storing time steps
dr = 0 # count the draining time steps
while True:
    # if the water level is below 0.95 and it hasn't been before, store energy.
    # if not, release the energy
```

```
    if ES[i-1] < 0.999*E_max and u == 0:
        Label = 'store'
        SiS = E_max - ES[i-1]
        if SiS < (ts/3600)*PP: # check if there is still enough space in storage
            P_in = (ts/3600)*PP
        else:
            P_in = SiS
        E_in[i] = P_in*Eta_pump # calculate energy that goes into storage
        Energy_in_act = np.add(Energy_in_act,E_in[i]) # add it to total energy in
        Energy_in = np.add(Energy_in,P_in) # calculate energy used
        st += 1
    else:
        u = 1 # time to release
        Label = 'release'
        if ES[i-1] < (ts/3600)*PT: # check if there is still enough energy in storage—
            P_out = (ts/3600)*PT
        else:
            P_out = ES[i-1]
        E_out[i] = P_out*Eta_turbine # calculate energy that reaches customer
        Energy_out = np.add(Energy_out,E_out[i]) # add it to total energy out
        Energy_out_pot = np.add(Energy_out_pot,P_out) # calculate energy out of storage
        dr += 1

    # calculate storage level  volume of the bladder
    if Label == 'store':
        ES[i] = ES[i-1] + E_in[i]
    elif Label == 'release':
        ES[i] = ES[i-1] - P_out

    # if the reservoir is almost empty, stop
    if ES[i] ¡ 0.0001*E_max and u == 1:
        break
    i += 1

# make efficiency calculations
Eta_total = Energy_out/Energy_in # calculate the roundtrip efficiency
Tot_Eta_pump = Energy_in_act/Energy_in # calculate the efficiency of the pump
Tot_Eta_turbine = Energy_out/Energy_out_pot # calculate the efficiency of the turbine

print(f'Efficiency of the pump = {Tot_Eta_pump}')
print(f'Efficiency of the turbine = {Tot_Eta_turbine}')
print(f'Round trip efficiency OG battery = {Eta_total}')
print(f'Total time to fill the storage = {(st*ts)} seconds')
print(f'Total time to drain the storage = {(dr*ts)} seconds')
print(f'Time to fill & drain the storage = {(i)*ts} seconds')
```

D Validation of the dynamical model

One of the validation techniques applied to validate the dynamical model was comparison to analytical calculations. It has been decided to analytically calculate the theoretical time it takes to fill and drain the storage and compare them to the model results. The analytical calculations are executed as follows. First, the maximum storage capacity was calculated by

$$E_{max} = V_{max} \cdot \Delta p_{av} = \frac{(25132 \cdot 350000)/3600}{10^6} = 2.44 \text{ MWh} \tag{38}$$

$$\Delta p_{av} = p_{ocean} - \frac{p_{atm}}{2} = 400000 - \frac{100000}{2} = 350000 \text{ Pa} \tag{39}$$

Then, the efficiency of the pump and the turbine were determined from the assigned values as $\eta_{pump} = 0.765$ and $\eta_{turbine} = 0.81$. A turbine capacity of $1MW$ is used. Effectively, of each MW that is used to drive the pump, only 0.765 MWh goes into storage due to efficiency losses. The time it takes to fill the storage is now calculated as

$$T_{fill} = \frac{E_{max}}{E_{in}} = \frac{2.44}{0.765} = 3.19 \text{ hours} \approx 11485 \text{ seconds} \tag{40}$$

Although the turbine also has efficiency losses, the energy that is drained from the storage is still equal to the turbine capacity. Efficiency losses occur before the energy reaches the customer. The time to drain the storage is calculated as

$$T_{drain} = \frac{2.44}{1} = 2.44 \text{ hours} \approx 8784 \text{ seconds} \tag{41}$$

The total time to fill and drain the storage is therefore

$$T = T_{fill} + T_{drain} = 11485 + 8784 = 20269 \text{ seconds} \tag{42}$$

E Basic settings for the validation simulations

This appendix consists of the basic settings used in the simulations with the purpose of validating the simulation models.

Validation of the MPC 1S1G model

For both simulations, the day-ahead data set from 2019 was used. All other parameters are listed in Table 37.

Parameter	Value	Description [units]
T_s	900	Sampling time $[s]$
P	4	Prediction horizon $[hours]$
nrS	4	Number of storage units in cluster $[-]$
p_{ocean}	400000	Ocean pressure $[Pa]$
p_{atm}	100000	Atmospheric pressure $[Pa]$
V_{max}	25132	Maximum volume of bladder $[m^3]$
TC	1	Capacity of the PaT $[MW]$

Table 37: Basic settings for the validation of the MPC 1S1G model by prediction validation and parameter variability.

Validation of the Heuristics 1S1G model

For the simulation of the parameter variability, the day-ahead price data from 2019 were used. The threshold price was set at the mean of the data set. All other parameters are listed in Table 38.

Parameter	Value	Description [units]
T_s	900	Sampling time $[s]$
nrS	4	Number of storage units in cluster $[-]$
p_{ocean}	400000	Ocean pressure $[Pa]$
p_{atm}	100000	Atmospheric pressure $[Pa]$
V_{max}	25132	Maximum volume of bladder $[m^3]$
TC	1	Capacity of the PaT $[MW]$

Table 38: Basic settings for the validation of the MPC 1S1G model by prediction validation and parameter variability.

Validation of the MPC MSMG model

For the qualitative validation, the day-ahead price data from 2019 were used and for the quantitative validation, the aFRR price data from 2019 were used. All other settings are listed in Table 39

Parameter	**Value**	**Description [units]**
T_s	1800	Sampling time $[s]$
P	3	Prediction horizon $[hours]$
nrS	3	Number of storage units in cluster $[-]$
p_{ocean}	400000	Ocean pressure $[Pa]$
p_{atm}	100000	Atmospheric pressure $[Pa]$
V_{max}	25132	Maximum volume of bladder $[m^3]$
TC	1	Capacity of the PaT $[MW]$
η_P	0.95	Efficiency of the pump mode of the PaT $[-]$
η_T	0.95	Efficiency of the turbine mode of the PaT $[-]$

Table 39: Basic settings for the validation of the MPC MSMG model by prediction validation and parameter variability.

F One-Storage-One-Generator RBC simulation model

```
import numpy as np
import xlrd
import time
import sys from statistics import mean

# import dataset
Price_Data = xlrd.open_workbook("FINAL_Price_Data.xlsx")
Power_Data = xlrd.open_workbook("FINAL_Power_Data.xlsx")
DayAhead = Price_Data.sheet_by_name('DayAhead')
aFRRup = Price_Data.sheet_by_name('aFRRup')
Windpower = Power_Data.sheet_by_name('2019') # or 2018 or 2017

# set printoptions: print values up to 2 decimals
np.set_printoptions(formatter='float': lambda x: "0:0.2f".format(x))

# initialize parameters
simtime = 31536000 # total simulation time [s] = 1 year
ts = 900 # sampling time [s] = 15 min
N = int(simtime/ts) # number of time steps
WT = 2 # number of wind turbines
C = 4 # 4 = 2019; 3 = 2018; 2 = 2017 p1 = 400000 # ocean pressure [Pa]
p2 = 100000 # atmospheric pressure [Pa]
V_max = 25132 # maximum volume of the tubes [m3]
Eta_pump = 0.85 # efficiency of pumping process [-]
Eta_turbine = 0.9 # efficiency of turbine process [-]
nrS = 4 # number of storage systems in a cluster [-]
TC = (ts/3600)*nrS # turbine capacity [MW]

# initialize vectors
ES = np.zeros(N) # energy stored [MWh]
EG = np.zeros(N) # wind turbine data [MW]
M = np.zeros(N) # prices of electricity [€]
R = np.zeros(N) # revenue [€]

# make vector with price data
for i in range(1,N+1):
    M[i-1] = aFRRup.cell_value(i,C) # aFRRup or DayAhead

# find mean price
mu = mean(M)
print(f'Mean: mu')
TP = mu
print(f'Threshold price = TP')
```

```
# make vector with generation data, based on ts = 15 mins
for j in range(1,N+1):
    EG[j-1] = (ts/3600)*Windpower.cell_value(j,2)

# calculate the maximum storage capacity [MWh]
dPav = p1 - (p2/2)
E_max = nrS*((V_max*dPav)/3600)/10**6

# calculate storage level and revenue at t = i
for i in range(N):
    if M[i] > TP: # sell energy
        if ES[i-1] > TC: # sell TC
            ES[i] = ES[i-1] - TC
            R[i] = M[i]*(EG[i] + Eta_turbine*TC)
        else: # sell EG
            ES[i] = 0
            R[i] = M[i]*(EG[i] + Eta_turbine*ES[i-1])
    else: # store energy
        SiS = E_max - ES[i-1] # calculate space in storage
        if SiS > 0:
            if SiS ≥ EG[i]:
                if EG[i] ≤ TC: # store EG
                    ES[i] = ES[i-1] + Eta_pump*EG[i]
                    R[i] = 0
                else: # store TC
                    ES[i] = ES[i-1] + Eta_pump*TC
                    R[i] = M[i]*(EG[i]-TC)
            else:
                if SiS ≥ TC: # store TC
                    ES[i] = ES[i-1] + Eta_pump*TC
                    R[i] = M[i]*(EG[i] - TC)
                else: # store SiS
                    ES[i] = ES[i-1] + Eta_pump*SiS
                    R[i] = M[i]*(EG[i] - SiS)
        else: # no space in storage
            ES[i] = ES[i-1]# nothing happens to ES
            if M[i] > 0: # only sell if price > 0
                R[i] = M[i]*EG[i]

# print total revenue
print(f'Total Revenue = €{np.sum(R[:])}')
```

G One-Storage-One-Generator MPC simulation model

```
import numpy as np
import xlrd
import time
import sys
from statistics import mean
from scipy.optimize import minimize
from matplotlib.pyplot import plot,show,figure,subplot,title,ylabel

# import dataset
Price_Data = xlrd.open_workbook("FINAL_Price_Data.xlsx")
Power_Data = xlrd.open_workbook("FINAL_Power_Data.xlsx")
DayAhead = Price_Data.sheet_by_name('DayAhead')
aFRRup = Price_Data.sheet_by_name('aFRRup')
Windpower = Power_Data.sheet_by_name('2019') # or 2018 or 2017

# set printoptions: print values up to 2 decimals
np.set_printoptions(formatter='float': lambda x:"0:0.2f".format(x),threshold=sys.maxsize)

# initialize parameters
simtime = 31536000 # total simulation time [s] = 1 year
ts = 900 # sampling time [s] = 15 min
N = int(simtime/ts) # number of time steps
WT = 2 # number of wind turbines
C = 4 # 4 = 2019; 3 = 2018; 2 = 2017 p1 = 400000 # ocean pressure [Pa]
p2 = 100000 # atmospheric pressure [Pa]
V_max = 25132 # maximum volume of the tubes [m3]
Eta_pump = 0.85 # efficiency of pumping process [-]
Eta_turbine = 0.9 # efficiency of turbine process [-]
nrS = 4 # number of storage systems in a cluster [-]
TC = (ts/3600)*nrS # turbine capacity [MW]
n = 2 # number of control variables [-]

# define prediction horizon
P = 24

# initialize vectors
ES = np.zeros(N) # energy stored [MWh]
EG = np.zeros(N) # wind turbine data [MW]
M = np.zeros(N) # prices of electricity [€]
R = np.zeros(N) # revenue [€]
u = np.zeros(n) # control variable [-]

# initialize prediction vectors
ES_hat = np.zeros(P) # prediction energy stored [MWh]
EG_hat = np.zeros(P) # prediction energy generated [MWh]
M_hat = np.zeros(P) # prediction prices of electricity [€]
R_hat = np.zeros(P) #predicted revenue [€]
```

```
# make vector with price data
for i in range(1,N+1):
    M[i-1] = aFRRup.cell_value(i,C) # aFRRup or DayAhead

# make vector with generation data, based on ts = 15 mins
for j in range(1,N+1):
    EG[j-1] = (ts/3600)*Windpower.cell_value(j,2)

# calculate the maximum storage capacity [MWh]
dPav = p1 - (p2/2)
E_max = nrS*((V_max*dPav)/3600)/10**6

globals()['u_hat_dict'] = {} # make dictionary to calculate all variables

def get_vars(u_hat):
    key = hash(u_hat.data.tobytes())
    u_hat_dict = globals()['u_hat_dict']
    if u_hat_dict.get(key):
        return u_hat_dict[key]
    es_hat = np.zeros(P_p)
    con1 = np.ones(P_p)
    con2 = np.ones(P_p)
    con3 = np.ones(P_p)

    for k in range(P_p):
        if k == 0:
            es_hat[-1] = ES[i - 1]
        EG_hat[k] = EG[k+i]
        es_hat[k] = es_hat[k - 1] + (1 - u_hat[n * k]) * Eta_pump * EG_hat[k]
            - u_hat[n * k + 1] * es_hat[k - 1]
        M_hat[k] = M[k + i]
        R_hat[k] = -M_hat[k] * (u_hat[n * k] * EG_hat[k] + u_hat[n * k + 1] * Eta_turbine
            * es_hat[k - 1])
        con1[k] = 0.0001 - (1 - u_hat[n * k]) * u_hat[n * k + 1]
        con2[k] = TC - (u_hat[n * k + 1] * es_hat[k - 1]) - (1 - u_hat[n * k]) * EG_hat[k]
        con3[k] = E_max - es_hat[k]
    objective = np.sum(R_hat[:])
    globals()['u_hat_dict'][key] = {
        'con1': con1,
        'con2': con2,
        'con3': con3,
        'r_hat':R_hat,
        'eg_hat':EG_hat,
        'es_hat':es_hat,
        'm_hat':M_hat,
        'objective': objective,
    }
    return globals()['u_hat_dict'][key]
```

```
# prediction model {}
def objective(u_hat):
    return get_vars(u_hat)['objective']

# definition of constraints
1: PaT cannot act as a pump and turbine simultaneously
def constraint1(u_hat):
    return get_vars(u_hat)['con1']

# 2: pump/turbine capacity has a maximum value
def constraint2(u_hat):
    return get_vars(u_hat)['con2']

# 3: the energy storage level cannot exceed the maximum storage level
def constraint3(u_hat):
    return get_vars(u_hat)['con3']

t = time.time()
iterations = []
for i     in range(N): # if i ≥ N-P, it cannot predict further into the future, adjust P
    if i ≥ N - P:
        P_p = N - i
    else:
        P_p = P

    # randomize initial guess
    Result = []
    it = 0
    while not Result:
        u_hat0 = np.random.uniform(low=0, high=1, size=(n * P_p))

        # MPC calculation
        bnds = [(0, 1)] * n * P_p
        cons1 = {'type':'ineq', 'fun': constraint1}
        cons2 = {'type':'ineq', 'fun': constraint2}
        cons3 = {'type':'ineq', 'fun': constraint3}
        cons = ([cons1, cons2, cons3])
        solution    =    minimize(objective,    u_hat0,    method='SLSQP',    bounds=bnds,
            constraints=cons)
        del globals()['u_hat_dict']
        globals()['u_hat_dict'] = {}
        u_hat = solution.x
        obj = -objective(u_hat)

        # check whether the generated u_hat satisfies the constraints
        con1 = constraint1(u_hat)
        con2 = constraint2(u_hat)
        con3 = constraint3(u_hat)
```

```
        min_const = -0.0001
        if all([np.all(con1 > min_const), np.all(con2 > min_const), np.all(con3 > min_const)]):
            Result.append(obj)
            u_hatbest = u_hat
        it += 1
    iterations.append(it)

    # calculate storage level and revenue at t = i
    u[0] = u_hatbest[0]
    u[1] = u_hatbest[1]
    ES[i] = ES[i - 1] + (1 - u[0]) * Eta_pump * EG[i] - u[1] * ES[i - 1]

print('Total Revenue = €{np.sum(R[:])}')
print('Theoretical max storage level = {E_max}')
print('Actual max storage level = {np.amax(ES)}')
print('Difference = {E_max - np.amax(ES)}')
print(f'Total amount of energy to storage = np.sum(ETS)')
print(f'Total amount of energy produced = np.sum(EG)')
elapsed = time.time() - t
print(elapsed)

# figure to show all relevant parameters  outcomes
figure(1)
subplot(211)
plot(ES)
ylabel('ES')
subplot(212)
plot(M)
ylabel('Price')
show()
```

H Multiple-Storage-Multiple-Generator MPC simulation model

```
import numpy as np
import xlrd
import time
import sys
from statistics import mean
from scipy.optimize import minimize
from matplotlib.pyplot import plot,show,figure,subplot,title,ylabel

# import dataset
Price_Data = xlrd.open_workbook("FINAL_Price_Data.xlsx")
Power_Data = xlrd.open_workbook("FINAL_Power_Data.xlsx")
Adjacency_Matrix = xlrd.open_workbook("Adjacency_Matrix.xlsx")
DayAhead = Price_Data.sheet_by_name('DayAhead')
aFRRup = Price_Data.sheet_by_name('aFRRup')
Windpower = Power_Data.sheet_by_name('2019') # or 2018 or 2017
A_Matrix = Adjacency_Matrix.sheet_by_index(0)

# set printoptions: print values up to 2 decimals
np.set_printoptions(formatter='float': lambda x:"0:0.2f".format(x),threshold=sys.maxsize)

# initialize parameters
simtime = 31536000 # total simulation time [s] = 1 year
ts = 1800 # sampling time [s] = 30 min
N = int(simtime/ts) # number of time steps
WT = 2 # number of wind turbines
C = 4 # 4 = 2019; 3 = 2018; 2 = 2017 p1 = 400000 # ocean pressure [Pa]
p2 = 100000 # atmospheric pressure
    Pa

V_max = 25132 # maximum volume of the tubes [m3]
Eta_pump = 0.95 # efficiency of pumping process [-]
Eta_turbine = 0.95 # efficiency of turbine process [-]
nrS = 3 # number of storage systems in a cluster [-]
TC = (ts/3600)*nrS # turbine capacity [MW]
S = 4 # number of Ocean Batteries
G = 2 # number of wind turbines
dim = S+G+1 # dimension of control variable

# define prediction horizon
P = 6

# initialize vectors
ES = np.zeros((S,N)) # energy stored [MWh]
EG = np.zeros((G,N)) # wind turbine data [MW]
ESav = np.zeros((dim,N)) # available energy [MWh]
```

```
EFT = np.zeros(N) # energy from wind turbine to storage [MWh]
M = np.zeros(N) # prices of electricity [€]
R = np.zeros((S+G,N)) # revenue [€]
Rtotal = np.zeros(N) # total revenues [€]
u = np.zeros(dim**2) # control variable [-]
u_form = np.zeros(dim**2) # make adjacency matrix
u_best = np.zeros(dim**2) # make adjacency matrix

# make vector with price data
for i in range(1,N+1):
    M[i-1] = aFRRup.cell_value(2*i,C) # aFRRup or DayAhead
    if M[i-1] < 0:
        M[i-1] = 0

# make vector with generation data, based on ts = 15 mins
for j in range(1,N+1):
    for i in range(G):
        EG[i,j-1] = (ts/3600)*Windpower.cell_value(2*j,2+i)

# import adjacency matrix
for a in range(A_Matrix.nrows):
    for b in range(A_Matrix.ncols):
        u_form[dim*a+b] = A_Matrix.cell_value(a,b)

# find size of u_hat
c = 0
CV = 0
while c < u_form.size:
    if u_form[c] == 1:
        CV += 1
    c += 1

# calculate the maximum storage capacity [MWh]
dPav = p1 - (p2/2)
E_max = nrS*((V_max*dPav)/3600)/10**6

globals()['u_hat_dict'] = {} # make dictionary to calculate all variables

def get_vars(u_hat):
    key = hash(u_hat.data.tobytes())
    u_hat_dict = globals()['u_hat_dict']
    if u_hat_dict.get(key):
        return u_hat_dict[key]
    es_hat = np.zeros((S,P_p))
    con1 = np.ones(S*P_p)
    con2 = np.ones(S*P_p)
    con3 = np.ones(S*P_p)
    con4 = np.ones(dim*P_p)
```

```
for k in range(P_p):
    if k == 0:
        es_hat[:,-1] = ES[:,i - 1] # start with the energy at the previous time step
    EG_hat[:,k] = EG[:,k + i] #import right values from EG
    M_hat[k] = M[k + i] #import right values from M
    #make available energy array
    ESav_hat[:S+G,k] = np.append(es_hat[:,k-1],EG_hat[:,k])
    ESav_hat[:,k] = np.append(ESav_hat[:S+G,k],0)

    # make a matrix of u_hat
    for a in range(A_Matrix.nrows):
        for b in range(A_Matrix.ncols):
            u_form[dim*a+b] = A_Matrix.cell_value(a,b)

    y = 0
    for t in range(dim**2):
        if u_form[t] == 1:
            u_form[t] = u_hat[k*CV+y]
            y = y + 1
        else:
            u_form[t] = 0

    # calculate updated storage levels
    for j in range(S):
        if u_form[j*dim+dim-1] > 0:
            for g in range(G):
                EFT_hat[g] = u_form[(S+g)*dim+j]*ESav_hat[S+g,k]
            es_hat[j,k] = es_hat[j,k-1] + Eta_pump*np.sum(EFT_hat[:])
                + Eta_turbine*Eta_pump*np.sum(u_form[j:S*dim:dim]*ESav_hat[:S,k])
                - np.sum(u_form[j*dim:j*dim+dim])*ESav_hat[j,k]
        else:
            es_hat[j,k] = es_hat[j,k-1] + Eta_turbine*Eta_pump*np.sum(u_form[j:S*dim:dim]
                *ESav_hat[:S,k]) - np.sum(u_form[j*dim:j*dim+dim-1])*ESav_hat[j,k]

    # calculate revenue
    for j in range(S): # revenue from storage units
        if u_form[j*dim+dim-1] > 0:
            R_hat[j,k] = -M_hat[k]*u_form[j*dim+dim-1]*Eta_turbine*es_hat[j,k-1]
        else:
            R_hat[j,k] = 0
    for j in range(G): # revenue from generators
        R_hat[S+j,k] = -M_hat[k]*(1-np.sum(u_form[(S+j)*dim:(S+j+1)*dim-1]))
            *EG_hat[j,k]
    Rtotal_hat[k] = np.sum(R_hat[:,k])

    # calculate constraints
    for j in range(S):
        # con1: PaT cannot act as pump and turbine at the same time
```

```
            con1[S*k+j] = 0.0001 - np.sum(u_form[j*dim:j*dim+dim])*np.sum(u_form[j::dim])
            # con2: there exists a turbine capacity of 1 MW
            con2[S*k+j] = TC - (np.sum(u_form[j*dim:j*dim+dim])*ESav_hat[j,k])
            - np.sum(u_form[j::dim]*ESav_hat[:,k])
            # con3: there exists a maximum storage level
            con3[S*k+j] = E_max - es_hat[j,k]
        for j in range(dim):
            # con4: the sum of the energy from an actor cannot exceed 100%
            con4[dim*k+j] = 1.0001 - np.sum(u_form[j*dim:j*dim+dim])

    # cost function
    objective = np.sum(Rtotal_hat[:])
    globals()['u_hat_dict'][key] = {
        'con1': con1,
        'con2': con2,
        'con3': con3,
        'con4': con4,
        'objective': objective,
    }
    return globals()['u_hat_dict'][key]

# prediction model {}
def objective(u_hat):
    return get_vars(u_hat)['objective']

# definition of constraints
def constraint1(u_hat):
    return get_vars(u_hat)['con1'

def constraint2(u_hat):
    return get_vars(u_hat)['con2']

def constraint3(u_hat):
    return get_vars(u_hat)['con3']

def constraint4(u_hat):
    return get_vars(u_hat)['con4']

start = time.time()
iterations = []
EnergyFromWT = 0
for i in range(N): # if i ≥ N-P, it cannot predict further into the future, adjust P
    if i >= N-P:
        P_p = N-i
    else:
        P_p = P
```

```
# initialize prediction vectors
ES_hat = np.zeros((S,P_p)) # prediction energy stored [MWh]
EG_hat = np.zeros((G,P_p)) # prediction energy generated [MWh]
EFT_hat = np.zeros(G) # predicted energy from wind turbines to storage units
ESav_hat = np.zeros((dim,P_p)) # predicted available energy [MWh]
M_hat = np.zeros(P_p) # prediction prices of electricity [€]
R_hat = np.zeros((S+G,P_p)) # predicted revenue [€]
Rtotal_hat = np.zeros(P_p)

#randomize initial guess
Result = []
it = 0
while not Result:
    u_hat0 = np.random.uniform(low=0,high=1,size=(CV*P_p))

    # MPC calculation
    bnds = [(0, 1)]*CV*P_p
    cons1 = {'type':'ineq', 'fun': constraint1}
    cons2 = {'type':'ineq', 'fun': constraint2}
    cons3 = {'type':'ineq', 'fun': constraint3}
    cons4 = {'type':'ineq', 'fun': constraint1}
    cons = ([cons1,cons2,cons3,cons4])
    solution = minimize(objective,u_hat0,method='SLSQP',bounds=bnds,
    constraints=cons)
    del globals()['u_hat_dict']
    globals()['u_hat_dict'] = {}
    u_hat = solution.x
    obj = -objective(u_hat)


    # check whether u_hat satisfies the constraints
    con1 = constraint1(u_hat)
    con2 = constraint2(u_hat)
    con3 = constraint3(u_hat)
    con4 = constraint4(u_hat)

    min_const = -0.0001
    if all([np.all(con1 > min_const), np.all(con2 > min_const), np.all(con3 > min_const),
    np.all(con4 > min_const)]):
        Result.append(obj)
        u_hatbest = u_hat
        # make a matrix of u_hatbest
        for a in range(A_Matrix.nrows):
            for b in range(A_Matrix.ncols):
                u_best[dim*a+b] = A_Matrix.cell_value(a,b)

        y = 0
        for t in range(dim**2):
```

```
            if u_best[t] == 1:
                u_best[t] = u_hatbest[k*CV+y]
                y = y + 1
            else:
                u_best[t] = 0
        for q in range(G):
            u_best[(S+q+1)*dim-1] = 1-np.sum(u_best[(S+q)*dim:(S+q+1)*dim-1])
    it+=1
iterations.append(it)
u = u_best

# construct array with available energy
ESav[:S+G,i] = np.append(ES[:,i-1],EG[:,i])
ESav[:,i] = np.append(ESav[:S+G,i],0)


#calculate updated storage levels
for j in range(S):
    if u_form[j*dim+dim-1] > 0:
        for g in range(G):
            EFT[g] = u[(S+g)*dim+j]*ESav[S+g,i]
        ES[j,i] = ES[j,i-1] + Eta_pump*np.sum(EFT[:])
            + Eta_turbine*Eta_pump*np.sum(u[j:S*dim:dim]*ESav[:S,i])
            - np.sum(u[j*dim:j*dim+dim])*ESav[j,i]
        EnergyFromWT += np.sum(EFT[:])
    else:
        ES[j,i] = ES[j,i-1]
            + Eta_turbine*Eta_pump*np.sum(u[j:S*dim:dim]*ESav[:S,i])
            - np.sum(u[j*dim:j*dim+dim-1])*ESav[j,i]

# calculate revenue
for j in range(S): # revenue from storage units
    if u[j*dim+dim-1] > 0:
        R[j,i] = M[i]*u[j*dim+dim-1]*Eta_turbine*ES[j,i-1]
    else:
        R[j,i] = 0
for j in range(G):# revenue from generators
    if 1-np.sum(u[(S+j)*dim:(S+j+1)*dim-1]) < 0:
        Portion_sold = 0
    else:
        Portion_sold = 1-np.sum(u[(S+j)*dim:(S+j+1)*dim-1])
        R[S+j,i] = M[i]*Portion_sold*EG[j,i]

# total revenue
Rtotal[i] = sum(R[:,i])
```

I Reference model: without storage

```
import numpy as np
import xlrd
import openpyxl

# import dataset
Price_Data = xlrd.open_workbook("FINAL_Price_Data.xlsx")
Power_Data = xlrd.open_workbook("FINAL_Power_Data.xlsx")
DayAhead = Price_Data.sheet_by_name('DayAhead')
aFRRup = Price_Data.sheet_by_name('aFRRup')
Windpower = Power_Data.sheet_by_name('2019') # or 2018 or 2017

# set printoptions: print values up to 2 decimals
np.set_printoptions(formatter={'float': lambda x: "0:0.2f".format(x)})

# initialize parameters
simtime = 31536000 # total simulation time [s] = 1 year
ts = 1800 # sampling time [s] = 15 min
N = int(simtime/ts) # number of time steps
WT = 2 # number of wind turbines
C = 4 # 4 = 2019; 3 = 2018; 2 = 2017

# initialize vectors
EG = np.zeros((WT,N)) # wind turbine data [MW]
M = np.zeros(N) # prices of electricity [€]
R = np.zeros((WT,N)) # revenue [€]

# make vector with price data
for i in range(1,N+1):
    M[i-1] = aFRRup.cell_value(2*i,C) # aFRRup or DayAhead

# activate this part if you have 1 wind turbine

### make vector with generation data
##for j in range(1,N+1):
##    EG[0,j-1] = (ts/3600)*Windpower.cell_value(2*j,2)
##
### calculate the revenue  eliminate negative prices
##for i in range(N):
##    if M[i] > 0:
##        R[0,i] = M[i]*EG[0,i]

# activate this part if you have >1 wind turbine

# make vector with generation data
for i in range(2,Windpower.ncols):
    for j in range(1,N+1):
        EG[i-2,j-1] = (ts/3600)*Windpower.cell_value(2*j,i)
```

```
# calculate the revenue  eliminate negative prices
for i in range(N):
    for j in rangerange(WT):
        if M[i] > 0:
            R[j,i] = M[i]*EG[j,i]
    print(R[:,i])

# print total revenue
print(f'Total Revenue = €{np.sum(R[:])}')
```

J Simulation results

Data set	**Revenue (€)**
Day-ahead market (2019)	751175
Day-ahead market (2019)	751165
Day-ahead market (2019)	751325
Day-ahead market (2019)	751266
Day-ahead market (2019)	751182
Day-ahead market (2019)	751206

Table 40: Test whether one iteration for the optimizer is sufficient with 1S1G MPC model.

Data set	**Revenue (€)** ($T_s = 900s$)	**Revenue (€)** ($T_s = 1800s$)	**Difference (%)**
Day-ahead market (2017)	803422	800165	0.4
Day-ahead market (2018)	988511	984317	0.4
Day-ahead market (2019)	751203	748317	0.4
aFRR market (2017)	1342228	1253838	7
aFRR market (2018)	1439498	1382827	4.1
aFRR market (2019)	1179923	1128615	4.5

Table 41: Test the effects of sampling time on the yearly revenues with 1S1G MPC model.

Number of storage units	**Revenue (€) day-ahead (2019)**	**Revenue (€) aFRR (2019)**
1	709992	863539
2	727247	986464
4	751357	1181008
6	766747	1325803

Table 42: Test the relation between the number of Ocean Batteries in a cluster and the yearly revenue with 1S1G MPC model.

Prediction horizon	**Revenue (€) day-ahead (2019)**	**Revenue (€) aFRR (2019)**
4 (1 hour)	697914 *(00:02:32)*	1026578 *(00:04:09)*
12 (3 hours)	745583 *(00:18:51)*	1159587 *(00:31:11)*
16 (4 hours)	751345 *(00:34:02)*	1180037 *(01:01:57)*
24 (6 hours)	757194 *(01:24:57)*	1201775 *(02:38:58)*
48 (12 hours)	762765 *(09:15:08)*	1215053 *(17:48:03)*

Table 43: Test the effects of prediction horizon on the yearly revenues with computation times of the simulation in *hh:mm:ss* with 1S1G MPC model.

η_p	η_t	**Revenue (€) day-ahead (2019)**	**Revenue (€) aFRR (2019)**
0.75	0.80	691004	996447
0.80	0.85	694706	1037290
0.85	0.90	702908	1081291
0.90	0.95	718445	1129617
1	1	757194	1201775

Table 44: Test the effects of the efficiency of the PaT on the yearly revenue with 1S1G MPC model.

Data set	**Revenue (€)**
Day-ahead market (2017)	749756
Day-ahead market (2018)	924766
Day-ahead market (2019)	703323
aFRR market (2017)	1236307
aFRR market (2017)	1323391
aFRR market (2017)	1082613

Table 45: Yearly revenues for the 1S1G MPC strategy.

η_p	η_t	**Revenue (€) day-ahead (2019)**	**Revenue (€) aFRR (2019)**
0.75	0.80	660928	906916
0.80	0.85	674802	944078
0.85	0.90	688466	981079
0.90	0.95	701933	1018599
1	1	721205	1083939

Table 46: Test the effects of the efficiency of the PaT on the yearly revenues of the RBC model.

Data set	Mean (€)	Revenue (€)
Day-ahead market (2017)	39.31	730969
Day-ahead market (2018)	52.53	902562
Day-ahead market (2019)	41.20	688466
aFRR market (2017)	43.18	1128840
aFRR market (2017)	52.41	1170752
aFRR market (2017)	42.55	981079

Table 47: Yearly revenues for the RBC strategy.

Year	Indirect model	Direct model
2017	€1198871	€1244271
2018	€1520417	€1576104
2019	€1142382	€1177447

Table 48: Yearly revenues (day-ahead market) for the MSMG simulations with the MPC strategy.

	Storage	2017	2018	2019
Indirect model	1	6,0	6,3	6,9
	2	1,3	1,4	1,3
	3	1,4	1,4	1,4
	4	6,0	6,0	6,1
Direct model	1	7,3	7,3	7,3
	2	7,3	7,3	7,3
	3	7,3	7,3	7,3
	4	7,3	7,3	7,3

Table 49: Maximum storage levels (day-ahead market) for the MSMG simulations with the MPC strategy.

	Storage	2017	2018	2019
Indirect model	1	1692	1483	1366
	2	19	31	30
	3	26	26	29
	4	1310	1208	1011
Direct model	1	1537	1347	1190
	2	1530	1380	1237
	3	1510	1387	1232
	4	1536	1316	1207

Table 50: Total energy sent to individual storage units (day-ahead market) for the MSMG simulations with the MPC strategy.

	2017	2018	2019
Total production (MWh)	30170	28967	27876
Sent to storage (MWh), Indirect model	2962	2639	2323
Sent to storage (MWh), Direct model	6434	5716	5123

Table 51: Total energy sent to storage units (day-ahead market) for the MSMG simulations with the MPC strategy.

Year	Indirect model	Direct model
2017	€1692001	€2165750
2018	€1990390	€2455104
2019	€1527080	€1955968

Table 52: Yearly revenues (aFRR market) for the MSMG simulations with the MPC strategy.

	Storage	2017	2018	2019
Indirect model (P = 3 hr)	1	5,7	6,0	7,1
	2	1,5	1,5	1,5
	3	1,5	1,4	1,7
	4	5,9	6,0	7,3
Indirect model (P = 15 min)	1	1,2	0,9	1,5
	2	0,2	0,6	0,2
	3	0,1	0,3	0,3
	4	1,0	1,1	1,3
Direct model	1	6,3	7,3	7,3
	2	6,4	7,3	7,3
	3	7,2	7,3	7,3
	4	6,0	7,3	7,3

Table 53: Maximum storage levels (aFRR market) for the MSMG simulations with the MPC strategy.

	Storage	2017	2018	2019
Indirect model (P = 3 hr)	1	4438	3954	4222
	2	122	90	113
	3	89	94	103
	4	3472	3243	3297
Indirect model (P = 15 min)	1	2927	2584	1753
	2	1	2	1
	3	1	1	2
	4	2177	1996	2028
Direct model	1	3265	2937	3018
	2	3177	2983	3093
	3	3238	3003	3113
	4	3209	3022	3050

Table 54: Total energy sent to individual storage units (aFRR market) for the MSMG simulations with the MPC strategy.

	2017	2018	2019
Total production (MWh)	30170	28967	27876
Sent to storage (MWh), Indirect model (P = 3 hr)	7720	7031	7324
Sent to storage (MWh), Indirect model (P = 15 min)	5102	4576	4779
Sent to storage (MWh), Direct model	13567	12574	12921

Table 55: Total energy sent to storage units (day-ahead market) for the MSMG simulations with the MPC strategy.

TC (MW)	**Energy stored** (MWh)	**Day-ahead** (2019)	**Energy stored** (MWh)	**aFRR** (2019)
1	2323	1142382	7324	1527080
2	2993	1147161	9679	1660317
3	3338	1148424	10780	1711480
4	3364	1148190	11304	1758889

Table 56: Yearly revenues from the turbine capacity sensitivity with MSMG MPC strategy.

Depth (m)	**Energy stored** (MWh)	**Day-ahead** (2019)	**Energy stored** (MWh)	**aFRR** (2019)
40	2323	1142382	7324	1527080
50	2296	1142414	7340	1532689
60	2290	1142044	7352	1531546
70	2289	1141822	7345	1534316

Table 57: Yearly revenues from the depth sensitivity with MSMG MPC strategy.

Depth (m)	**Day-ahead** (2019)	**aFRR** (2019)	**Max capacity** (MWh)
40	6.85	7.33	7.33
50	7.42	6.4	9.42
60	6	6.93	11.52
70	6	6.33	13.61

Table 58: Maximum storage levels from the depth sensitivity with MSMG MPC strategy.

Year	**Indirect model**	**Indirect model + BFM**
2017	€1692001	€2197474
2018	€1990390	€2518177
2019	€1527080	€1994398

Table 59: Yearly revenues (aFRR market) for the MSMG simulations with the MPC strategy + buy from market.

	Storage	**2017**	**2018**	**2019**
Indirect model	1	5,7	6,0	7,1
	2	1,5	1,5	1,5
	3	1,5	1,4	1,7
	4	5,9	6,0	7,3
Indirect model	1	7,33	7,33	7,33
+ buy from market	2	1,35	5,21	3,86
	3	2,24	4,06	4,33
	4	7,33	7,33	7,33

Table 60: Maximum storage levels (aFRR market) for the MSMG simulations with the MPC strategy + buy from market.

	Storage	**2017**	**2018**	**2019**
Indirect model	1	4438	3954	4222
	2	122	90	113
	3	89	94	103
	4	3472	3243	3297
Indirect model	1	7927	7633	8014
+ buy from market	2	13	15	8
	3	12	20	9
	4	7908	7649	7979

Table 61: Total energy sent to individual storage units (aFRR market) for the MSMG simulations with the MPC strategy + buy from market.

	2017	**2018**	**2019**
Total production (MWh)	30170	28967	27876
Sent to storage (MWh), Indirect model	7720	7031	7324
Sent to storage (MWh)	1086	1008	1015
Bought from market (MWh) Indirect model + BFM	15829	15392	16088

Table 62: Total energy sent to storage units (day-ahead market) for the MSMG simulations with the MPC strategy + buy from market.

K Optimization problem in Chapter 6.6

$$\max_{\hat{u}} \quad J = \sum_{k=1}^{N}\left(\sum_{i=1}^{\#S} R_i(k) + \sum_{j=1}^{\#G} R_j(k)\right) \tag{43}$$

s.t.:

$$\begin{aligned}
\hat{E}_{i,k+1} = \hat{E}_{i,k} &+ \eta_P \sum_{j=1}^{\#G} \hat{u}^{RG}_{i,j,k} \cdot \hat{E}^{G}_{j,k+1} + \eta_T \cdot \eta_P \sum_{j=1, i\neq j}^{\#S} \hat{u}^{RS}_{i,j,k} \cdot \hat{E}_{j,k} \\
&+ \eta_P \cdot \hat{u}^{RC}_{i,k} \cdot E^M - \eta_T \cdot \hat{E}_{i,k} \left[\left(\sum_{j=1, i\neq j}^{\#S} \hat{u}^{SS}_{i,j,k} \right) + \hat{u}^{SC}_{i,k} \right], && i = 1,..,S \\
(\hat{u}^{RG}_{i,k} + \hat{u}^{RS}_{i,k}) \cdot (\hat{u}^{SS}_{i,k} + \hat{u}^{SC}_{i,k}) &= 0, && i = 1,..,S \\
TC - \eta_P \sum_{j=1}^{\#G} \hat{u}^{RG}_{i,j,k} \cdot \hat{E}^{G}_{j,k+1} &+ \eta_T \cdot \eta_P \sum_{j=1, i\neq j}^{\#S} \hat{u}^{RS}_{i,j,k} \cdot \hat{E}_{j,k} \\
&+ \eta_P \cdot \hat{u}^{RC}_{i,k} \cdot E^M - \eta_T \cdot \hat{E}_{i,k} \left[\left(\sum_{j=1, i\neq j}^{\#S} \hat{u}^{SS}_{i,j,k} \right) + \hat{u}^{SC}_{i,k} \right] &\geq 0, & \quad i = 1,..,S \\
E_{max} - \left(\eta_P \sum_{j=1}^{\#G} \hat{u}^{RG}_{i,j,k} \cdot \hat{E}^{G}_{j,k+1} + \eta_T \cdot \eta_P \sum_{j=1, i\neq j}^{\#S} \hat{u}^{RS}_{i,j,k} \cdot \hat{E}_{j,k} + \eta_P \cdot \hat{u}^{RC}_{i,k} \cdot E^M \right) &\geq 0, && i = 1,..,S \\
\left[\left(\sum_{j=1, i\neq j}^{\#S} \hat{u}^{SS}_{i,j,k} \right) + \hat{u}^{SC}_{i,k} \right] &\leq 1, && i = 1,..,S \\
\left[\left(\sum_{j=1}^{\#S} \hat{u}^{SS}_{i,j,k} \right) + \hat{u}^{GC}_{i,k} \right] &\leq 1, && i = 1,..,G \\
0 \leq \hat{u}^{RG}, \hat{u}^{RS}, \hat{u}^{RC} \hat{u}^{SS}, \hat{u}^{SC}, \hat{u}^{GC} &\leq 1
\end{aligned}$$

In this optimization problem, R_i and R_j are calculated from (36) and (22), respectively. $\hat{E}^G$ is imported from the wind power production data set and E^M is an unlimited amount of energy that can be bought from the market.